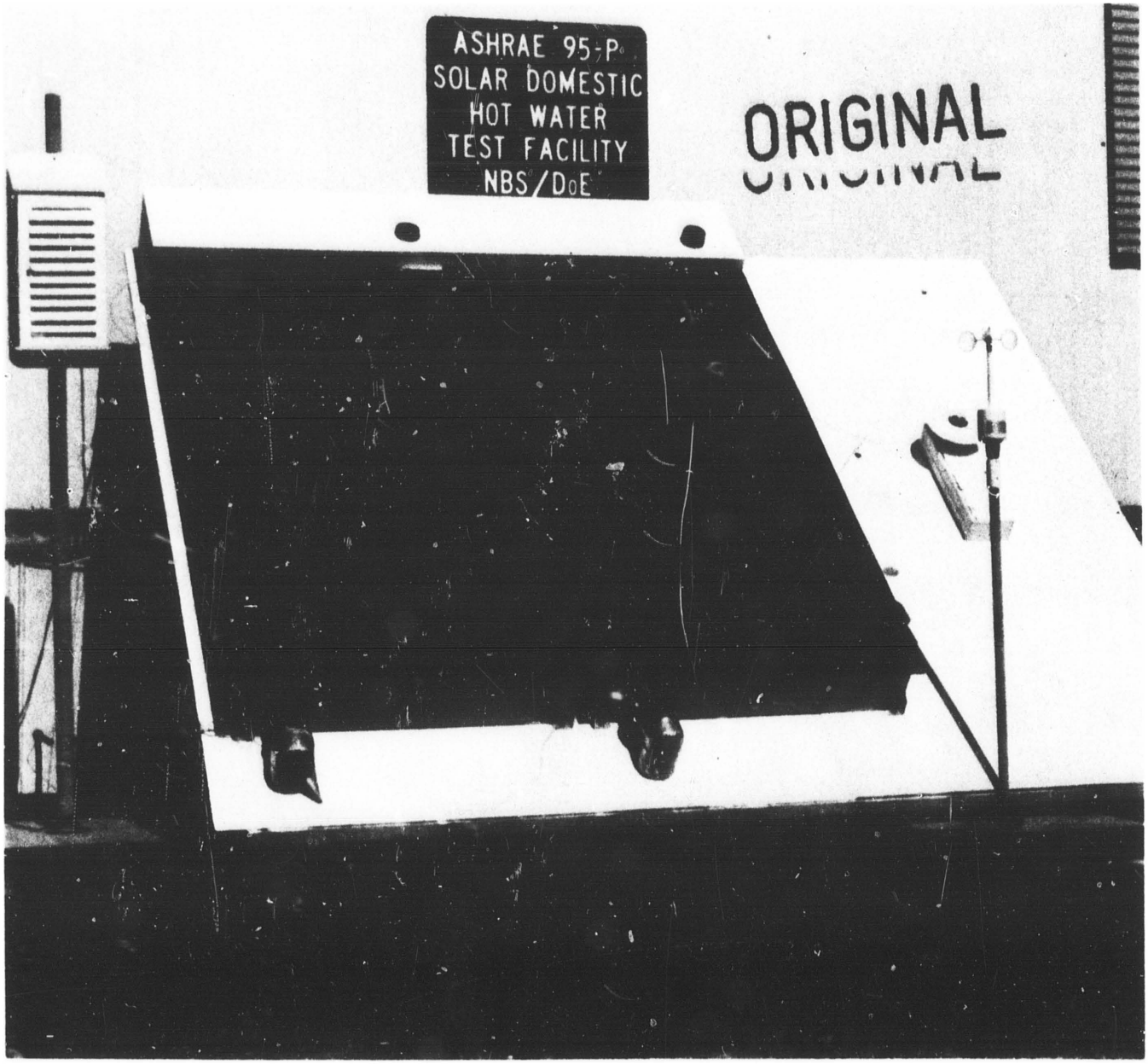

NBS BUILDING SCIENCE SERIES 140

Analytical and Experimental Analysis of Procedures for Testing Solar Domestic Hot Water Systems

U.S. DEPARTMENT OF COMMERCE • NATIONAL BUREAU OF STANDARDS

NATIONAL BUREAU OF STANDARDS

The National Bureau of Standards[1] was established by an act of Congress on March 3, 1901. The Bureau's overall goal is to strengthen and advance the Nation's science and technology and facilitate their effective application for public benefit. To this end, the Bureau conducts research and provides: (1) a basis for the Nation's physical measurement system, (2) scientific and technological services for industry and government, (3) a technical basis for equity in trade, and (4) technical services to promote public safety. The Bureau's technical work is performed by the National Measurement Laboratory, the National Engineering Laboratory, and the Institute for Computer Sciences and Technology.

THE NATIONAL MEASUREMENT LABORATORY provides the national system of physical and chemical and materials measurement; coordinates the system with measurement systems of other nations and furnishes essential services leading to accurate and uniform physical and chemical measurement throughout the Nation's scientific community, industry, and commerce; conducts materials research leading to improved methods of measurement, standards, and data on the properties of materials needed by industry, commerce, educational institutions, and Government; provides advisory and research services to other Government agencies; develops, produces, and distributes Standard Reference Materials; and provides calibration services. The Laboratory consists of the following centers:

Absolute Physical Quantities[2] — Radiation Research — Thermodynamics and Molecular Science — Analytical Chemistry — Materials Science.

THE NATIONAL ENGINEERING LABORATORY provides technology and technical services to the public and private sectors to address national needs and to solve national problems; conducts research in engineering and applied science in support of these efforts; builds and maintains competence in the necessary disciplines required to carry out this research and technical service; develops engineering data and measurement capabilities; provides engineering measurement traceability services; develops test methods and proposes engineering standards and code changes; develops and proposes new engineering practices; and develops and improves mechanisms to transfer results of its research to the ultimate user. The Laboratory consists of the following centers:

Applied Mathematics — Electronics and Electrical Engineering[2] — Mechanical Engineering and Process Technology[2] — Building Technology — Fire Research — Consumer Product Technology — Field Methods.

THE INSTITUTE FOR COMPUTER SCIENCES AND TECHNOLOGY conducts research and provides scientific and technical services to aid Federal agencies in the selection, acquisition, application, and use of computer technology to improve effectiveness and economy in Government operations in accordance with Public Law 89-306 (40 U.S.C. 759), relevant Executive Orders, and other directives; carries out this mission by managing the Federal Information Processing Standards Program, developing Federal ADP standards guidelines, and managing Federal participation in ADP voluntary standardization activities; provides scientific and technological advisory services and assistance to Federal agencies; and provides the technical foundation for computer-related policies of the Federal Government. The Institute consists of the following centers:

Programming Science and Technology — Computer Systems Engineering.

[1]Headquarters and Laboratories at Gaithersburg, MD, unless otherwise noted; mailing address Washington, DC 20234.
[2]Some divisions within the center are located at Boulder, CO 80303.

NBS BUILDING SCIENCE SERIES 140

Analytical and Experimental Analysis of Procedures for Testing Solar Domestic Hot Water Systems

A. H. Fanney[1]
W. C. Thomas[2]
C. A. Scarbrough[1]
C. P. Terlizzi[1]

[1]Center for Building Technology
National Engineering Laboratory
National Bureau of Standards
Washington, DC 20234

[2]Department of Mechanical Engineering
Virginia Polytechnic Institute and State University
Blacksburg, VA 24061

Sponsored by the
Office of Solar Applications for Buildings
U.S. Department of Energy
Washington, DC 20585

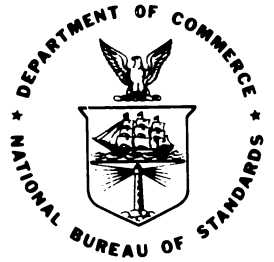

U.S. DEPARTMENT OF COMMERCE, Malcolm Baldrige, Secretary
NATIONAL BUREAU OF STANDARDS, Ernest Ambler, Director

Issued February 1982

I

Library of Congress Catalog Card Number: 81-600191

National Bureau of Standards Building Science Series 140
Nat. Bur. Stand. (U.S.), Bldg. Sci. Ser. 140, 158 pages (Feb. 1982)
CODEN: BSSNBV

U.S. GOVERNMENT PRINTING OFFICE
WASHINGTON: 1982

For sale by the Superintendent of Documents, U.S. Government Printing Office, Washington, DC 20402

ABSTRACT

A repeatable test method independent of outdoor environmental conditions and laboratory geographical location is required in order to provide a means by which solar domestic hot water systems may be rated and compared. Three experimental techniques which allow the net thermal output of an irradiated solar collector array to be reproduced indoors without the use of a solar simulator are investigated. These techniques include use of an electric heat source only, use of a nonirradiated collector array in series with an electric heat source, and the use of electric strip heaters which are attached to the back of nonirradiated absorber plates. Expressions are developed to compute the input power required for each experimental technique. Solar collectors connected in parallel and series combinations are considered.

All three test techniques were shown to reproduce the outdoor daily collector array thermal output within four percent. Two of the techniques allow the actions of the circulator controller for an outdoor irradiated system to be duplicated indoors. One technique applies to solar hot water systems which operate on the thermosyphon principle.

Experiments conducted to determine the effect of storage tank temperature stratification on system performance for a single-tank direct solar hot water system are described. Several return tube designs, which introduce the solar-heated water into the storage tank, were fabricated and tested to determine the influence of thermal stratification on system performance. The best return tube design increased the performance of a single-tank direct system approximately ten percent compared to a conventional return tube design.

An analytical model for a single-tank direct hot water system is developed. The model is used to support parametric studies for the thermal performance characteristics which result from the use of each test method to duplicate the net thermal output of an irradiated array. The model is also used to assess thermal performance differences which occur due to indoor versus outdoor environmental conditions.

Key words: ASHRAE Standard 95; collectors in parallel; electric strip heaters; environmental conditions; indoor testing; modeling; NBS; solar; solar domestic hot water system; stratification; test method.

PREFACE

This reseach was sponsored by the Office of Solar Applications for Buildings, U.S. Department of Energy, Washington, D.C. 20585.

DISCLAIMER

Certain commercial equipment, instruments, or materials are identified in this paper in order to adequately specify the experimental procedure. Such identification does not imply recommendation or endorsement by the National Bureau of Standards, nor does it imply that the materials or equipment identified are necessarily the best available for the purpose.

TABLE OF CONTENTS

LIST OF FIGURES

LIST OF FIGURES (cont.)

LIST OF FIGURES (cont.)

LIST OF FIGURES (cont.)

LIST OF TABLES

LIST OF TABLES (cont.)

NOMENCLATURE

A_a	Collector aperture area, m^2
A_c	Cross-sectional area of storage tank, m^2
A_e	Collector edge area, m^2
A_g	Collector gross area, m^2
A_{si}	Surface area of storage tank segment i which experiences heat loss to the environment, m^2
$\frac{A_a}{A_g} F_R(\tau\alpha)_n$	Intercept of the collector efficiency curve determined in accordance with ASHRAE 93-77, dimensionless
$\frac{A_a}{A_g} F_R U_L$	Slope of the collector efficiency curve determined in accordance with ASHRAE 93-77, $W/(m^2 C)$
CL_{CON}	Daily combustion heat loss from a conventional water heater, kJ
C_p	Specific heat, kJ/(kg C)
$C_{p,c}$	Specific heat of the transfer fluid used in the collector during the ASHRAE Standard 93-77 tests, kJ/(kg C)
$C_{p,s}$	Specific heat of the transfer fluid used in the collector during the solar hot water system test, kJ/(kg C)
d_h	Hydraulic diameter of flow tube, m
D	Flow tube outside diameter, m
e	Fractional energy savings, dimensionless
E_{c1}	Emissive power of cover 1, W/m^2
E_p	Emissive power of absorber plate, W/m^2
E_s	Emissive power of sky, W/m^2
F	Fin efficiency, dimensionless
F_i^c	Collector control function for node i, dimensionless
F'	Collector efficiency factor, dimensionless
F_R	Collector heat removal factor, dimensionless

F_{R2}	Collector heat removal factor for two collectors connected in series, dimensionless
G	Total global irradiance incident upon the aperture plane of the collector, W/m^2
$\dot{G}$	Fluid mass flow rate per unit collector aperture area, $kg/(m^2 s)$
h_f	Heat transfer coefficient between the fluid and tube wall, $W/(m^2 C)$
h_{pc1}	Conductance, natural convection, between absorber and cover 1, $W/(m^2 C)$
h_w	Conductance, outside cover to ambient air, $W/(m^2 C)$
HL_{CON}	Daily heat loss from a conventional water heater, kJ
J	Heating element control logic, dimensionless
$\tilde{J}_{bj}$	Solar beam radiosity, jth surface, dimensionless
$\tilde{J}_{dj}$	Solar diffuse radiosity, jth surface, dimensionless
$\tilde{J}_j$	Longwave diffuse radiosity, jth surface, dimensionless
k_e	Thermal conductivity, edge insulation, W/(m C)
k_i	Thermal conductivity, back insulation, W/(m C)
k_p	Thermal conductivity, absorber plate, W/(m C)
k_w	Thermal conductivity, water, W/(m C)
$K_{\alpha\tau}$	Incident angle modifier, dimensionless
L	Number of time steps in test period, dimensionless; length of absorber plate, m
L_e	Thickness of edge insulation, m
L_i	Thickness of back insulation, m
L_i^c	Control logic function for node i, dimensionless
m	Parameter defined by equation 34, m^{-1}
$\dot{m}$	Mass flow rate, kg/s
$\dot{m}_c$	Mass flow rate of the transfer fluid through the collector during the ASHRAE Standard 93-77 tests, kg/s

$\dot{m}_L$	Mass flow rate of hot water draw, kg/s
$\dot{m}_s$	Mass flow rate of the transfer fluid through the collector array during the solar hot water system test, kg/s
M	Number of parallel rows of collectors, dimensionless
M_i	Mass of water contained in storage tank node i, kg
n	Number of time steps during which hot water draws occur, dimensionless
N	Number of collectors connected in series, dimensionless; number of segments into which the storage tank is divided, dimensionless
Nu	Nusselt number, dimensionless
Pr	Prandtl number, dimensionless
P_w	Wetted perimeter, m
q_{acl}	Fraction of total solar irradiance absorbed by cover, W/m^2
$\dot{Q}$	Power supplied to storage tank, W
Q_{CON}	Daily energy supplied to a conventional water heater, kJ
$\dot{Q}_{HE}$	Thermal output of storage tank heating element, W
Q_{HE}	Daily energy consumed by storage tank heating element, kJ
$\dot{Q}_{hs}$	Thermal output of conventional heat source, W
$\dot{Q}^*_{hs}$	Thermal output of conventional heat source when located upstream of a nonirradiated array, W
Q_L	Daily energy extracted from storage tank, kJ
Q_{SA}	Daily thermal output of irradiated collector array, kJ
$\dot{Q}_{sh}$	Thermal output of electric strip heaters, W
$\dot{Q}_{SI}$	Heat loss from the section of pipe located in the laboratory which supplies the collector array, W
Q_{ST}	Change in storage tank internal energy during the test day, kJ
Q_T	Daily energy supplied to storage tank from solar collector array, kJ

$\dot{Q}''_t$	Heat loss per unit time and aperture area through absorber-cover assembly, W/m^2
$\dot{Q}_u$	Net thermal output of collector array, W
Re	Reynolds number, dimensionless
S	Quantity of solar irradiance absorbed by the absorber plate of a single collector, W
t_a	Ambient temperature, C
$t_{a\ell}$	Laboratory ambient temperature, C
t_{co}	Fluid temperature leaving the collector array, C
t_{c1}	Temperature, mean, cover 1, C
t_{fi}	Fluid temperature entering the collector array, C
t^*_{fi}	Fluid temperature entering the nonirradiated collector array with an upstream heat source, C
t_{fm}	Mean fluid temperature, C
t_H	Upper temperature limit for the heating element thermostat, C
$\bar{t}_h$	Average fluid temperature within the heat source, C
t_{hi}	Fluid temperature entering the heat source, C
t_{ho}	Fluid temperature leaving the heat source, C
t_i	Temperature of storage tank segment i, C
t_i^n	Predicted future temperature of storage tank segment i, C
t_L	Lower temperature limit for the heating element thermostat, C
t_{MW}	Temperature of supply water entering the storage tank, C
t_p	Mean absorber plate temperature, C
t_{pn}	Mean absorber plate temperature of a nonirradiated collector, C
t^*_{pn}	Mean absorber plate temperature of a nonirradiated collector with upstream heat source, C
t_R	Temperature of the solar-heated fluid as it enters the storage tank, C

t_{set}	Ultimate desired hot water delivery temperature, C
t_{sw}	Temperature of the collector supply fluid as it leaves the interior of the laboratory, C
t_w	Temperature, tube wall, C
T_{sky}	Effective sky temperature, K
Δt_M	Log-mean temperature difference, C
U_b	Collector back and edge loss coefficient, $W/(m^2C)$
U_L	Collector overall loss coefficient, $W/(m^2C)$
U_{LT}	Storage tank loss coefficient, $W/(m^2C)$
U_T	Collector top loss coefficient, $W/(m^2C)$
$(UA)_{hs}$	Heat loss coefficient-area product for heat source, W/C
$(UA)_{RI}$	Heat loss coefficient-area product for interior portion of solar collector array return pipe, W/C
$(UA)_{RO}$	Heat loss coefficient-area product for exterior portion of solar collector array return pipe, W/C
$(UA)_{SI}$	Heat loss coefficient-area product for interior portion of solar collector array supply pipe, W/C
$(UA)_{SO}$	Heat loss coefficient-area product for exterior portion of solar collector array supply pipe, W/C
V	Volume of storage tank segment, m^3
V_w	Wind velocity, m/s
W	Tube spacing, m
α_n	Absorptance of the collector absorber coating to the solar spectrum at the normal incidence, dimensionless
α_p	Absorptance, plate, dimensionless
θ	Angle of incidence between the direct solar beam and the normal to the collector aperture, deg
δ	Absorber plate thickness, m
η	Collector efficiency based on the net area, dimensionless

η_{hs}	Heat source efficiency, dimensionless
μ	Fluid viscosity, kg/(m s)
ρ	Density, kg/m^3
ρ_{bl}	Reflectance, solar beam irradiance, cover 1, dimensionless
ρ_{dl}	Reflectance, solar diffuse irradiance, cover 1, dimensionless
ρ_{cl}	Reflectance, longwave diffuse irradiance, cover 1, dimensionless
ρ_p	Reflectance, longwave diffuse irradiance, absorber, dimensionless
σ	Stefan-Boltzmann constant, $W/(m^2\ K^4)$
τ_{bl}	Transmittance, solar beam irradiance, cover 1, dimensionless
τ_{dl}	Transmittance, solar diffuse irradiance, cover 1, dimensionless
τ_{cl}	Transmittance, longwave diffuse irradiance, cover 1, dimensionless
τ_n	Effective transmittance at normal incidence, dimensionless
$(\tau\alpha)_n$	Effective transmittance-absorptance product for the collector at normal incidence, dimensionless
$\Delta\tau$	Length of time step, s

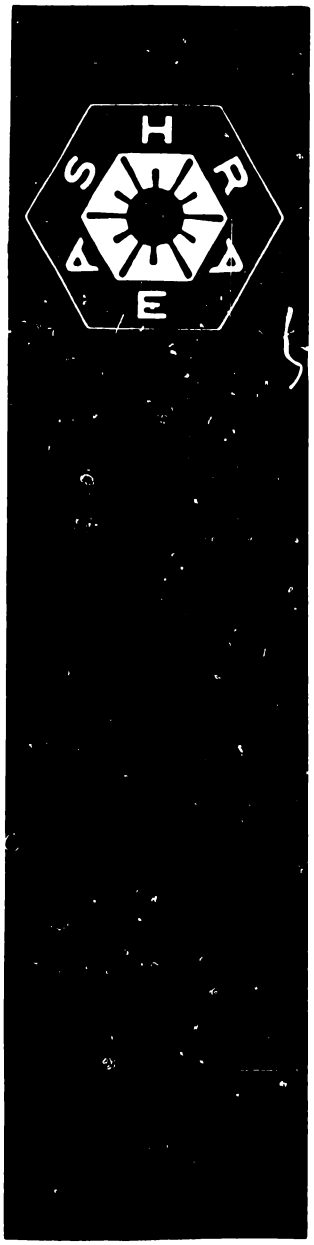

ASHRAE 95P

ASHRAE STANDARD

Method of Testing TO DETERMINE THERMAL PERFORMANCE OF PACKAGED RESIDENTIAL SOLAR WATER HEATERS

DRAFT
April 20, 1979

The American Society of Heating, Refrigerating, and Air-Conditioning Engineers, Inc.
345 East 47th Street, New York, N.Y. 10017

1. INTRODUCTION AND BACKGROUND

1.1 PURPOSE

The purpose of this analytical and experimental investigation is to develop a test method for solar domestic hot water (SDHW) systems. Although the primary components of a SDHW system are the collector modules and storage tanks, for which standards have been adopted, the interaction between components has not been established. Consequently, a standard test method for a SDHW system is needed. Once a test method is adopted, an industry rating association such as the Air Conditioning and Refrigeration Institute (ARI) or the Solar Energy Industries Association (SEIA) may develop and adopt a companion rating standard that specifies the number of tests to be conducted, the test conditions to be used, and the manner in which performance results are to be reported.

A repeatable test method, independent of outdoor environmental conditions and laboratory geographical location, is required in order to provide a means by which SDHW systems may be rated and compared. One possible method employs a solar simulator to irradiate the solar panels which are part of the SDHW system being tested. Another method, which is the subject of this research, requires that the energy normally furnished by an outdoor irradiated solar collector array be replaced by an equivalent amount of energy supplied by a conventional energy source.

Three experimental techniques which allow the net thermal output of an irradiated collector array to be duplicated without the use of a solar simulator are described in detail. Governing equations required for each technique are developed. Experiments performed at the National Bureau of Standards to validate each technique are described and the results are presented. The influence of temperature stratification on system performance and the repeatability of test results are investigated using one selected test method. A numerical model of a single-tank direct solar hot water system is developed. The model is used to predict the effects of different test methods and meteorological conditions on system performance.

1.2 BACKGROUND

The Steering Committee of the American National Standards Institute on Solar Energy Standards designated the American Society of Heating, Refrigerating and Air-conditioning Engineers (ASHRAE) to develop a standard test method for SDHW systems. The ASHRAE then formed Standards Project Committee 95-P in February 1977 to begin this task.

During the early deliberations of the Committee, alternative methods of testing a complete SDHW system were proposed. One method considered would require installation of each system to be tested in a particular location. The solar collector array of the system would be subjected to normal outdoor meteorological conditions. System performance would be monitored during the test interval. This method was eliminated due to the nonrepeating nature of outdoor environmental conditions.

Analytical methods based on mathematical models to predict system performance were also considered. The programs TRNSYS [1], f-CHART [2], and Solcost [3] are widely used in predicting the thermal performance of solar hot water systems since, for some systems, these computer codes have been shown to predict long-term performance generally in good agreement with experimental data [4]. The credibility of these codes for general rating purposes has not been established. Additionally, the system input parameters including the heat exchanger effectiveness, the overall heat loss coefficient for the storage tanks, and the performance characteristics of the solar collector modules have to be measured in order to achieve acceptable agreement with experimental results.

A third method considered [5] uses a combination of experimental results and analytical modeling. This concept is based on conducting single-day outdoor tests of the system and a "baseline" SDHW system. The ratio of the performance of the test system to the baseline system is called the daily relative solar

rating. Long-term performance for the test SDHW system would be determined from the daily relative solar rating, a correlation procedure based on computer simulations, and long-term measured performance results for the baseline system. Preliminary results for single-tank direct systems in sunny climatic regions are encouraging. Comparison of test results from different laboratories may prove difficult as a result of the variability in the performance of baseline systems. Difficulties may also be encountered in attempting to use a computer program, such as TRNSYS, to model all types of SDHW systems which may be encountered.

The Standard Projects Committee considered a test method which employs a solar simulator to irradiate the solar panels which are part of the SDHW system being tested. The irradiance on the collectors is varied throughout the test day as specified by an industry rating association. Specified quantities of energy are withdrawn from the storage tanks at selected times during the test period. The test continues until system performance is nearly identical for two successive days. This method of testing is included in the final ASHRAE Standard 95, Method of Testing to Determine the Thermal Performance of Solar Domestic Water Heating Systems [6]. The advantages of this method include repeatability of test conditions, independence from outdoor meteorological conditions, and elimination of analytical modeling. Additionally, a separate test to determine the thermal performance characteristics of an individual collector module [7] is not required. The use of a solar simulator enables testing of thermosyphon and integral storage systems. These systems pose formidable difficulties for some other test methods. However, among the disadvantages of using a solar simulator are high costs, limited availability, and the physical constraint that most solar simulators are designed to irradiate a single panel rather than an array consisting of several panels.

Two test methods are considered employing a conventional heat source such as an in-line electrical resistance heater. One method employs a conventional heat source instead of an irradiated collector array to supply the net quantity of power normally supplied by an irradiated array. The use of a heat source only to supply the net thermal output of an irradiated array results in excellent agreement between outdoor and laboratory system performance [8]. The influence of collector performance on total system performance may be evaluated without changing the experimental apparatus. Kotas and Wood [9] describe an apparatus and control system to automate this testing sequence. However, there are several disadvantages to using only an electric heat source to supply the quantity of power normally delivered by an irradiated array: 1) outdoor stagnation (no flow) conditions cannot be duplicated; 2) thermosyphon systems cannot be tested using this technique since the power input is localized rather than distributed along the length of the absorber plates contained within the solar collector modules; and 3) the solar industry may object to a system test in which the collector array is not part of the experimental apparatus.

The second heat source method employs a conventional heat source in series with the nonirradiated SDHW system collector array. The combination of a heat source and nonirradiated array supplies the net quantity of thermal power normally supplied by the irradiated array. The use of a conventional heat source in series with a nonirradiated collector array and a storage tank bypass loop allows outdoor stagnation conditions to be simulated. The heat source may be

located upstream or downstream of the nonirradiated array when the proper governing equation is used to compute the quantity of power supplied to the heat source [10]. As before, this technique does not apply to thermosyphon systems because it uses a localized heat source. The ASHRAE Standards Project Committee incorporated this method of testing into ASHRAE Standard 95. Validation of this test procedure is part of the present investigation.

In another method, the problem of the localized heat source is eliminated. Solar energy absorbed by irradiated solar collector absorber plates is replaced with energy supplied by electric strip heaters attached to the back side of nonirradiated absorber plates. Thermosyphon systems may be tested using this technique. Also, outdoor stagnation conditions can be duplicated within the laboratory using this technique. The calculation procedure required to determine the quantity of power supplied to the strip heaters is independent of mass flow rate and fluid composition. Additionally, testing of an individual collector module is not necessary if the optical properties of the collector are known. A disadvantage of this method is the requirement that the collector modules must be disassembled to install the heaters. Since this concept was advanced by NBS after the proposed Standard 95 was submitted for approval, this method has not yet been incorporated into the test standard. The present investigation is concerned with establishing the feasibility and validity of this method, which is important for testing thermosyphon systems.

2. ANALYSIS

Three methods were investigated which allowed the net thermal output of an irradiated collector array to be duplicated under nonirradiated conditions. The first method uses an electric heat source only. The second method uses a non-irradiated collector array in series with an electric heat source. The third method employs electric strip heaters attached to the back of nonirradiated absorber plates. Governing equations used in determining the power supplied to the electric heat source and strip heaters are developed in this chapter.

An analytical model is developed to simulate the performance of an entire solar domestic hot water system. The model is used to support parametric studies of

the thermal performance characteristics which result from the use of each method to duplicate the net thermal output of an irradiated array. The model is also used to assess thermal performance differences which occur as a result of indoor versus outdoor environmental conditions.

2.1 ANALYSIS OF IRRADIATED COLLECTOR ARRAYS

Under steady-state conditions, the useful energy from a single irradiated solar collector can be expressed in accordance with the Hottel-Whillier-Bliss (H-W-B) analysis as

$$\dot{Q}_u = A_g\left[K_{\alpha\tau}\frac{A_a}{A_g} F_R\,(\tau\alpha)_n\, G - \frac{A_a}{A_g} F_R U_L\,(t_{fi} - t_a)\right] \tag{1}$$

The useful energy output of an array consisting of M collectors connected in parallel is

$$\dot{Q}_u = MA_g\left[K_{\alpha\tau}\frac{A_a}{A_g} F_R\,(\tau\alpha)_n\, G - \frac{A_a}{A_g} F_R U_L\,(t_{fi} - t_a)\right] \tag{2}$$

The useful energy output of an array which includes collectors connected in series can be represented similarly, taking into account modification of the heat removal factor, F_R. For a single solar collector module

$$F_R = \frac{\dot{m}C_p}{U_L A_a}\left[1 - \exp\left(-\frac{A_a F' U_L}{\dot{m}C_p}\right)\right] \tag{3}$$

Consider the case where two collectors are connected in series. Each solar collector module experiences the same mass flow rate. However, the inlet temperature to the downstream collector is higher. The collector efficiency factor, F', is weakly influenced by the fluid temperature through its effect on the convective heat transfer coefficient. The overall heat loss coefficient, U_L, is somewhat more dependent on fluid temperature, but, in this analysis, both F' and U_L are assumed constant. With these assumptions, eq (3) becomes

$$F_{R2} = \frac{\dot{m}C_p}{U_L 2A_a}\left[1 - \exp\left(-\frac{2A_a F' U_L}{\dot{m}C_p}\right)\right] \tag{4}$$

Algebraic manipulation of eqs (3) and (4) gives

$$F_{R2} = F_R\left[1 - \frac{(F_R U_L)A_a}{2\dot{m}C_p}\right] \tag{5}$$

Thus for two collectors in series

$$(F_R U_L)_2 = (F_R U_L)\left[1 - \frac{(F_R U_L)A_a}{2\dot{m}C_p}\right] \tag{6}$$

and

$$(F_R(\tau\alpha)_n)_2 = (F_R(\tau\alpha)_n)\left[1 - \frac{(F_RU_L)A_a}{2\dot{m}C_p}\right] \tag{7}$$

Generalizing to any number, N, of identical collectors in series

$$(F_RU_L)_N = \frac{\dot{m}C_p}{NA_a}\left[1 - \left(1 - \frac{(F_RU_L)A_a}{\dot{m}C_p}\right)^N\right] \tag{8}$$

and

$$(F_R(\tau\alpha)_n)_N = \frac{(F_R(\tau\alpha)_n)\dot{m}C_p}{(F_RU_L)^N A_a}\left[1 - \left(1 - \frac{(F_RU_L)A_a}{\dot{m}C_p}\right)^N\right] \tag{9}$$

For N irradiated collectors connected in series, the useful energy output is

$$\dot{Q}_u = NA_g\left[K_{\alpha\tau}\frac{A_a}{A_g}(F_R(\tau\alpha)_n)_N G - \frac{A_a}{A_g}(F_RU_L)_N(t_{fi} - t_a)\right] \tag{10}$$

Substitution of eqs (8) and (9) into eq (2) yields the useful energy output of a solar collector array consisting of M rows of N collectors connected in series

$$\dot{Q}_u = MNA_g\left[K_{\alpha\tau}\frac{A_a}{A_g}(F_R(\tau\alpha)_n)_N G - \frac{A_a}{A_g}(F_RU_L)_N(t_{fi} - t_a)\right] \tag{11}$$

2.2 REPLACEMENT OF THE IRRADIATED ARRAY WITH A CONVENTIONAL HEAT SOURCE ONLY

A conventional heat source is used to replace the irradiated solar collector array. This method requires that the solar collector be tested according to ASHRAE Standard 93-77 [7] and values of F_RU_L, $F_R(\tau\alpha)_n$, and $K_{\alpha\tau}$ be determined. The inlet fluid temperature to the heat source, t_{fi}, is measured. The required thermal output of the heat source is calculated using the above information in conjunction with specified meteorological conditions and eq (11). It should be noted with reference to eq (3) that the value of F_R is dependent upon mass flow rate of the transfer fluid and the properties of the heat transfer fluid. ASHRAE Standard 95-P requires that the fluid used in the system test be identical to the one used in the required collector test. If the flow rate of the transfer fluid through the collector during the system test is different from the value used in the collector test, the value of F_R must be modified. Appendix A gives the ASHRAE Standard 95-P modification procedure.

2.3 REPLACEMENT OF THE IRRADIATED ARRAY WITH A CONVENTIONAL HEAT SOURCE IN SERIES WITH A NONIRRADIATED ARRAY

This method employs a conventional heat source upstream or downstream of a nonirradiated solar collector array. The useful energy output of a single collector may be expressed as

$$\frac{\dot{Q}_u}{A_a} = K_{\alpha\tau} (\tau\alpha)_n G - U_L(t_p - t_a) \tag{12}$$

Equating eqs (1) and (12) and solving for t_p

$$t_p = F_R (t_{fi} - t_a) + \frac{K_{\alpha\tau}(\tau\alpha)_n G}{U_L} (1 - F_R) + t_a \tag{13}$$

For a nonirradiated solar collector, eq (13) reduces to

$$t_{pn} = F_R (t_{fi} - t_{a\ell}) + t_{a\ell} \tag{14}$$

where t_{pn} is the mean plate temperature of a nonirradiated collector. The above equations can be used to calculate the necessary thermal output of a heat source used in series with a nonirradiated array.

Consider a conventional heat source located downstream of a single nonirradiated solar collector, as shown in figure 1. In order for the net thermal output of a nonirradiated solar collector and heat source to be equivalent to the output of a normally irradiated array, the following is required

$$\frac{\dot{Q}_{hs}}{A_a} - U_L (t_{pn} - t_{a\ell}) = K_{\alpha\tau} F_R(\tau\alpha)_n G - F_R U_L (t_{fi} - t_a) \tag{15}$$

The left side of eq (15) represents the net energy output from the collector simulator. The right side of eq (15) represents the net output that would occur from an irradiated array. Since the heat source is downstream of the nonirradiated array, the inlet fluid temperature to the nonirradiated array is identical to the inlet fluid temperature for the corresponding irradiated array. Consequently, eq (14) can be introduced into the left side of eq (15) and the resulting equation solved for Q_{hs}

$$\dot{Q}_{hs} = K_{\alpha\tau} \frac{A_a}{A_g} F_R (\tau\alpha)_n G A_g - \frac{A_a}{A_g} F_R U_L (t_{a\ell} - t_a) A_g \tag{16}$$

Another possibility is to locate the conventional heat source upstream of the nonirradiated collector as depicted in figure 2. Equating the net energy output from the nonirradiated collector with upstream heat source to that of an irradiated collector yields

$$\frac{\dot{Q}^*_{hs}}{A_a} - U_L(t^*_{pn} - t_{a\ell}) = K_{\alpha\tau} F_R(\tau\alpha)_n G - F_R U_L (t_{fi} - t_a) \tag{17}$$

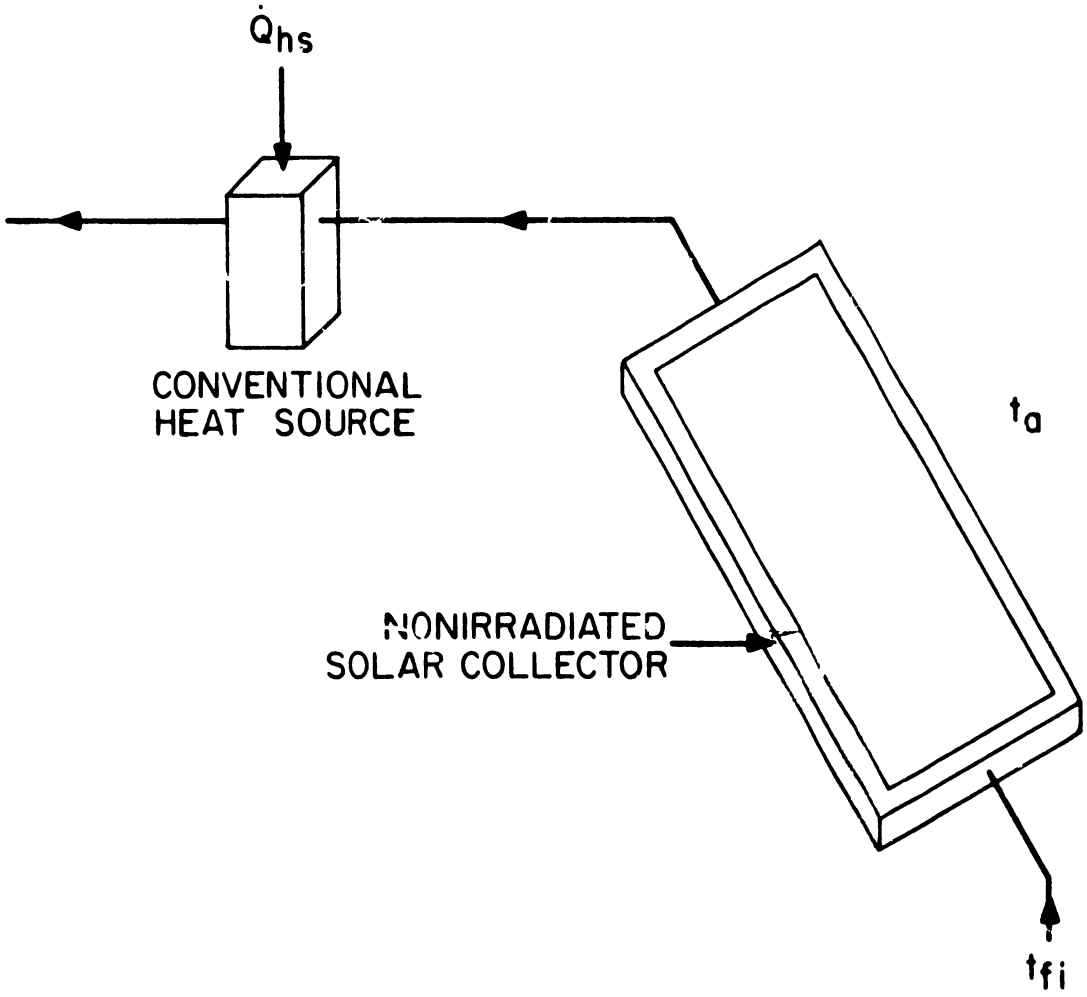

Figure 1. Nonirradiated solar collector with downstream conventional energy source

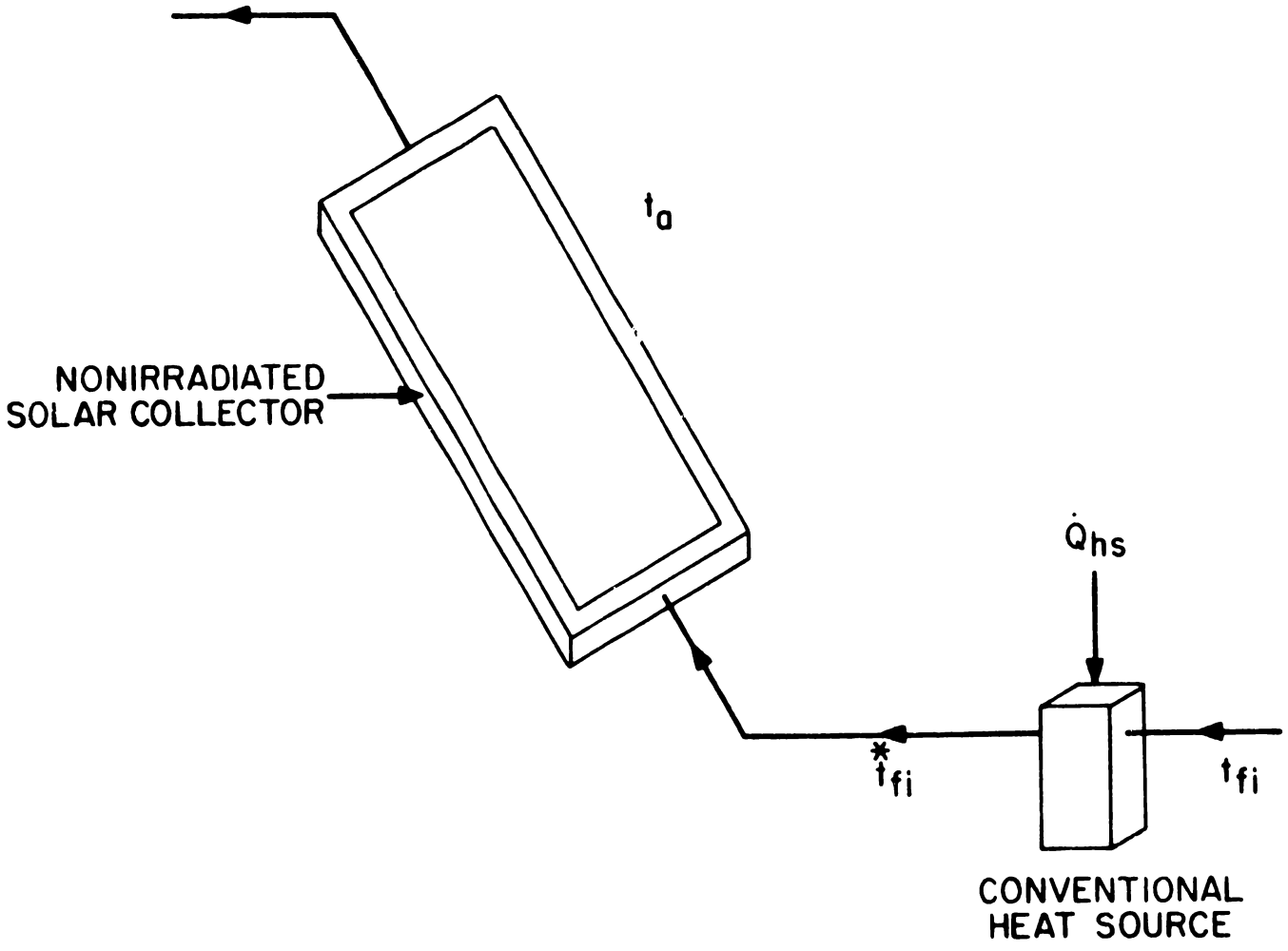

Figure 2. Nonirradiated solar collector with upstream conventional energy source

The asterisk indicates that t_{pn} is different from the previous case because the collector loop heater is now upstream of the irradiated collector. Equation (14) is still valid except that the inlet fluid temperature to the nonirradiated collector array is different from the previous case as a result of the electric heat source location

$$t^*_{pn} = F_R\,(t^*_{fi} - t_{a\ell}) + t_{a\ell} \tag{18}$$

An energy balance on the heat source results in the following expression for the exit fluid temperature from the heater in terms of the inlet fluid temperature to the heater

$$t^*_{fi} = t_{fi} + \frac{\dot{Q}_{hs}}{mC_p} \tag{19}$$

Solving eqs (17), (18), and (19) simultaneously

$$\dot{Q}_{hs} = \frac{K_{\alpha\tau}\frac{A_a}{A_g} F_R(\tau\alpha)_n\, G\, A_g - \frac{A_a}{A_g}(F_RU_L)\,(t_{a\ell} - t_a)\,A_g}{1 - \frac{\frac{A_a}{A_g} F_RU_LA_g}{\dot{m}C_p}} \tag{20}$$

This analysis is readily extended to combinations of M parallel rows of N collectors connected in series as shown in figure 3. Consider the situation where there are M collectors connected in parallel and no collectors connected in series, (N=1). Equation (16) becomes

$$\dot{Q}_{hs} = K_{\alpha\tau}\frac{A_a}{A_g} F_R(\tau\alpha)_n\, GMA_g - \frac{A_a}{A_g} F_RU_L\,(t_{a\ell} - t_a)\,MA_g \tag{21}$$

and eq (20) becomes

$$\dot{Q}_{hs} = \frac{K_{\alpha\tau}\frac{A_a}{A_g} F_R(\tau\alpha)_n\, GMA_g - \frac{A_a}{A_g}(F_RU_L)\,(t_{a\ell} - t_a)MA_g}{1 - \frac{\frac{A_a}{A_g} F_RU_LMA_g}{\dot{m}C_p}} \tag{22}$$

Collectors connected in series require that the heat removal factor, F_R, be modified according to eqs (8) and (9). Therefore, in the most general case where the heat source is located downstream of M rows of N collectors connected in series,

$$\dot{Q}_{hs} = K_{\alpha\tau}\frac{A_a}{A_g}(F_R(\tau\alpha)_n)_N\, GMNA_g - \frac{A_a}{A_g}(F_RU_L)_N(t_{a\ell} - t_a)\,MNA_g \tag{23}$$

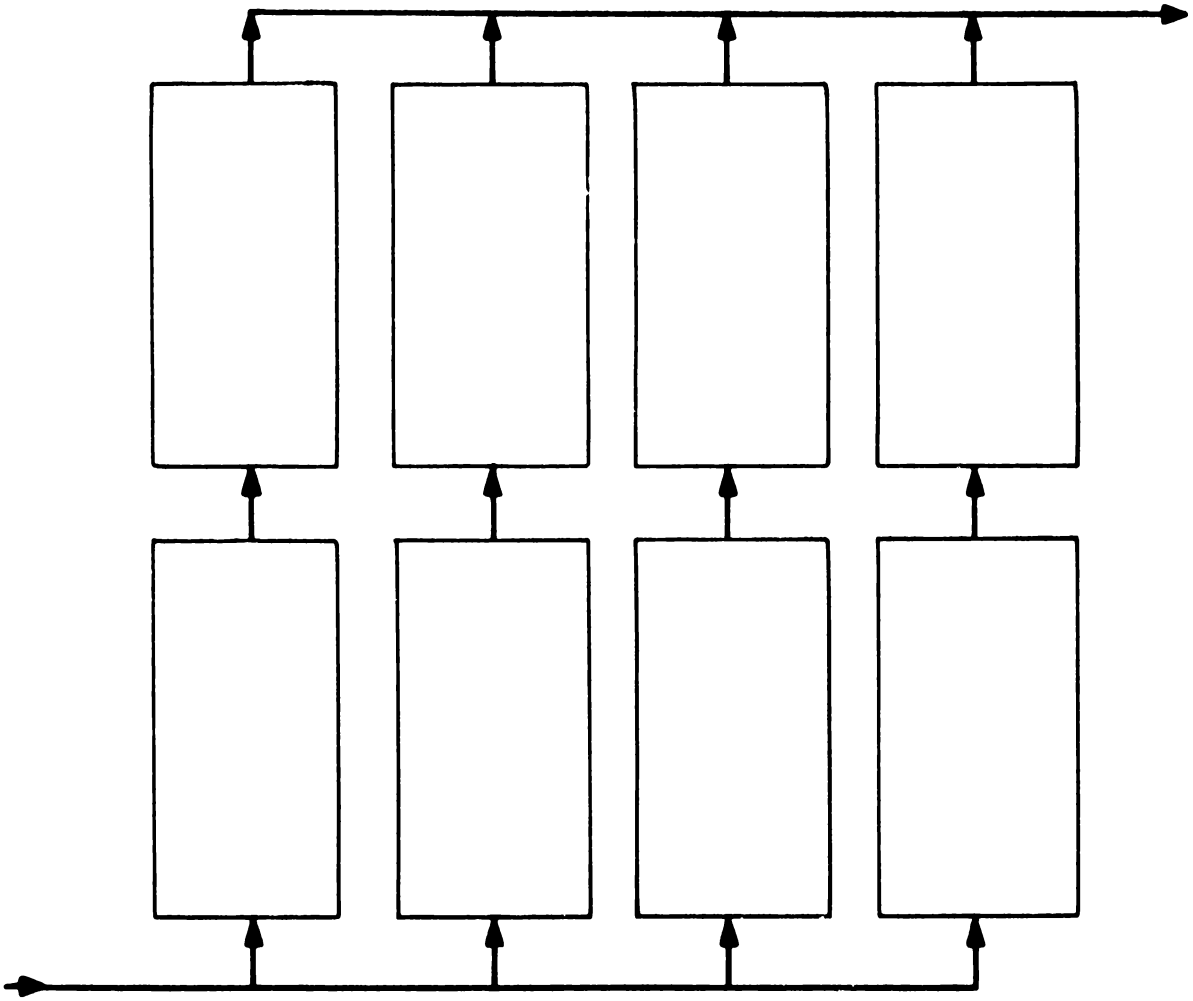

Figure 3. M parallel rows of N collectors connected in series

With the heat source located upstream of M rows of N collectors connected in series, eq (22) becomes

$$\dot{Q}_{hs} = \frac{K_{\alpha\tau}\frac{A_a}{A_g}(F_R(\tau\alpha)_n)_N\, GMNA_g - \frac{A_a}{A_g}(F_RU_L)_N(t_{a\ell} - t_a)MNA_g}{1 - \frac{\frac{A_a}{A_g}(F_RU_L)_N\, MNA_g}{\dot{m}C_p}} \tag{24}$$

Therefore, the proper quantity of energy to be supplied to a conventional heat source in series with a nonirradiated array may be computed using eq (23) or eq (24).

2.4 REPLACEMENT OF AN IRRADIATED ARRAY WITH STRIP HEATERS ATTACHED TO NONIRRADIATED SOLAR COLLECTORS

Solar energy absorbed by an irradiated collector array is replaced by energy supplied by electric strip heaters attached to the back of nonirradiated absorber plates. The quantity of solar energy absorbed by the absorber plate of a single collector is

$$S = A_a\, K_{\alpha\tau}\, (\tau\alpha)_n\, G \tag{25}$$

Thus, the amount of energy to be supplied by the strip heaters can be expressed as

$$Q_{sh} = MNA_a\, K_{\alpha\tau}\, (\tau\alpha)_n\, G \tag{26}$$

Simulation of a collector array consisting of M parallel rows of N collectors connected in series requires that

$$\dot{Q}_{sh} = MNA_a\, K_{\alpha\tau}\, (\tau\alpha)_n\, G \tag{27}$$

Input values of energy into the strip heaters are calculated using the prescribed radiation values, G, and the optical characteristics of the collectors. Thus, if the values of $(\tau\alpha)_n$ and $K_{\alpha\tau}$ are known, an ASHRAE 93-77 test is not required.

2.5 SOLAR DOMESTIC HOT WATER SYSTEM MODEL DEVELOPMENT

An analytical model has been developed for a solar domestic hot water system. A discussion of each model component follows.

2.5.1 Solar Collectors

The collector model is based on the Hottel-Whillier-Bliss (H-W-B) analysis. The following summary of analytical expressions for a single-cover flat-plate collector is directly from reference 11.

Collector efficiency (based on net area) is given by

$$\eta = \frac{\dot{Q}_u}{G\ A_a} \times 100\% \tag{28}$$

where G is the total solar irradiance on the outer surface of the cover. The useful energy, $\dot{Q}_u$, is given by

$$\dot{Q}_u = A_a F_R \{K_{\alpha\tau} (\tau\alpha)_n G - U_L [t_{fi} - t_a]\} \tag{29}$$

The loss coefficient, U_L, is the sum of the top loss coefficient U_t and the back (and edge) loss coefficient U_b. An initial estimate of the back conductance U_b is

$$U_b = \frac{k_i}{L_i} + \frac{k_e A_e}{L_e A_a} \tag{30}$$

The expressions and procedure for determining U_t are given in Appendix B. Since U_t depends on the mean absorber plate temperature, the following expression is used in an iterative approach

$$t_p = F_R [t_{fi} - t_a + K_{\alpha\tau} (\tau\alpha)_n G/U_L] + t_a - K_{\alpha\tau} (\tau\alpha)_n G/U_L \tag{31}$$

It should be noted that, in the H-W-B analysis, U_L is assumed constant over the temperature range $t_p(0)$ to $t_p(L)$ and accounts for heat losses by convection and longwave radiation. The expression for the collector flow factor F_R depends on the flow tube-absorber plate configuration. The tube-plate configuration is reflected in the expressions for the efficiency factor F' which accounts for tubes below, above, and integral with the plate. The values of F' for these three configurations differ only if the thermal bond between the tube and plate is poor. Since the bond resistance is negligible for the collectors under consideration, the expression for the efficiency factor is taken as

$$F' = \frac{1}{\frac{WU_L}{P_w h_f} + \frac{W}{D + [W-D]F}} \tag{32}$$

where

$$F = \frac{\tanh (m[W-D]/2)}{m\ [W-D]/2} \tag{33}$$

$$m = (U_L/[k_p \delta])^{1/2} \tag{34}$$

For the parallel-flow collectors which are being modeled,

$$F_R = [\dot{G}C_p/U_L] [1 - \exp (-F'U_L/\{\dot{G}C_p\})] \tag{35}$$

and

$$t_{fm} = [F_R/F'] [t_{fi} - t_a + K_{\alpha\tau} (\tau\alpha)_n G/U_L] + K_{\alpha\tau} (\tau\alpha)_n G/U_L \quad (36)$$

The heat transfer coefficient, h_f, calculated using the procedure outlined in Appendix B, is based on the mean fluid temperature which is determined by using eq (36) in an iterative procedure.

The algorithm for calculating the thermal performance of a collector is organized as follows:

Step 1. The operating conditions, design parameters and heat transfer properties, and fluid inlet temperature are specified.

Step 2. Collector and material parameters which do not vary with temperature are calculated. An initial estimate of t_p, in terms of t_{fi}, is made.

Step 3. With the current estimate of t_p, the heat loss through the cover assembly and U_t are determined (in a subroutine). Next, U_L and F_R are calculated. An estimate of t_{fm}, in terms of t_p, is made.

Step 4. With the current estimate for t_{fm}, h_f is calculated in a separate subroutine using a supporting fluids properties routine. The factors F' and F_R are calculated from eqs (32) and (35) to obtain an improved estimate of t_{fm}, and Step 4 is repeated until t_{fm} converges.

Step 5. Equation (31) is used to improve the estimate of t_p. Steps 3, 4, and 5 are repeated in an iterative procedure until t_p converges.

Step 6. The outputs $\dot{Q}_u$ and η are calculated from eqs (29) and (28), respectively, along with other parameters of interest.

2.5.2 Storage Tank

A one-dimensional heat transfer analysis is performed on the storage tank in the manner outlined in reference 12. The tank is divided vertically into N elements as illustrated in figure 4. An energy balance on the element i yields the following differential equation

$$(\rho C_p V)_i \frac{\partial t_i}{\partial \tau} = (\dot{m} C_p)_i \Delta y_i \frac{\partial t_i}{\partial y} + k A_c \Delta y_i \frac{\partial^2 t_i}{\partial y^2} \quad (37)$$

$$- U_{LT} \Delta A_{si} (t_i - t_{a\ell}) + \dot{Q}$$

The left hand side of eq (37) represents the increase in the internal energy of the element. The first term on the right hand side represents the convective heat transfer within the tank, the second term heat transfer due to conduction, the third term heat loss to the surroundings, and the fourth term external energy addition to the element. The conduction term was found to be negligible and is ignored in this analysis. Thus eq (37) becomes

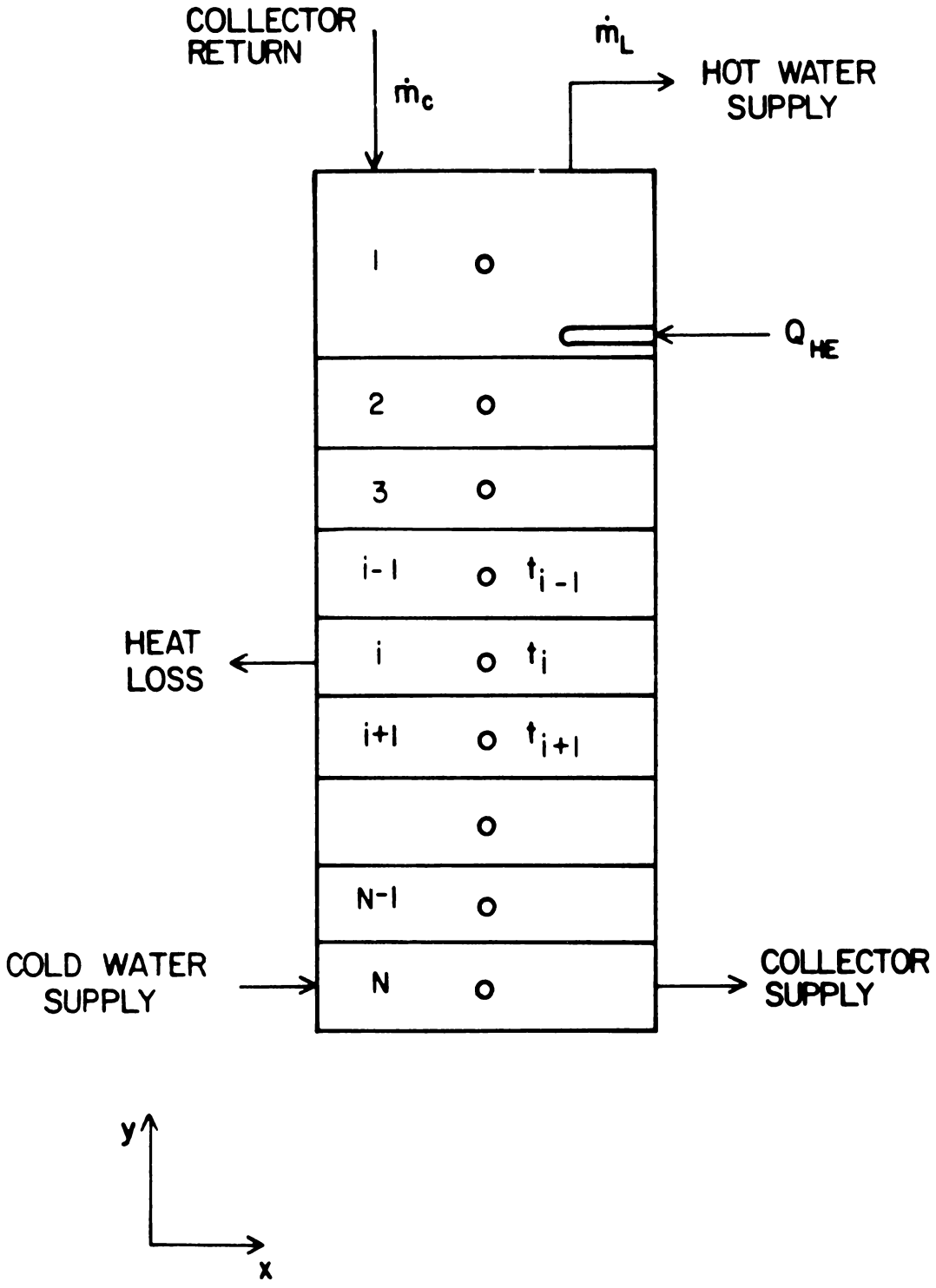

Figure 4. Solar storage tank model

$$(\rho C_p V)_i \frac{\partial t_i}{\partial \tau} = (\dot{m}C_p)_i \Delta y_i \frac{\partial t_i}{\partial y} - U_{LT}\ \Delta A_{si}\ (t_i - t_{a\ell}) + \dot{Q} \tag{38}$$

Expressing the partial derivatives in eq (38) in terms of finite difference approximations results in the following finite-difference equation

$$(\rho C_p V)_i \frac{t_i^{n} - t_i}{\Delta \tau} = (\dot{m}C_p)_i\ \Delta y_i \frac{t_{i+1} - t_i}{\Delta y_i} - U_{LT} \Delta A_{si}\ (t_i - t_{a\ell}) + \dot{Q} \tag{39}$$

The volume of the i^{th} node may be expressed as

$$V_i = \Delta y_i\ A_c \tag{40}$$

where A_c is the cross-sectional area of the tank.

Substitution of eq (40) into eq (39) gives

$$(\rho C_p A_c\ \Delta y)_i \frac{t_i^{n} - t_i}{\Delta \tau} = (\dot{m}\ C_p)_i\ \Delta y_i \frac{t_{i+1} - t_i}{\Delta y_i} - U_{LT}\ \Delta A_{si}\ (t_i - t_{a\ell}) + \dot{Q} \tag{41}$$

Mass flow rate through a node can be expressed as the sum of two components,

$$\dot{m}_i = (\dot{m}_L - \dot{m}_c)_i \tag{42}$$

where $\dot{m}_c$ is the mass flow rate circulating through the collector array, and $\dot{m}_L$ is the hot water load mass flow rate. Substitution of eq (42) into (41) and subsequent rearrangement yields the general equation

$$(\dot{m}C_p)_c \frac{(t_i - t_{i-1})}{\Delta y_i} + (\dot{m}C_p)_L \frac{(t_{i+1} - t_i)}{\Delta y_i} - U_{LT} \Delta A_{si} \frac{(t_i - t_{a\ell})}{\Delta y_i} + \frac{\dot{Q}}{\Delta y_i} \tag{43}$$

$$= (\rho C_p A_c)_i \frac{t_i^{n} - t_i}{\Delta \tau}$$

This generalized analysis is applied to the particular storage tank used in this investigation. A thermostatically controlled electric heating element located in the storage tank maintains the water above it within a specified temperature range. Hot water is withdrawn from the tank upper node, i = 1, and makeup water enters the bottom node, i = N. Supply water to the collector array is withdrawn from the bottom node. It is assumed that the returning heated water enters the tank at a location such that

$$t_{i-1} \geq t_R > t_i \tag{44}$$

where t_R is the temperature of the returning fluid as it enters the storage tank.

Applying eq (43) to the upper portion of the storage tank, i = 1, yields

$$(\dot{m}C_p)_c\ F_1^c\ (t_R - t_1) + (\dot{m}C_p)_L\ (t_2 - t_1) - U_{LT}\Delta A_{si}\ (t_1 - t_{a\ell}) + J\dot{Q}_{HE} = (\rho C_p V)_1 \frac{t_1^n - t_1}{\Delta\tau} \tag{45}$$

where F^c and J are control logic functions.

The collector control function for this node is defined as

$$F_1^c = \begin{cases} 1 \text{ if } t_R \geq t_1 \\ 0 \text{ if } t_R < t_1 \end{cases} \tag{46}$$

The heating control element function is defined as

$$J = \begin{cases} 1 \text{ if } t_1 < t_L \\ 0 \text{ if } t_1 > t_H \end{cases} \tag{47}$$

where t_L and t_H are the "turn-on" and "turn-off" temperature levels of the thermostat. Applying eq (43) to nodes 2 through N-1 results in

$$(\dot{m}C_p)_c\ F_i^c\ (t_R - t_i) + (\dot{m}C_p)_c\ L_i^c\ (t_{i-1} - t_i) + (\dot{m}C_p)_L\ (t_{i+1} - t_i) - U_{LT}\Delta A_{si}(t_i - t_{a\ell}) = (\rho C_p V)_i \frac{t_i^n - t_i}{\Delta\tau} \tag{48}$$

The control logic functions are

$$F_i^c = \begin{cases} 1 \text{ if } t_{i-1} \geq t_R > t_i \\ 0 \text{ otherwise} \end{cases} \tag{49}$$

and

$$L_i^c = \begin{cases} 1 \text{ if } t_R > t_{i-1} \\ 0 \text{ otherwise} \end{cases} \tag{50}$$

Applying eq (43) to the bottom node of the tank, i = N, yields

$$(\dot{m}C_p)_c \; F_N^c \; (t_R - t_N) + (\dot{m}C_p)_c \; L_N^c (t_{N-1} - t_N) + (\dot{m}C_p)_L \; (t_{MW} - t_N)$$

$$- U_{LT} \Delta A_{SN} \; (t_N - t_{a\ell}) = (\rho C_p V)_N \frac{t_N^n - t_N}{\Delta\tau} \tag{51}$$

where the control logic functions are

$$F_N^c = \begin{cases} 1 \text{ if } t_{N-1} \geq t_R > t_N \\ \\ 0 \text{ otherwise} \end{cases} \tag{52}$$

and

$$L_N^c = \begin{cases} 1 \text{ if } t_R > t_{N-1} \\ \\ 0 \text{ otherwise} \end{cases} \tag{53}$$

Modeling of the entire storage tank is achieved with the system of equations developed above.

2.5.3 Heat Source

The solar domestic hot water system model includes subroutines which allow the modeling of a hot water system where the irradiated array has been replaced with an electric heat source or an electric heat source used in series with a nonirradiated array. This section deals with the analytical model for the heat source.

Energy supplied to a conventional heat source used in series with nonirradiated collectors is computed using eq (23) or eq (24). An energy balance for the heat source under steady-state conditions yields

$$\dot{Q}_{hs} = \dot{m}C_p \; (t_{ho} - t_{hi}) + (UA)_{hs} \; (\bar{t}_h - t_{a\ell}) \tag{54}$$

where

$$\bar{t}_h = \frac{t_{hi} + t_{ho}}{2} \tag{55}$$

Defining the efficiency of a heat source as

$$\eta_{hs} = \frac{\dot{m}C_p \; (t_{ho} - t_{hi})}{\dot{Q}_{hs}} \tag{56}$$

gives

$$t_{ho} = \frac{\eta_{hs} Q_{hs}}{\dot{m} C_p} + t_{hi} \tag{57}$$

where $\eta_{hs} = 1$ corresponds to an adiabatic heat source. The product $(UA)_{hs}$ was determined experimentally. Equation (57) is used in the simulation model for t_{ho}.

2.5.4 Pipe Thermal Losses

The model accounts for heat losses from the collector array supply and return pipes. The supply pipe is divided into two sections, indoors and outdoors, for the heat loss analysis. Thermal losses for the section located within the test facility may be expressed as

$$\dot{Q}_{SI} = (UA)_{SI} \Delta t_m \tag{58}$$

The log-mean temperature difference is defined as

$$\Delta t_m = \frac{(t_{sw} - t_{a\ell}) - (t_N - t_{a\ell})}{\ln\left[\frac{t_{sw} - t_{a\ell}}{t_N - t_{a\ell}}\right]} \tag{59}$$

Substitution of eq (59) into eq (58) yields

$$\dot{Q}_{SI} = (UA)_{SI} \frac{t_{sw} - t_N}{\ln\left[\frac{t_{sw} - t_{a\ell}}{t_N - t_{a\ell}}\right]} \tag{60}$$

The thermal losses may also be expressed as

$$\dot{Q}_{SI} = \dot{m} C_p (t_N - t_{sw}) \tag{61}$$

Combining eqs (60) and (61) yields

$$t_{sw} = t_{a\ell} + (t_N - t_{a\ell}) \exp\left(-\frac{(UA)_{SI}}{\dot{m} C_p}\right) \tag{62}$$

Equation (62) predicts the supply fluid temperature as it leaves the interior of the test facility. With this temperature, the temperature entering the solar collector array is predicted in an identical manner, i.e.

$$t_{fi} = t_a + (t_{sw} - t_a) \exp\left(-\frac{(UA)_{SO}}{\dot{m} C_p}\right) \tag{63}$$

Substitution of eq (62) into eq (63) allows the collector array inlet fluid temperature to be calculated in terms of the fluid temperature entering the pipe and the indoor and outdoor surrounding ambient temperatures. Thus,

$$t_{fi} = t_a \left[1 - \exp\left(-\frac{(UA)_{SO}}{\dot{m}C_p}\right)\right] + t_N \exp\left(-\left(\frac{(UA)_{SI} + (UA)_{SO}}{\dot{m}C_p}\right)\right) + t_{a\ell}\left[\exp\left(-\frac{(UA)_{SO}}{\dot{m}C_p}\right)\left[1 - \exp\left(-\frac{(UA)_{SI}}{\dot{m}C_p}\right)\right]\right] \quad (64)$$

The return pipe from the outlet of the solar collector array to the storage tank also experiences heat loss. The fluid temperature returning to the storage tank can be expressed in terms of the exit fluid temperature of the array and the interior and exterior ambient temperatures

$$t_R = t_{a\ell}\left[1 - \exp\left(-\frac{(UA)_{RI}}{\dot{m}C_p}\right)\right] + t_{co}\left[\exp\left(-\frac{(UA)_{RO} + (UA)_{RI}}{\dot{m}C_p}\right)\right] + t_a\left[\exp\left(-\frac{(UA)_{RI}}{\dot{m}C_p}\right)\left[1 - \exp\left(-\frac{(UA)_{RO}}{\dot{m}C_p}\right)\right]\right] \quad (65)$$

The overall heat loss coefficients used were calculated using the measured length and diameter of each section, the thickness of the insulating material, and the values of thermal conductivity as supplied by the manufacturer. The use of an electric heat source upstream or downstream of the nonirradiated array introduces a small amount of additional interconnecting pipe. However, calculations show that the additional thermal pipe losses are negligible.

2.5.5 Computation Sequence For An Irradiated System

The various component models discussed above, in conjunction with recorded meteorological data, allow simulation of the solar domestic hot water system. Solar collector, storage tank, and piping model components are used when simulating an irradiated system. Nodes within the storage tank are set to an initial temperature. Collector array flow rate and circulator pump status recorded during operation of the actual system are supplied to the model. Equation (64) predicts the fluid temperature entering the collector array using recorded indoor and outdoor ambient temperatures. The collector model, using measured meteorological data, calculates the fluid temperature leaving the array. The fluid temperature entering the tank is predicted using eq (65). Storage tank nodal temperatures are recalculated every minute with eqs (45), (48), and (51).

In the actual system, a hot water withdrawal occurs at specific time intervals. This situation is simulated as follows

$$Q_L = \sum_{j=1}^{n} (\dot{m}_L C_p (t_1 - t_{mw}))_j \Delta\tau \quad (66)$$

Values of $\dot{m}_L$ and n are selected such that the amount of energy extracted is equivalent to that withdrawn from the actual system.

The computer model predicts the auxiliary energy needed to maintain the upper node of the storage tank within the control temperature range of the thermostat. Daily energy consumption may be expressed as

$$Q_{HE} = \sum_{j=1}^{L} J_j \dot{Q}_{HE} \Delta\tau \tag{67}$$

For comparison with experimental data, the quantity of energy transferred from the solar collector array to the storage tank is calculated using the computer model. The daily thermal output of the irradiated collector array may be calculated as

$$Q_{SA} = \sum_{j=1}^{L} (\dot{m}C_p (t_{co} - t_{fi}))_j \Delta\tau \tag{68}$$

Energy supplied to the storage tank may be expressed as

$$Q_T = \sum_{j=1}^{L} (\dot{m}C_p (t_R - t_N))_j \Delta\tau \tag{69}$$

Subtraction of eq (69) from eq (68) yields the amount of energy lost during transport to and from the collector array. The change in stored energy within the storage tank during the simulation period is

$$Q_{ST} = \sum_{i=1}^{N} (M_i C_p t_i)_{\tau = L\Delta\tau} - \sum_{i=1}^{N} (M_i C_p t_i)_{\tau = 0} \tag{70}$$

Once the above quantities have been predicted, the daily performance of the solar system is compared to that of a conventional system. An energy balance performed on a conventional system yields

$$Q_{CON} = Q_L + HL_{CON} + CL_{CON} + Q_{ST} \tag{71}$$

For an electric hot water heater, $CL_{CON} = 0$, and eq (71) reduces to

$$Q_{CON} = Q_L + HL_{CON} + Q_{ST} \tag{72}$$

A comparison between the performance of a solar hot water system and that of a conventional system meeting the same load requirements is possible by defining a parameter called the "fractional energy savings," i.e.

$$e = 1 - \frac{Q_{HE}}{Q_{CON}} \tag{73}$$

The rationale behind this definition is as follows. If the solar system met the required load with no auxiliary energy required, $Q_{HE} = 0$, the fractional energy savings would be 1.0. If the same amount of energy is required to operate the solar system as the conventional system, the fractional energy savings would be zero.

2.5.6 Computation Sequence For A Nonirradiated System in Series With A Conventional Heat Source

The computer model can accommodate a heat source located upstream or downstream of a nonirradiated solar collector array. The fluid temperature entering the heat source is predicted using the storage tank and pipe component models when the heat source is upstream of a nonirradiated array. Fluid temperature leaving the heat source is predicted using eq (57). This temperature is subsequently supplied to the collector model in which the incident radiation has been set to zero. The remainder of the system simulation is identical to that for an irradiated system. When the heat source is downstream of the nonirradiated array, the tank and pipe component models predict the entrance temperature to the nonirradiated array. The predicted collector outlet temperature is used to calculate the heat source outlet temperature. The remainder of the system simulation is again identical to that described earlier.

2.5.7 Computation Sequence For Nonirradiated Collectors With Attached Strip Heaters

The computation sequence is identical to that for an irradiated system. However, the collector component model must be modified slightly. Under irradiated conditions the collector model computes the amount of energy absorbed by the absorber plate using the known incident radiation conditions and the optical properties of the cover system. The calculation is not required when modeling collectors with strip heaters attached to the absorber plates. The absorbed energy is given directly by eq (27).

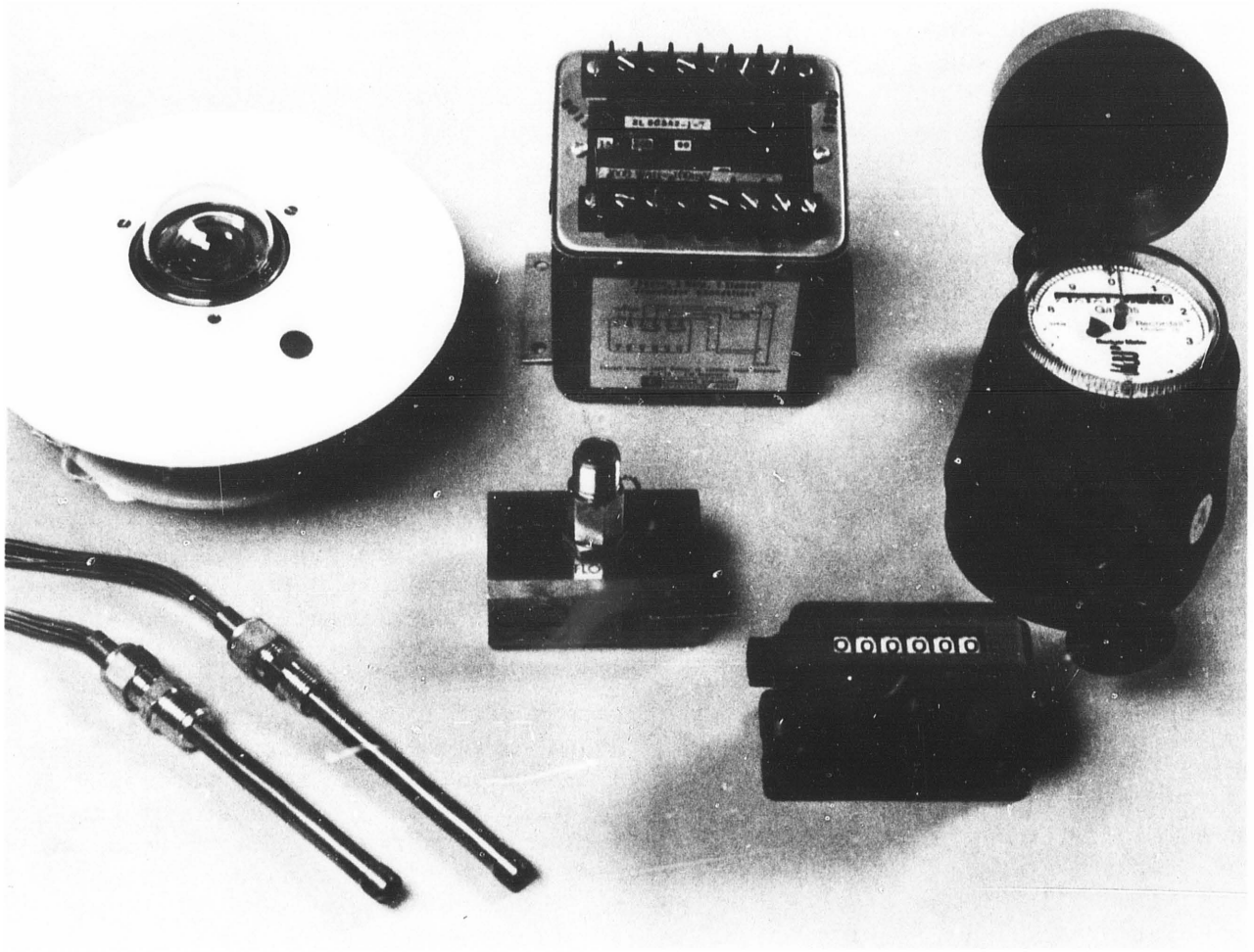

3. EXPERIMENTAL APPARATUS AND INSTRUMENTATION

A test facility has been fabricated at the National Bureau of Standards to aid in the development of a test method for solar hot water systems. Two solar domestic hot water systems are located within the test facility. The solar collector array of one system is subjected to outdoor meteorological conditions, while the second system uses a thermal simulator. Thermal simulation is achieved by using an electric heat source only, an electric heat source in series with nonirradiated collectors, or by attaching strip heaters to nonirradiated absorber plates. Instrumentation and data recording equipment for monitoring the thermal performance of each system and environmental conditions are included within the facility. A water conditioning loop supplies constant

temperature water to both systems. The test facility is located at Gaithersburg, Maryland, where the latitude is 39.1° and the longitude is 77.2°. Altitude of the facility is 130 m above sea level.

3.1 SOLAR HOT WATER SYSTEM WITH IRRADIATED COLLECTOR ARRAY

A schematic of the single-tank direct system with irradiated collectors is given in figure 5. This system consists of two solar collectors connected in parallel, one water storage tank, an "on-off" differential controller, circulating pumps, piping, and insulation. Two flat-plate, liquid-type collectors (as shown in figure 6), set at a 39° tilt angle, are used in this system. Collector dimensions and properties are summarized in Appendix C. A black chrome coating applied to the steel absorber plate enhances short wavelength (solar) radiation absorptance and reduces longwave (infrared) radiation losses. Silicone rubber pads thermally isolate the absorber plate from the galvanized sheet steel enclosure.

A State Industries conventional electric water heater, as shown in figure 7, is used for storage. This tank has a nominal 0.310 m^3 capacity and outside dimensions of 1.57 m in height by 0.61 m in diameter. The particular tank used in this experiment has a capacity of 0.290 m^3 and a working pressure of 1034 kPa. The inner surface of the tank is lined with vitrified glass to minimize corrosion. Glass fiber insulation, thickness 51 mm, surrounds the actual storage tank, which in turn is covered by a thin metal jacket. A temperature and pressure relief valve rated at 1034 kPA and 99 C is located at the top of the storage tank. The lower heating element was not used in this experiment. The upper heating element, located 1.27 m above the tank bottom, is a 208 volt, 3.5 kW, direct immersion heating element. The heating element is controlled by a thermostat which senses the temperature of the storage tank immediately above it.

A solid-state controller, Hawthorne Industry Model H-1504-A "Fixflow," activates the circulator pumps when an 8.9 C temperature difference exists between the collector sensor and the storage tank sensor. A temperature difference of less than 1.7 C deactivates the pumps. The temperature sensors are hermetically sealed thermistors. The collector thermistor senses the temperature of the copper outlet pipe at a distance of 38 mm external to the collector enclosure. The sensor is clamped to the outside surface of the pipe and covered with glass fiber insulation. The storage tank sensor is located on the exterior tank surface, underneath the insulation, at an elevation of 153 mm above the bottom of the tank.

Two Grundfos UPS 20-42 pumps connected in series circulate the water through the solar collector array. These two three-speed pumps in series with flow control valves provide the capability of varying the mass flow rate through the collector array. Performance characteristics, i.e., head vs flow rate, are given in figure 8. Isolation valves are installed on each side of the pumps to facilitate easy removal.

The water supply line to the storage tank consists of 12.7-mm-diameter hard copper tubing. The inlet water supply flows through a gate valve, an integrating volumetric meter, and a temperature-measuring well before entering the tank. A drain valve, located 92 mm above the bottom of the storage tank, was

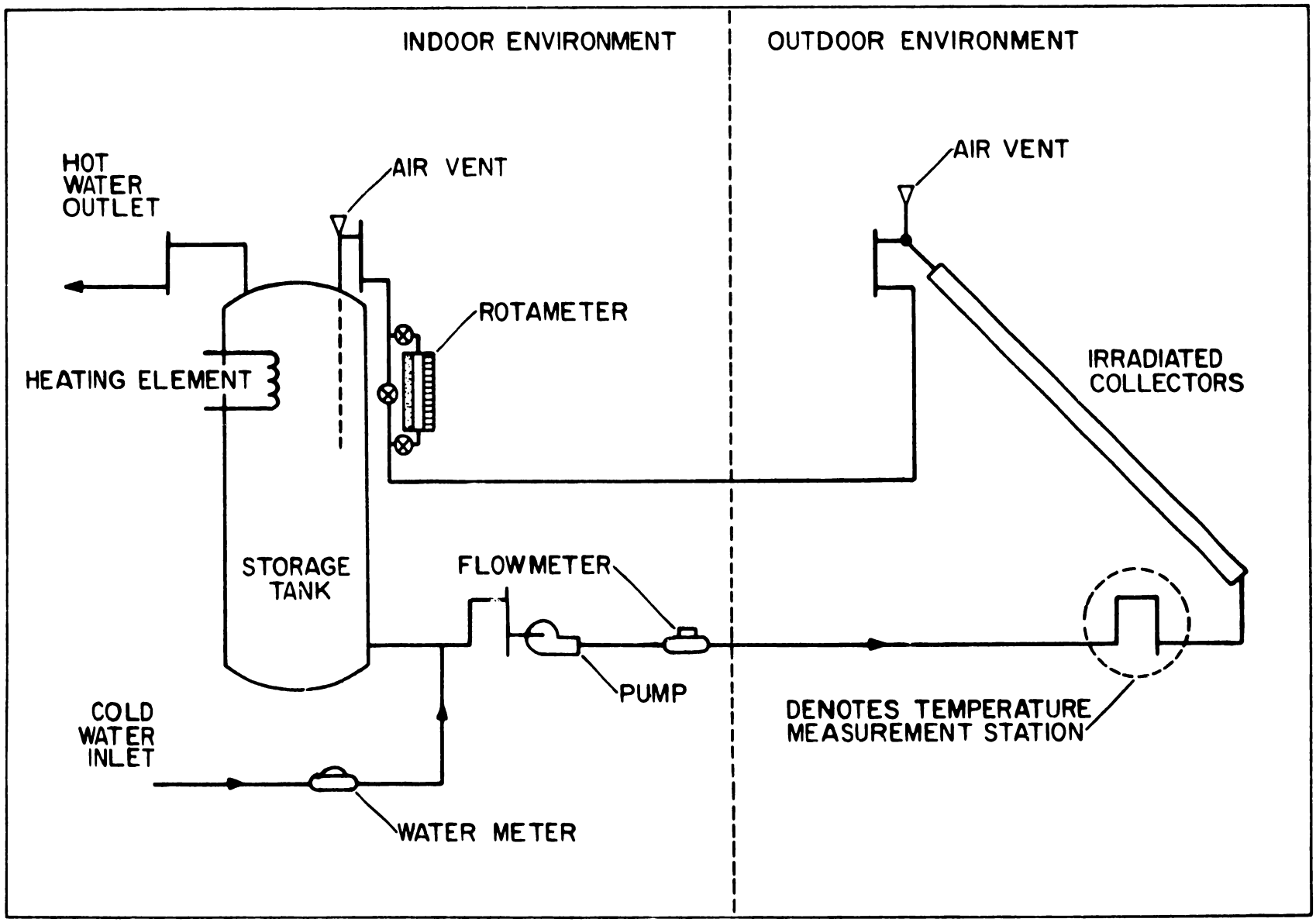

Figure 5. Single-tank direct system schematic

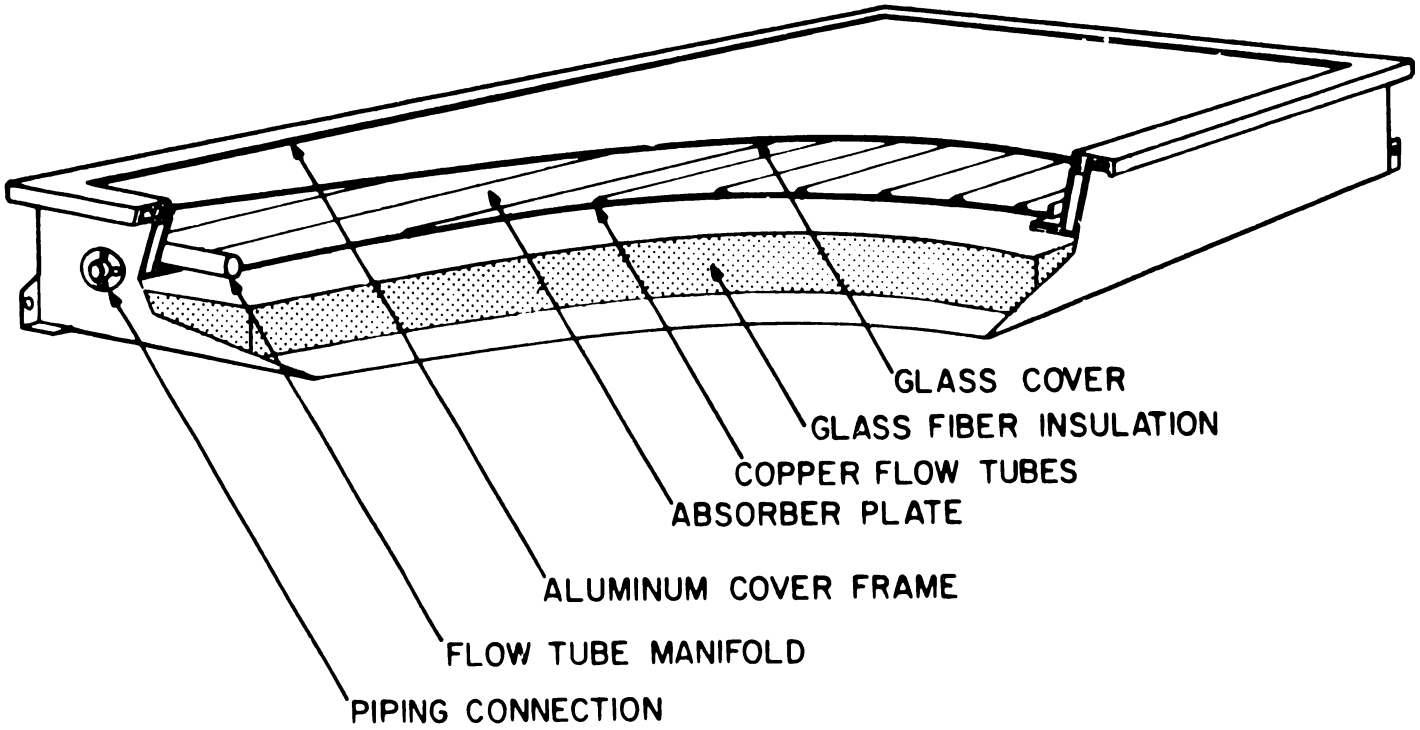

Figure 6. Flat-plate liquid collector

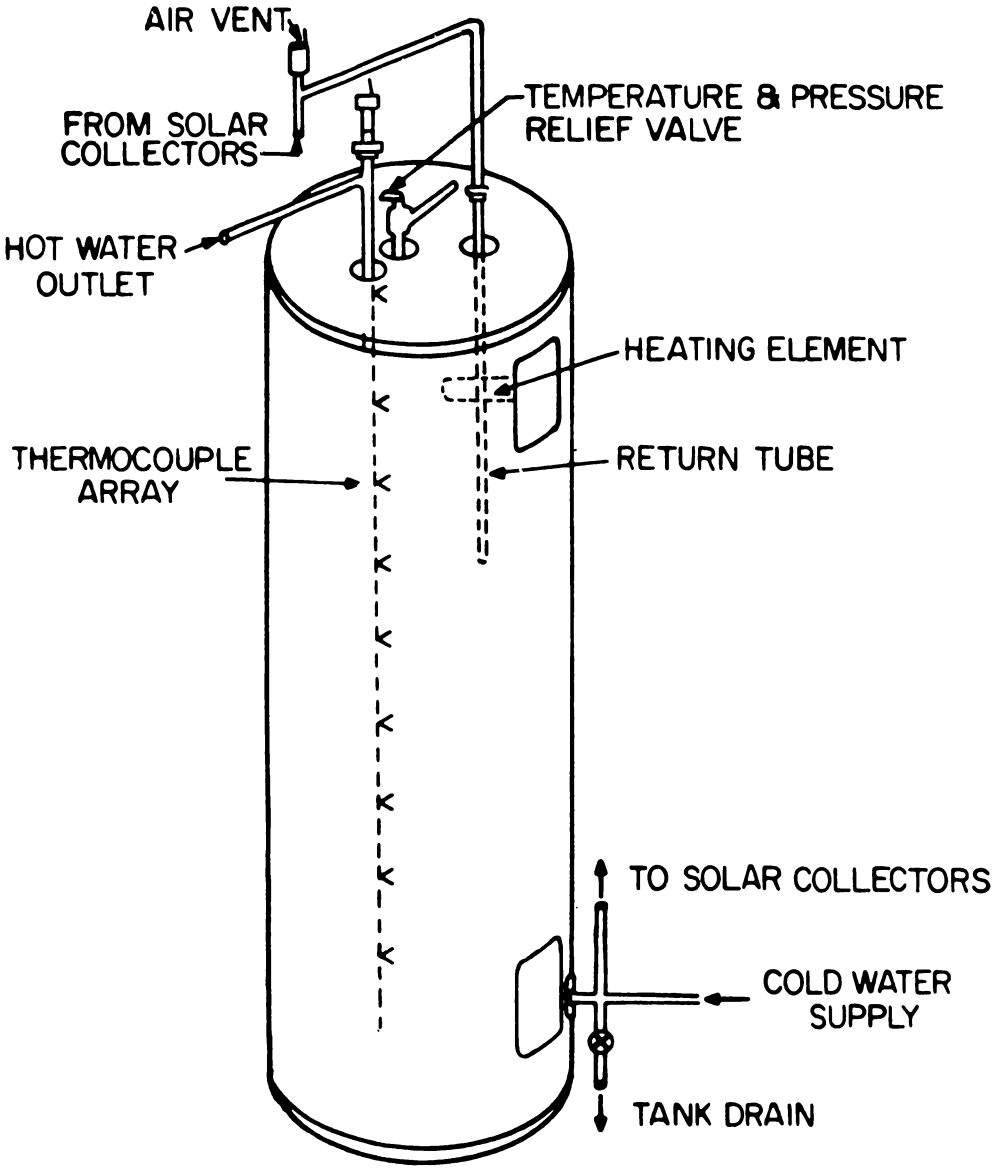

Figure 7. Hot water storage tank

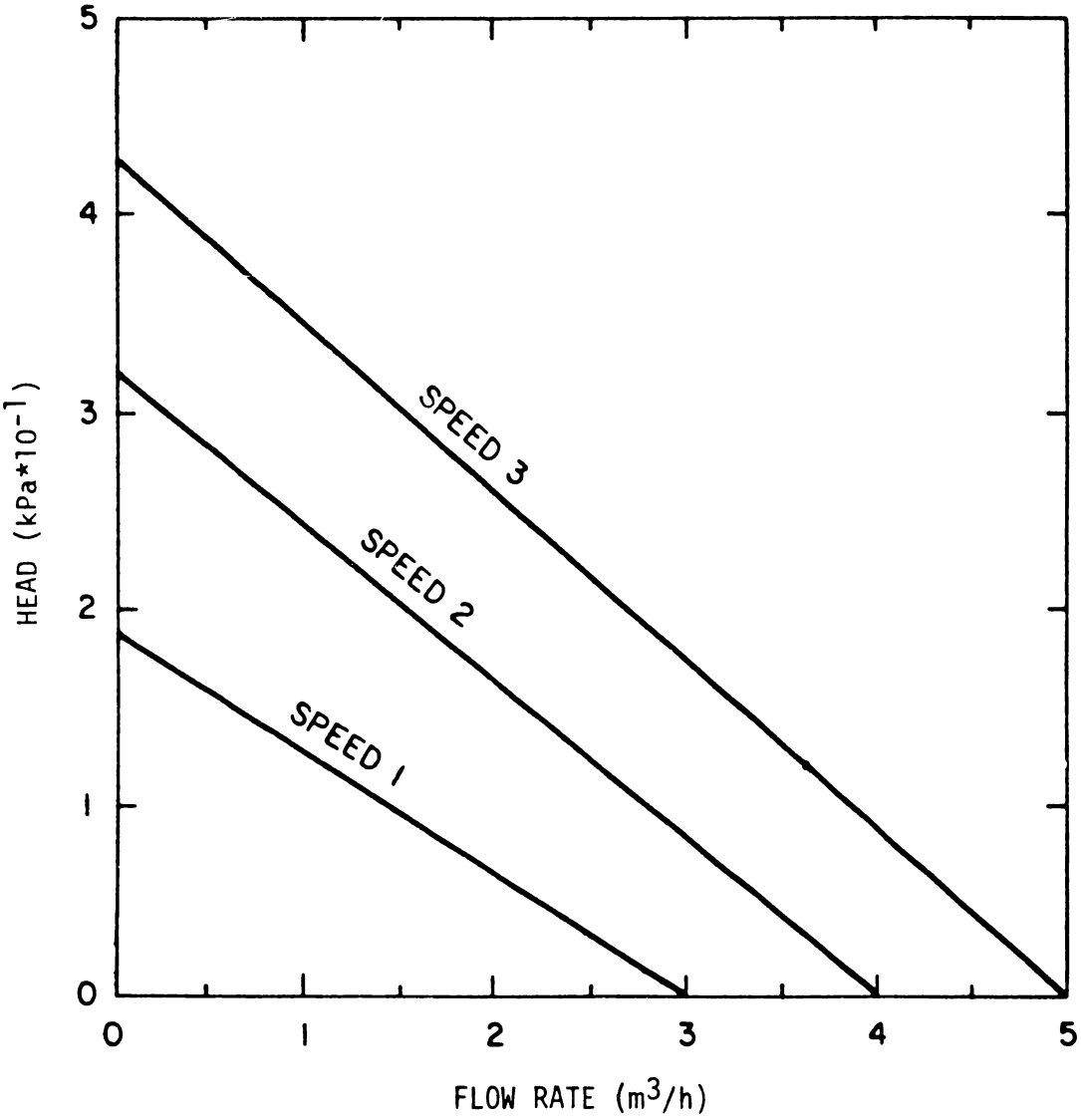

Figure 8. Circulator performance characteristics

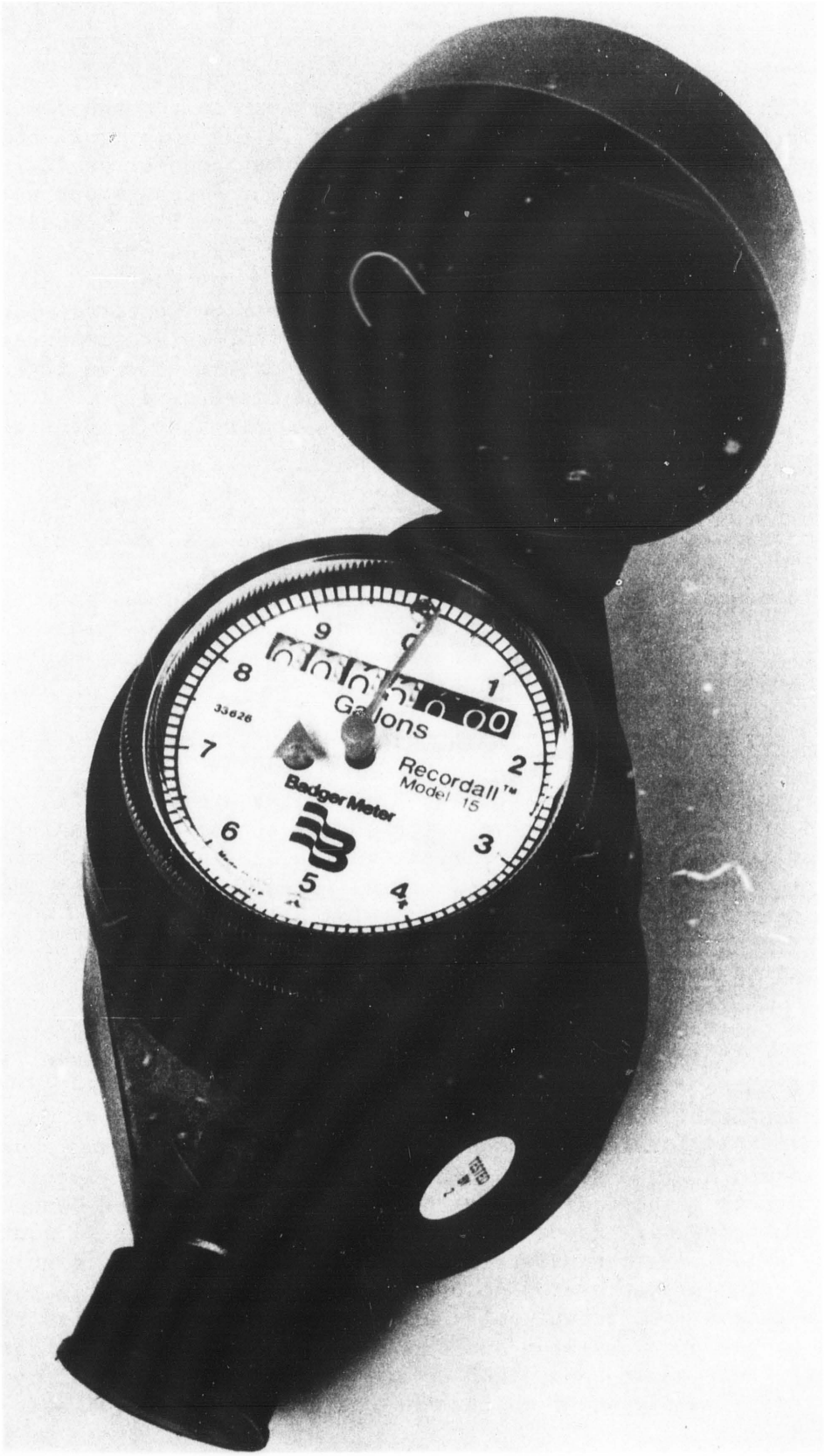

Integrating volumetric flowmeter used to monitor the quantity of hot water withdrawn from system

replaced with a tee fitting. The water supply enters through one port of the tee, while the second port supplies water to the solar collector array. The supply and return lines to the collector array consist of 12.7-mm-diameter copper tubing. The supply includes two temperature-measurement wells, one at the storage tank and one at the collector array, a turbine flowmeter, valves, and two Grundfos UPS 20-42 pumps. The two solar collectors are connected in parallel using 25.4-mm-diameter copper tubing. A reverse "Z" pattern (figure 9) is used in order to ensure equal flow through both collectors. The return line includes a check valve to prevent back flow, a temperature measurement well at the array, a rotameter, and a temperature well at the storage tank. The solar-heated water enters the tank through a 12.7-mm-diameter dip tube extending 597 mm from the upper storage tank surface. An air vent is provided at the top of the storage tank to release trapped air.

The hot water supplied from the storage tank passes by a temperature- easurement well a ıd through a needle valve before entering an open weigh tank.

Rubatex closed-cell insulation, 12.7 mm thickness, provides internal pipe insulation. Exterior insulation consists of 31.8-mm-thick glass fiber insulation covering the 12.7 mm piping, while 51.0 mm glass fiber insulation encases the 25.4-mm-diameter collector headers.

3.2 SOLAR HOT WATER SYSTEM WITH THERMALLY SIMULATED COLLECTOR ARRAY

All components of the indoor nonirradiated system are identical to those of the irradiated system discussed above, with the exception of the solar collector array. During this experimental investigation, three different techniques were used to supply the quantity of energy normally supplied by the irradiated array. A description of each is given below.

3.2.1 Electric Heat Source

This system (as shown in figure 10) employs an electric heat source to supply the net energy gain of a solar collector array. The heat source (figure 11) consists of three Chromalox Immersion Heaters. Each immersion heater, having a maximum capacity of 1 kW, is encased within a 19 1-mm-diameter copper tube. A mixing chamber is located at the entrance and exit of the heat source. The three rod heaters and associated piping are located within an insulated vacuum jar. The jar is suspended in polyethylene foam inside a box constructed of 12.7-mm-thick plywood. Power input to the electric heaters is controlled by a Powerstat Variable Autotransformer. Electrical specifications are given in Appendix C. The pressure drop across the simulated collector array has been matched to that of the actual solar collector array, as shown in figure 12. In addition, a copper canister and copper tubing were placed in series with the electric heat source and sized so that the time constant of the simulated array is approximately equal to that of the actual array (304 s).

3.2.2 Electric Heat Source In Series With Nonirradiated Array

This experimental technique employs nonirradiated solar collectors in series with the electric heat source described above, as shown in figure 13. A

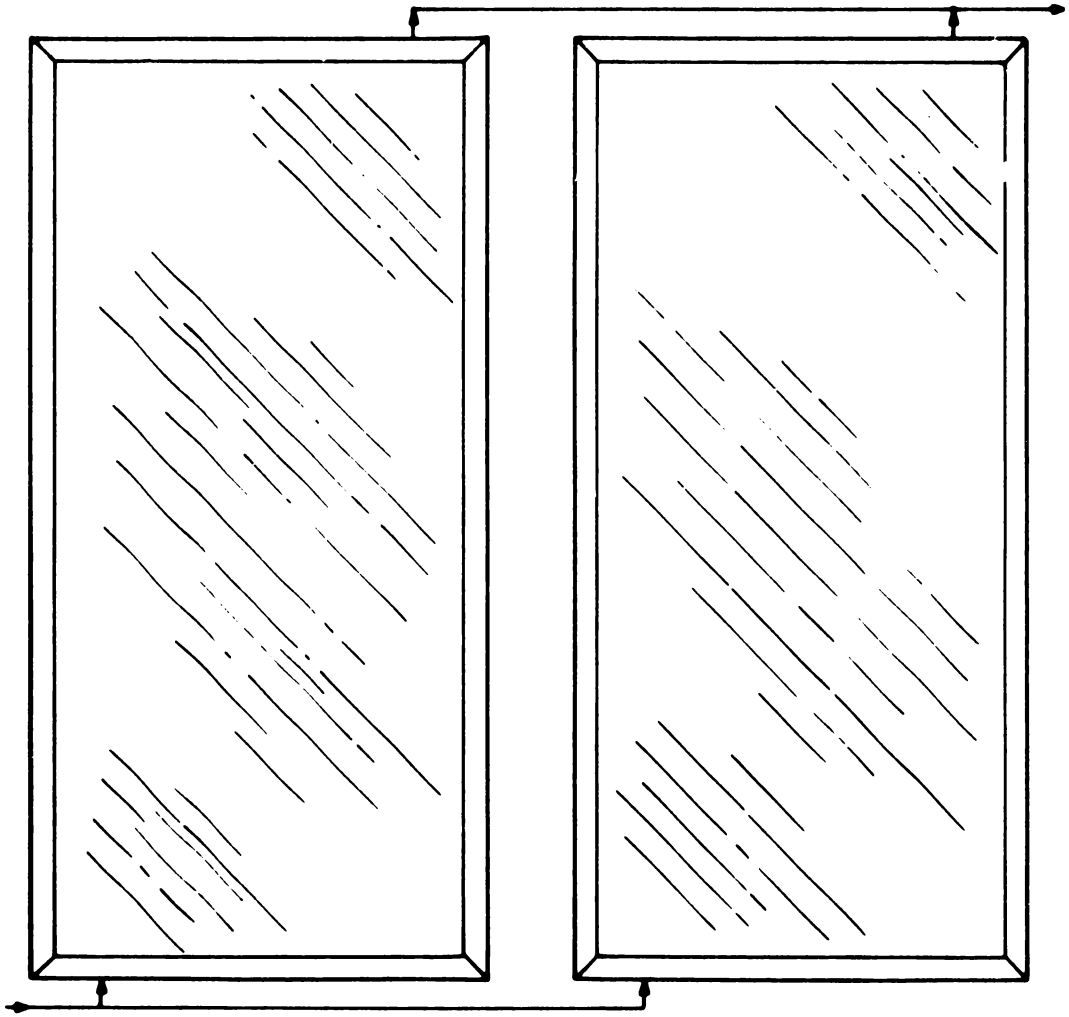

Figure 9. Solar collector plumbing schematic

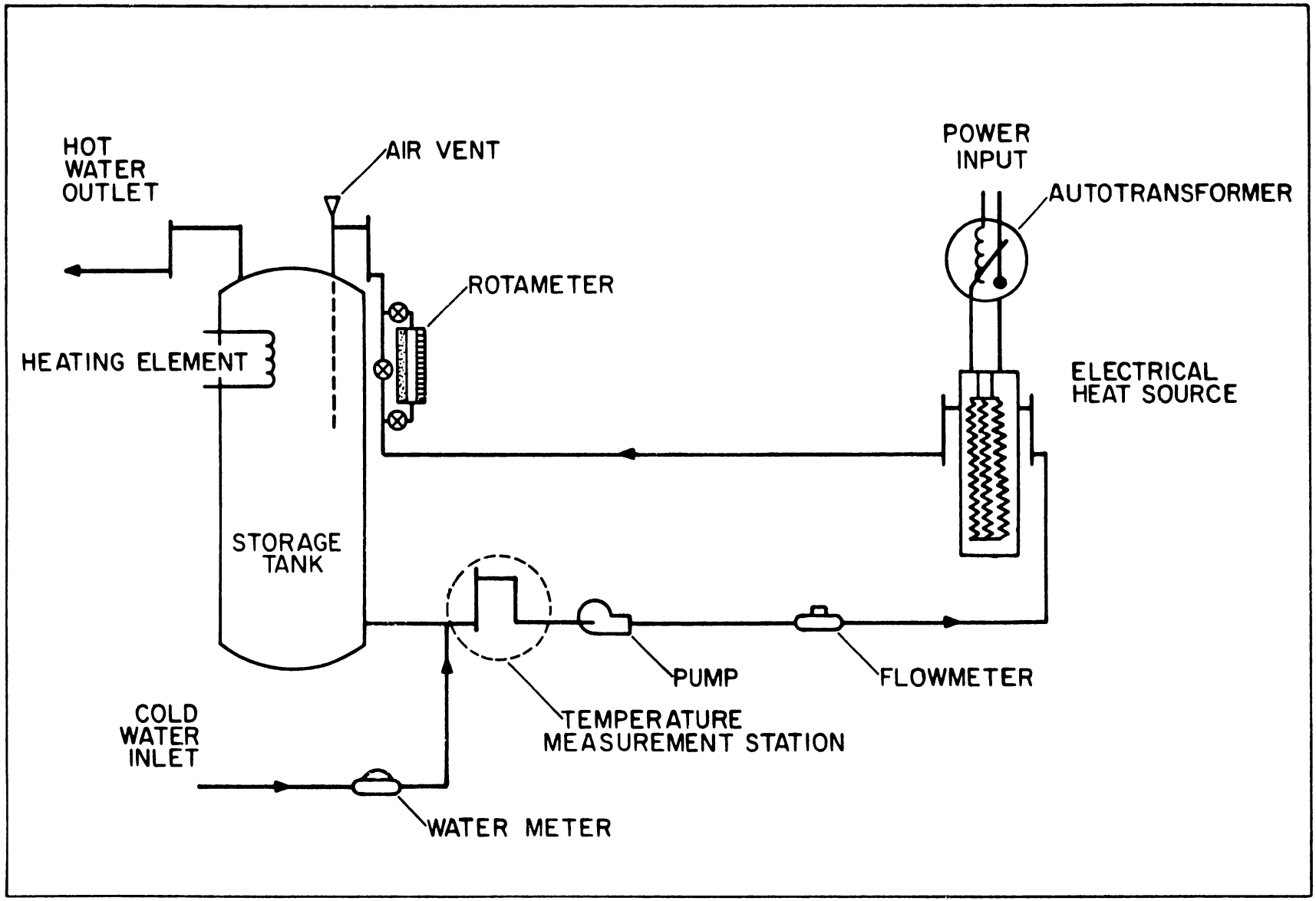

Figure 10. Solar hot water system with the irradiated collector array replaced with an electric heat source

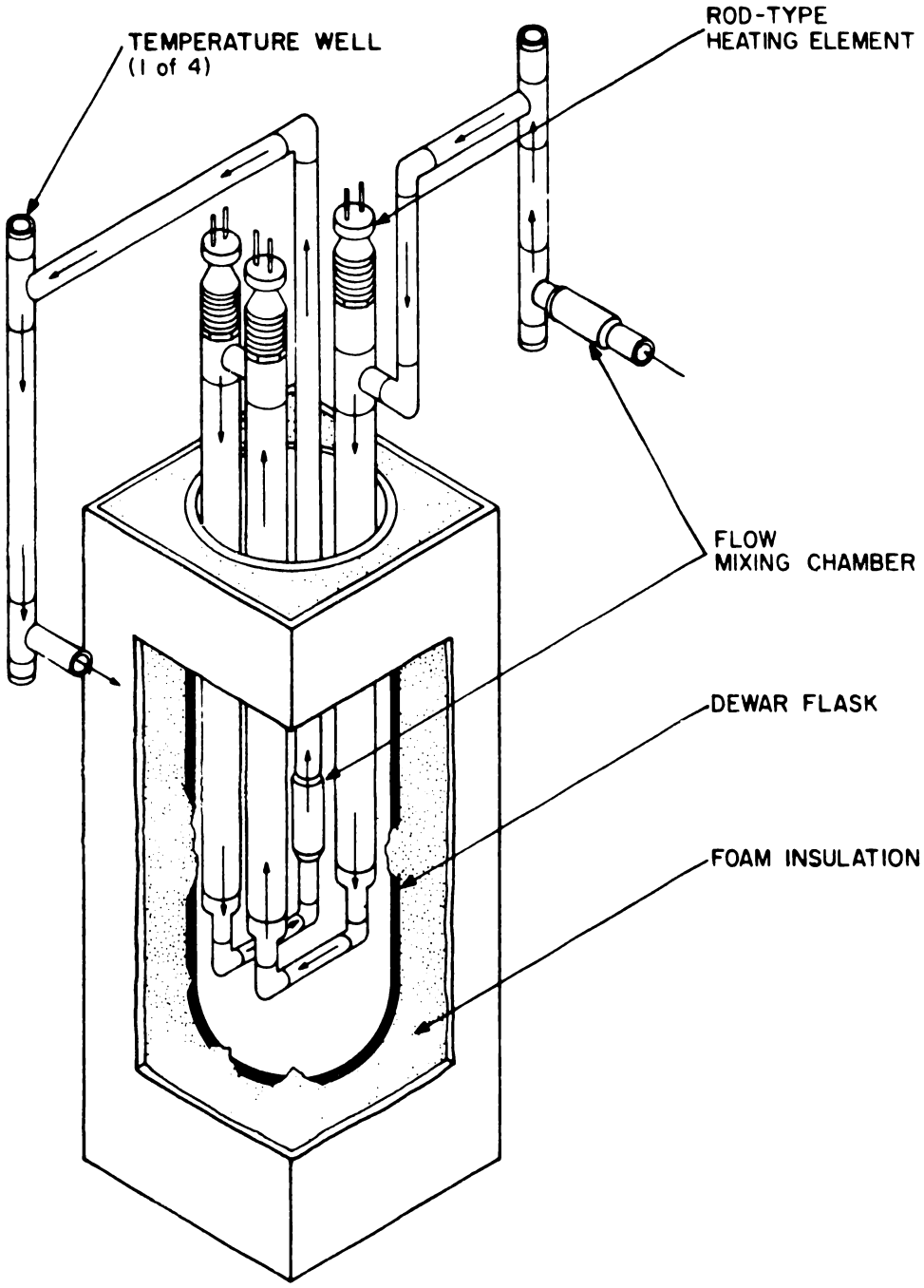

Figure 11. Electric heat source

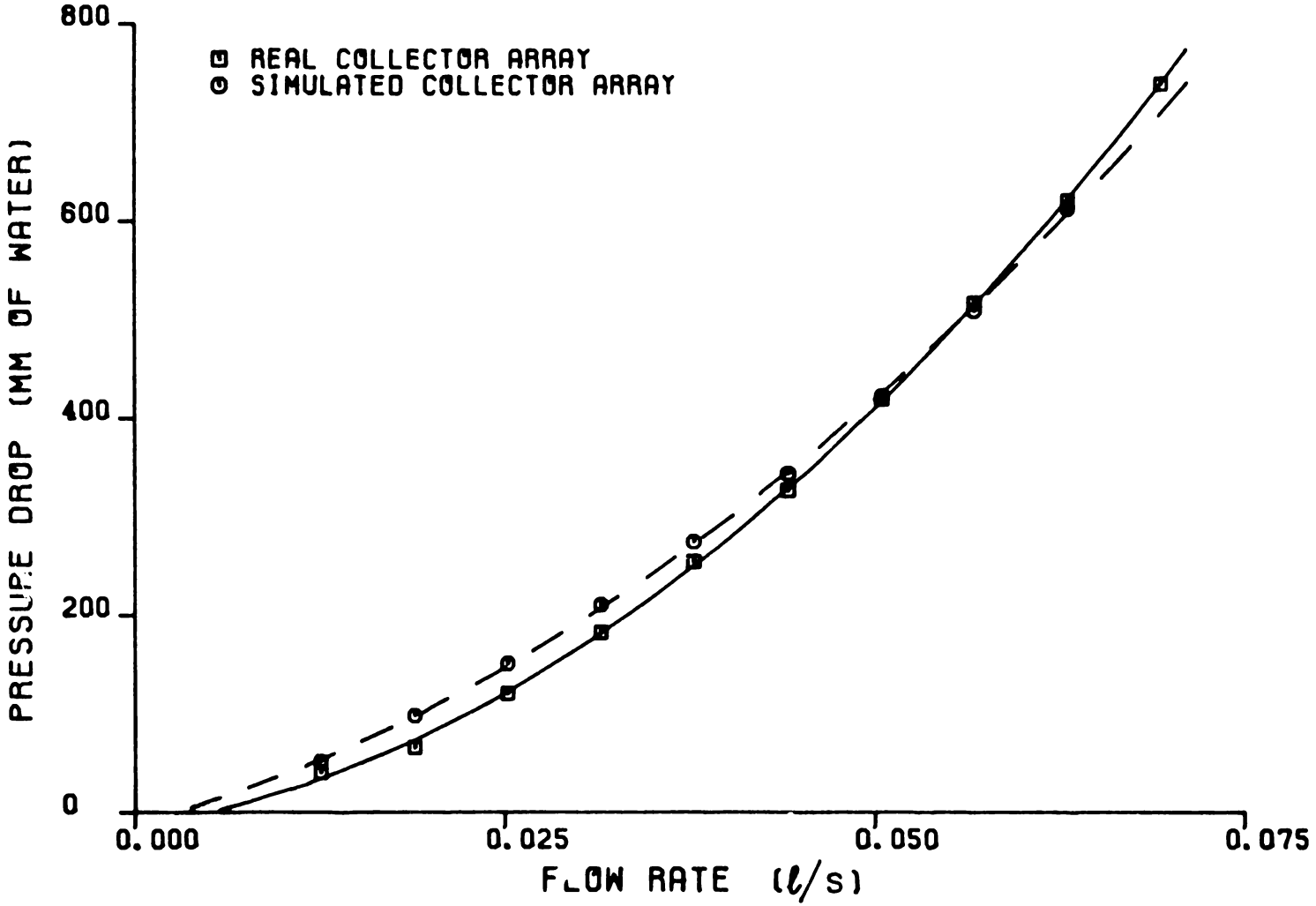

Figure 12. Pressure drop across the irradiated collector array and across the electric heat source

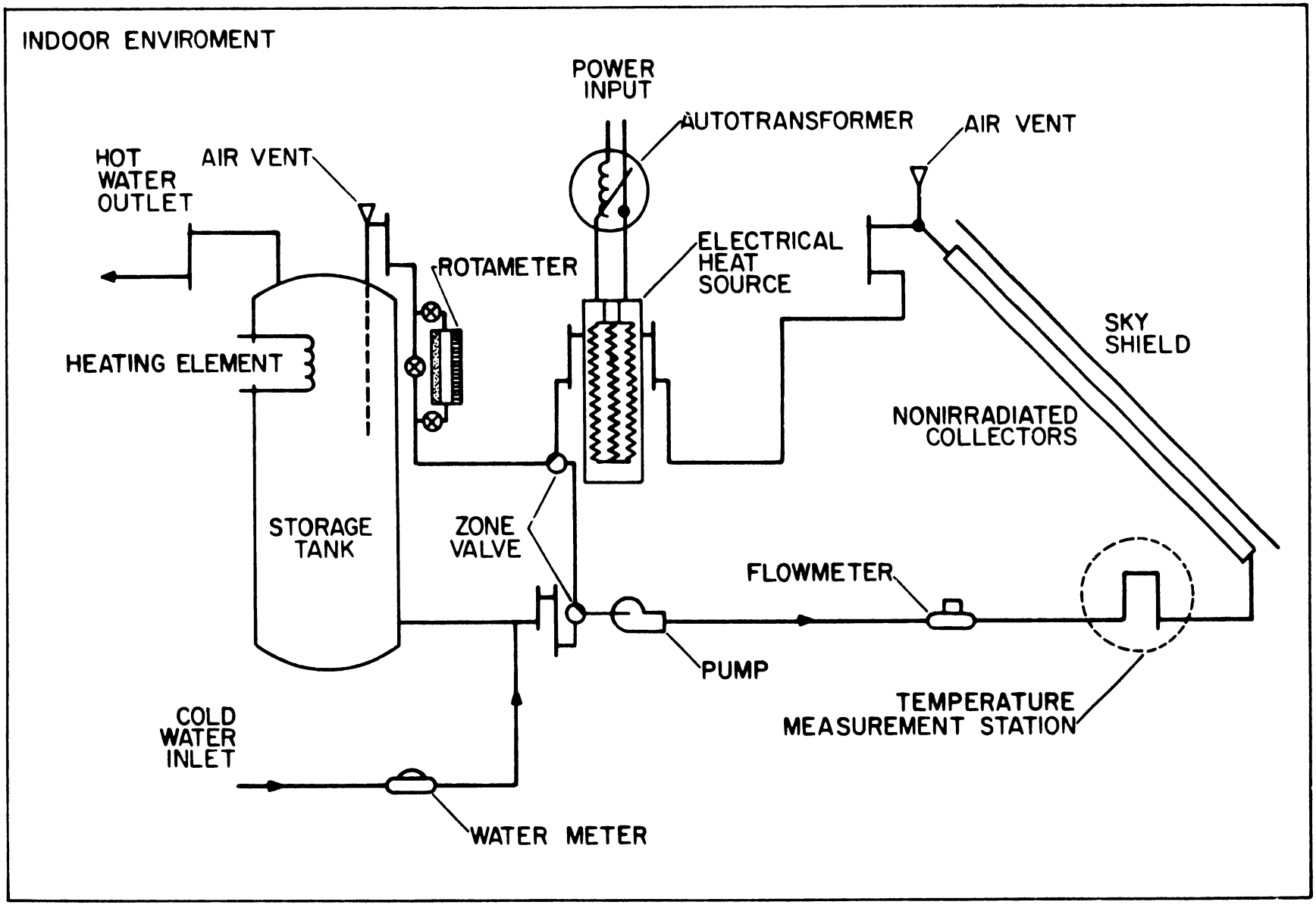

Figure 13. Solar hot water system with the irradiated collector array replaced with a nonirradiated collector array with downstream heat source

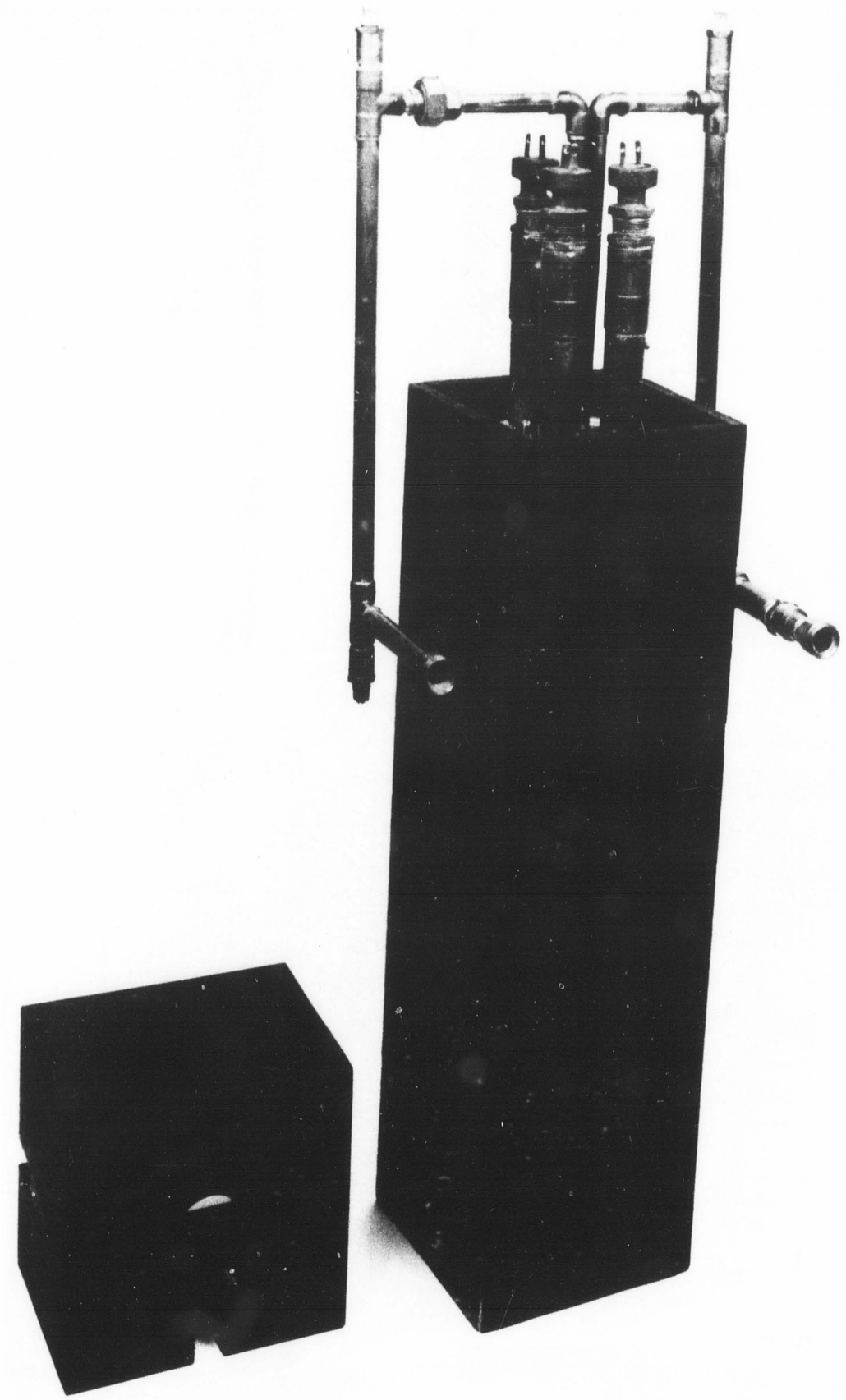

Electric heat source consisting of three immersion heaters

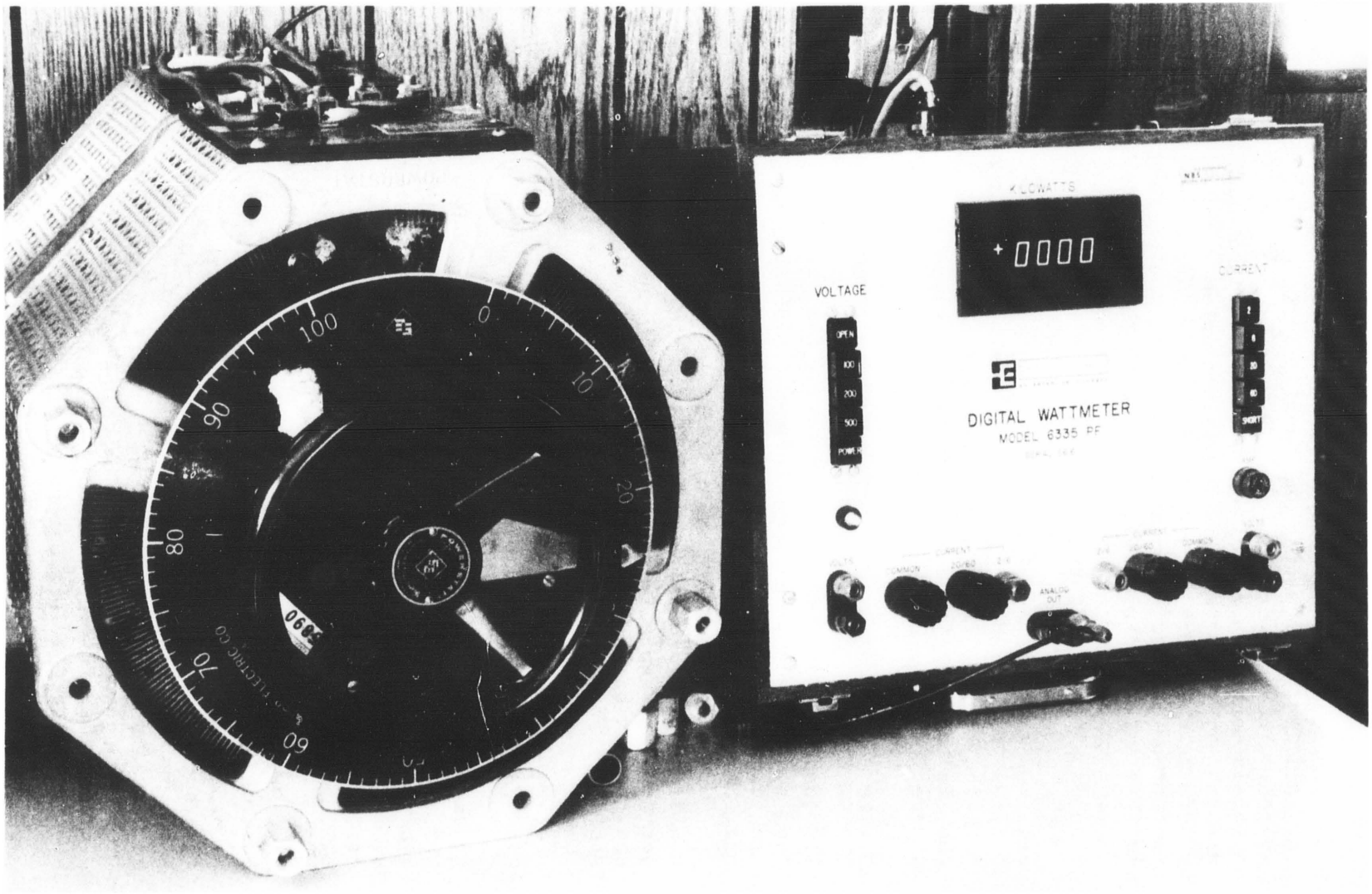

Autotransformer used to control heat source power input

collector array identical to that used for the irradiated array was constructed inside the test facility. All piping and insulation is equivalent to that of the outdoor system. The collector tilt angle is the same (39°). A 6.4-mm-thick plywood shield mounted parallel and 203 mm above the nonirradiated array provides a uniform "sky" temperature. The shield extends 203 mm beyond the outer boundary of the collector array. As discussed in the analysis section, the heat source may be located upstream or downstream of the nonirradiated array. During this experimental investigation, the heat source was located downstream. A storage tank bypass loop allows outdoor collector stagnation conditions to be duplicated indoors. When an 8.9 C temperature difference exists between the pipe leaving the heat source and the storage tank sensor, the controller positions two three-way zone valves such that the flow path is identical to that of an irradiated system. When the temperature difference becomes less than 1.7 C, the storage tank is bypassed. In this mode of operation, power supplied by the electric heat source is partially dissipated as heat from the nonirradiated array.

3.3 NONIRRADIATED COLLECTORS WITH ATTACHED STRIP HEATERS

Energy normally absorbed by the irradiated solar collector is supplied by strip heaters attached to the back side of the absorber plates. The quantity of energy supplied to the strip heaters is dependent on the simulated outdoor radiation conditions and the optical characteristics of the collector.

Strip heaters having a maximum power density of 0.0031 W/cm^2 were used in this series of experiments. Figure 14 shows the strip heater layout on one absorber plate. Three different sizes were attached to each absorber plate. The combination consists of fifteen 50.8 mm by 1.524 m strip heaters, three 50.8 mm by 609 mm strip heaters, and three 50.8 mm by 228.6 mm heaters. Use of three different sizes avoids the need for specially sized strip heaters. Brush-on silicone adhesive was used to bond the heaters to the absorber plates.

The strip heaters were electrically connected in parallel using 14-gage Teflon™-coated stranded wire. Power regulation was provided by the autotransformer previously described. The controller sensor locations are identical to the locations for the irradiated system.

3.4 INLET TEMPERATURE CONDITIONING SYSTEM

The inlet water temperature to both solar hot water systems is held at a preset temperature by a water-circulating loop, as shown in figure 15. The system consists of two storage tanks, 0.310 m^3 and 0.159 m^3, a water chiller, a circulating pump, and a temperature controller. Supply water enters the 0.310 m^3 tank. This tank has a 4.5 kW heating element located near the bottom. Water leaves the top of the tank and enters the 0.159 m^3 tank which provides additional storage capacity. A constant displacement pump draws water from the bottom of the smaller tank. The water circulates through a closed loop, which contains a Temprite Model R-30 Water Chiller, before returning to the bottom of the large storage tank. A Honeywell Model R7350 Digital Set Point Temperature Controller, with a Type T thermocouple sensor located in the 0.310 m^3 storage tank, senses the temperature deviation from the set point. The controller then activates the

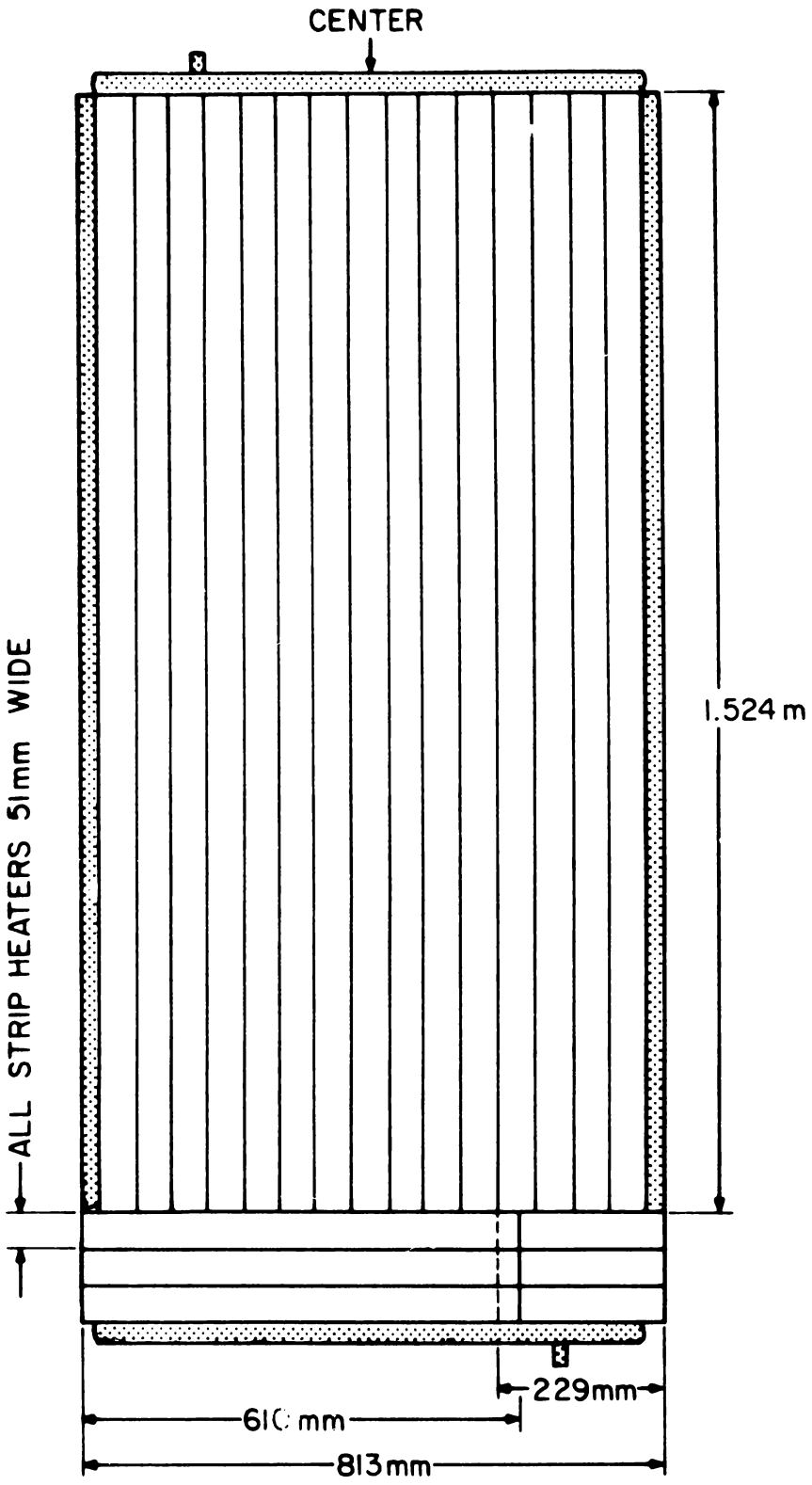

Figure 14. Location of strip heaters on the back of solar collector absorber plate

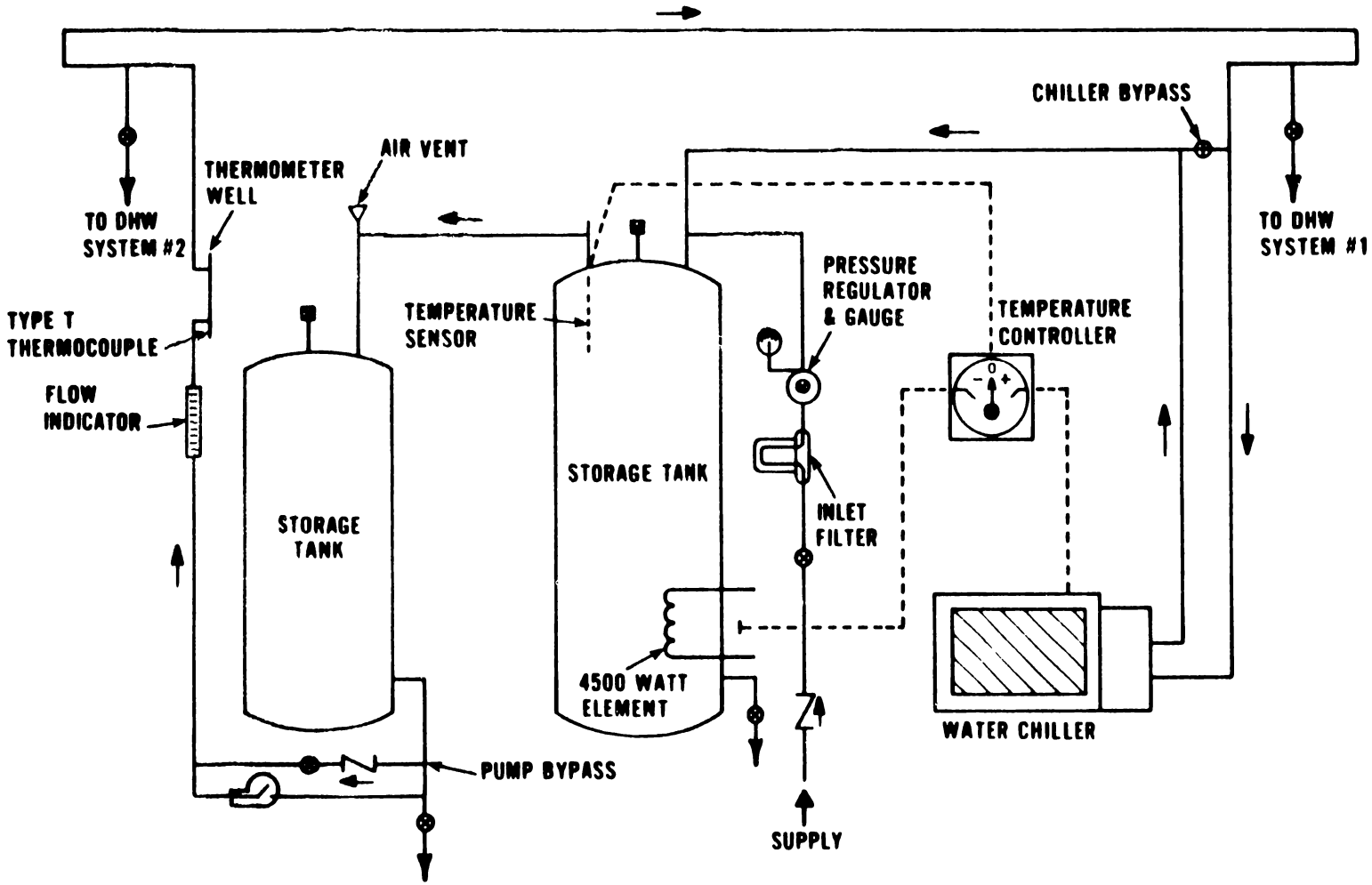

Figure 15. Schematic of supply water conditioning loop

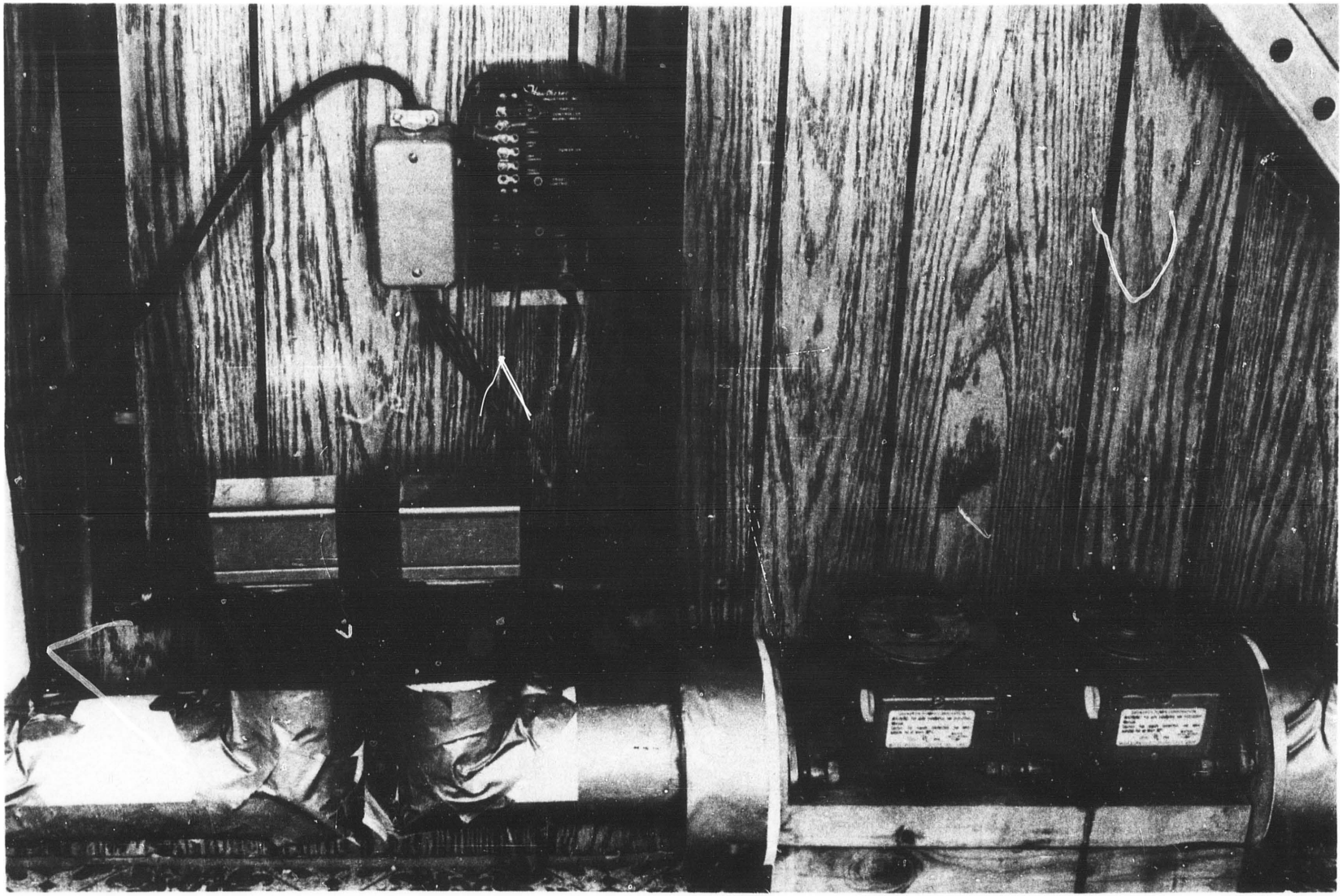

Differential temperature controller and two three-way zones valves used for indoor duplication of outdoor stagnation conditions

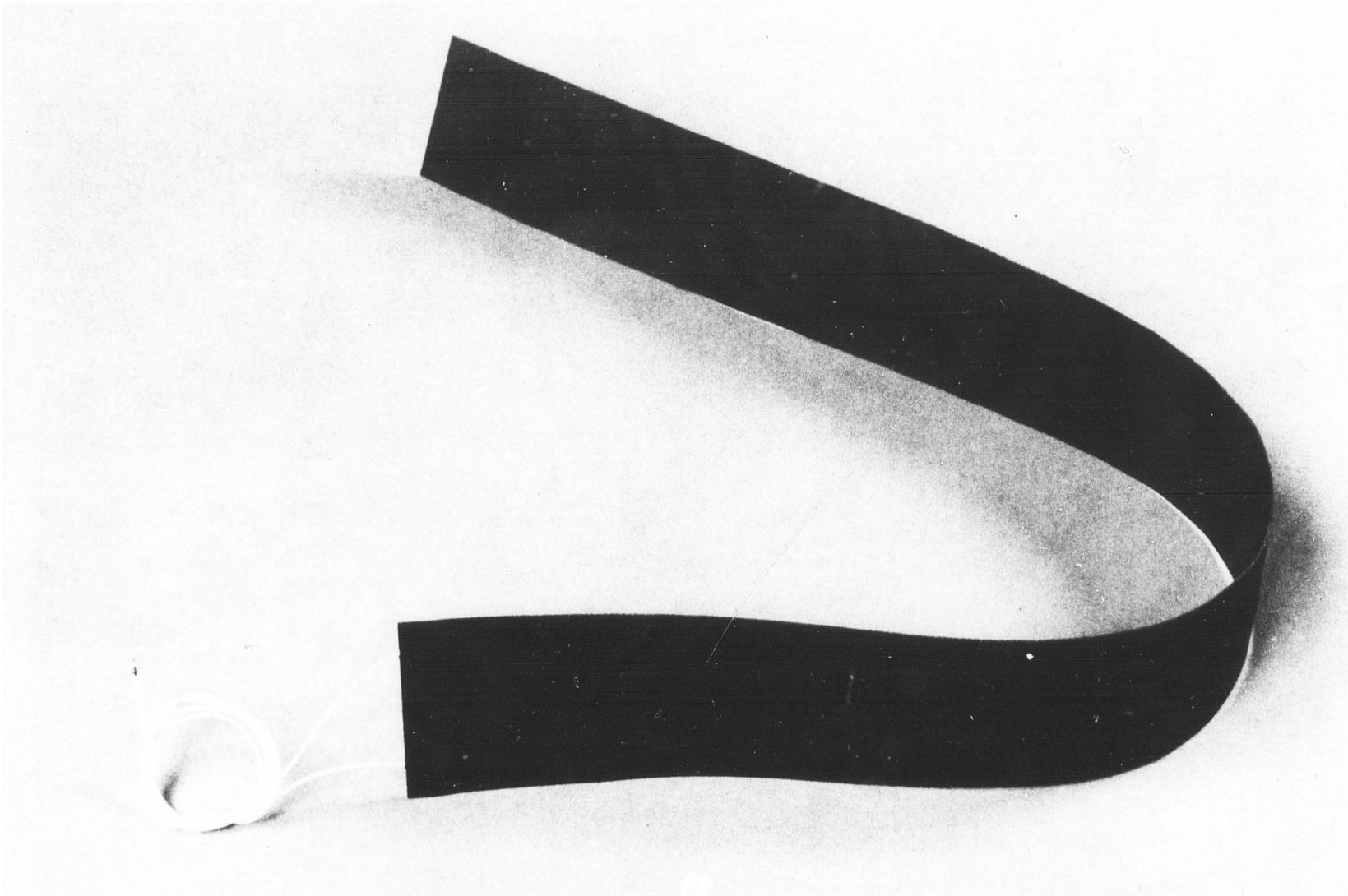

A representative electric strip heater

chiller or heating element as necessary. The fluid temperature in the loop is generally maintained within ± 2 C of the set point.

3.5 INSTRUMENTATION

Volumetric flow, temperature, power, and environmental conditions are monitored during the operation of each solar system. These measurements allow determination of system thermal performance. The irradiated and nonirradiated solar hot water systems are identically instrumented, with two exceptions. Pertinent outdoor meteorological conditions are measured for the irradiated system, while the input power to the electric heat source or strip heaters is measured for the nonirradiated system.

Premium grade thermocouple wire which has a nominal accuracy of ± 0.5 C was used in all thermocouple and thermopile construction. All wire runs are continuous from the temperature sensors to the data acquisition system. All thermopiles were calibrated using constant temperature baths and NBS-certified thermometers. A vertical array of type T (copper-constantan) thermocouples, with the junctions at 152 mm intervals, is located inside each water storage tank. Construction details are shown in figure 16. Thermocouples are used to measure the inlet and outlet potable water temperatures and a three-junction thermopile measures the temperature difference when a hot water load occurs. Two shielded thermocouples, supported by a wooden rod, located 1.5 m from the tank, are used to measure the surrounding ambient temperature. The thermocouples have elevations of 0.53 m and 1.05 m, respectively, above the floor. Thermocouples and a six-junction thermopile are used to monitor the irradiated or simulated solar collector array supply and return temperatures at the storage tank. Thermocouples are located in the inlet and outlet of the collector array. A six-junction thermopile is used to measure the temperature difference across the array.

The apparatus used to supply the quantity of energy supplied by an irradiated array may consist of an electric heat source, strip heaters attached to nonirradiated collector absorber plates, or nonirradiated collectors in series with an electric heat source. Thermocouples are placed at the inlet and outlet of each component while a six-junction thermopile measures the temperature difference across each component. An additional thermopile is placed across the nonirradiated array-heat source combination. Two thermocouples measure the sky-shield temperature above the nonirradiated array. The absorber plate temperatures are monitored in four locations along the center line of the plate as shown in figure 17.

Flow rate through the collector array is measured with a Flow Technology, Model FTM-N10-LB, Omniflo Turbine Flowmeter. This volumetric flowmeter uses a bladed rotor to generate a digital signal. An orifice directs the flow tangentially past the underside of a rotor, figure 18. The turbine rotor rotates at a speed proportional to the velocity of the fluid. A variable reluctance transducer located adjacent to the rotor has generated within it an electrical current whose frequency is proportional to the rotational speed of the rotor. The pulses generated are fed to a Flow Technology Series 7050 digital processor. The turbine flowmeter and digital processor are calibrated, as a unit, before each experiment using the dead weight method. A typical resulting calibration

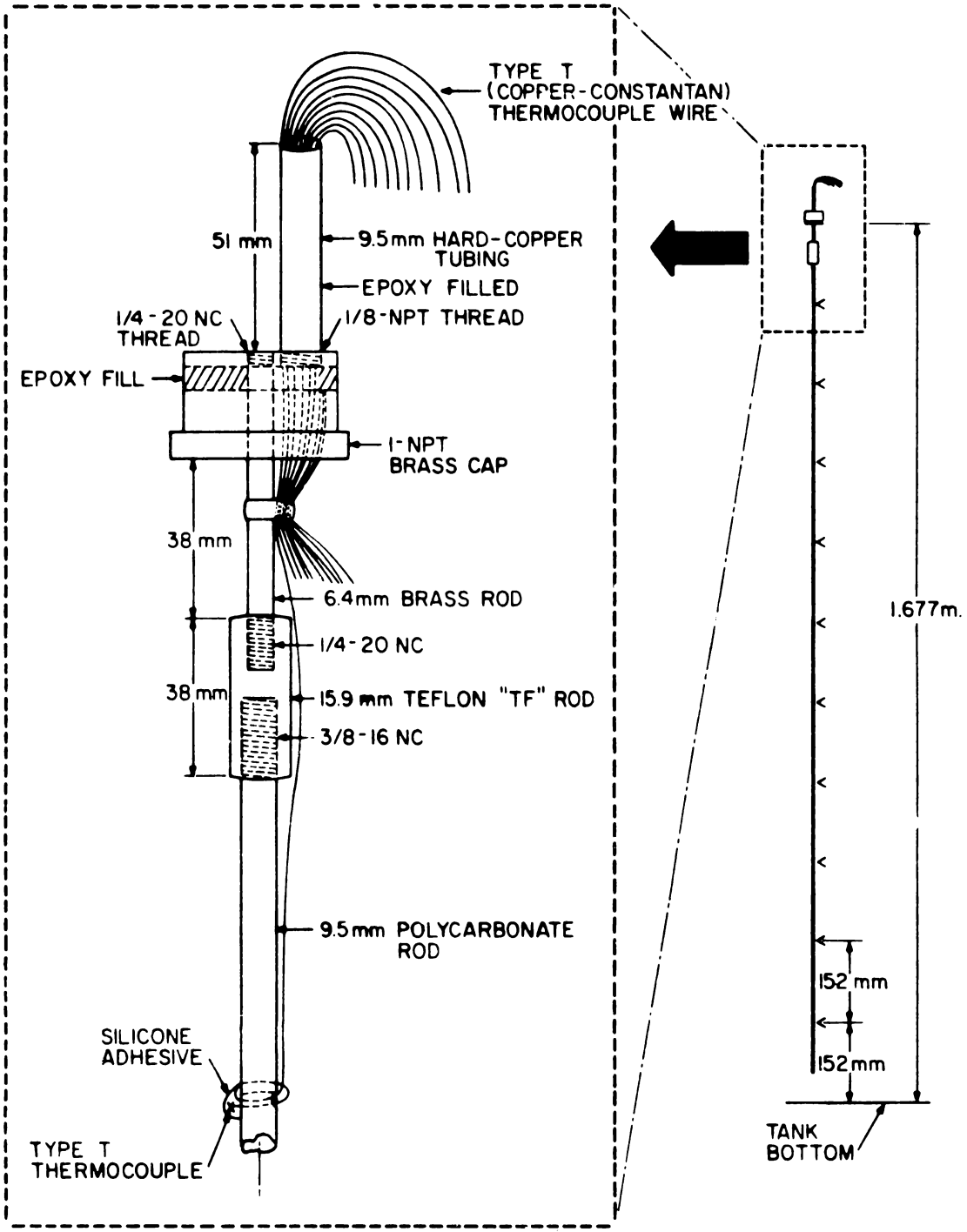

Figure 16. Vertical thermocouple array construction details

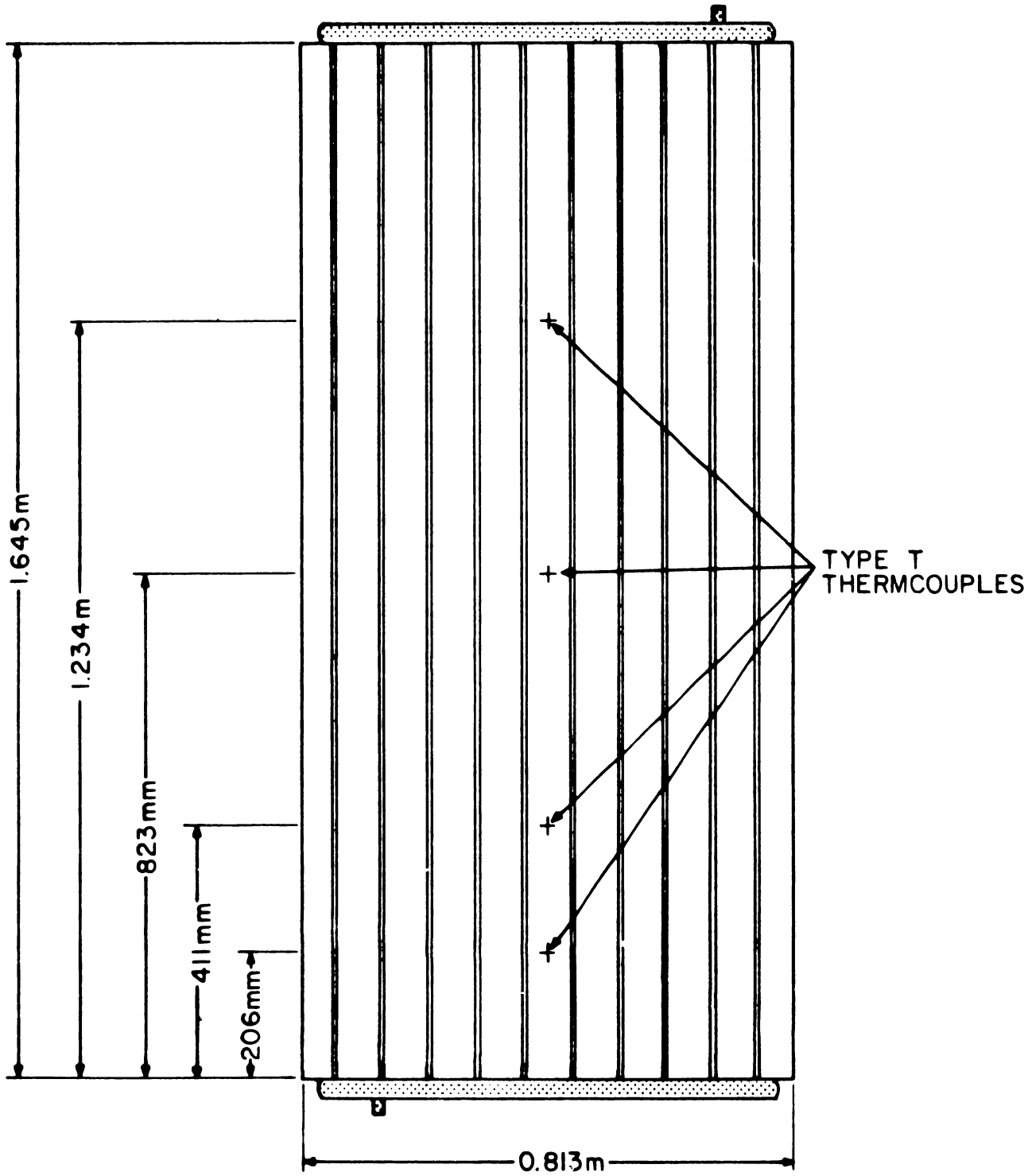

Figure 17. Location of absorber plate thermocouples

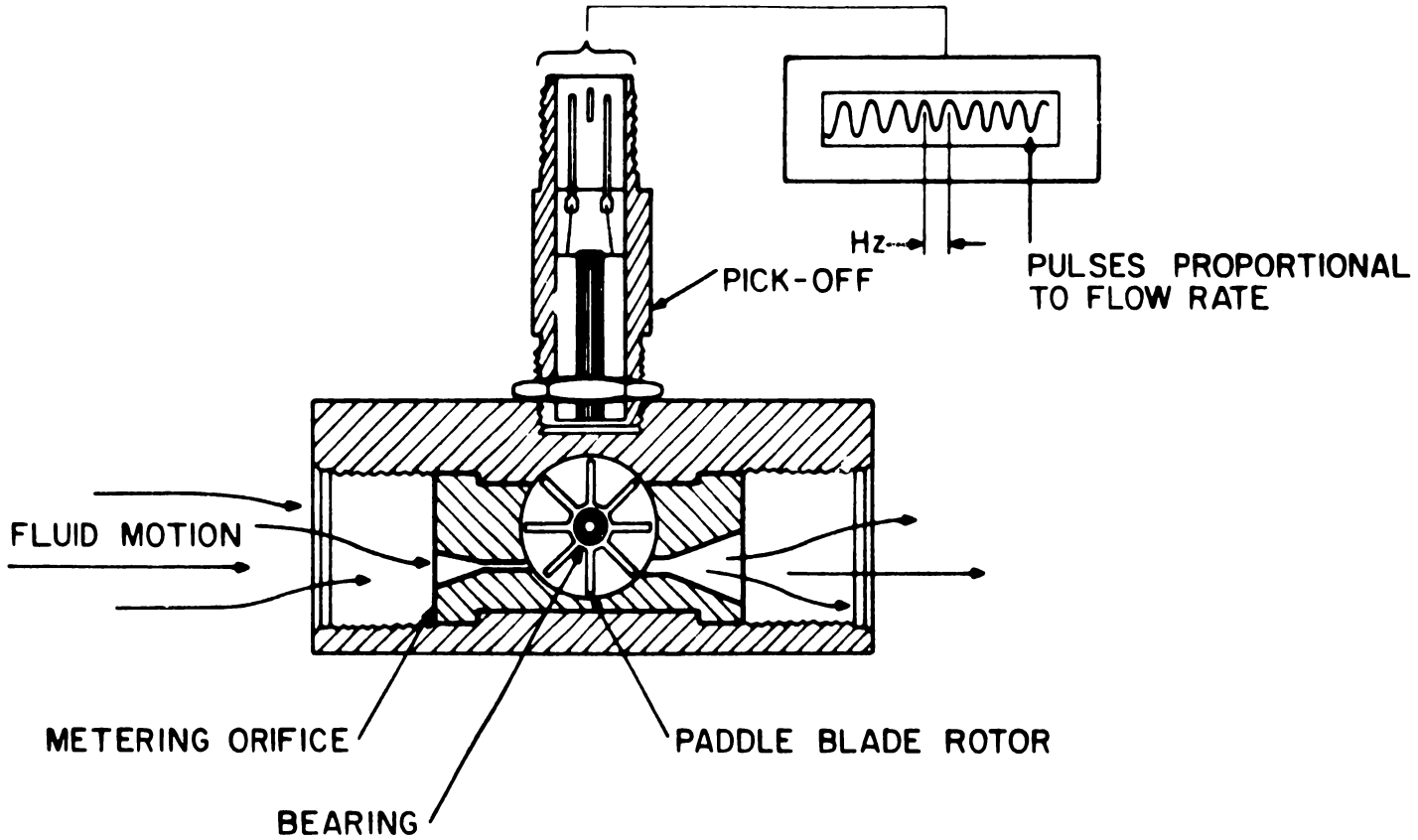

Figure 18. Volumetric flowmeter schematic

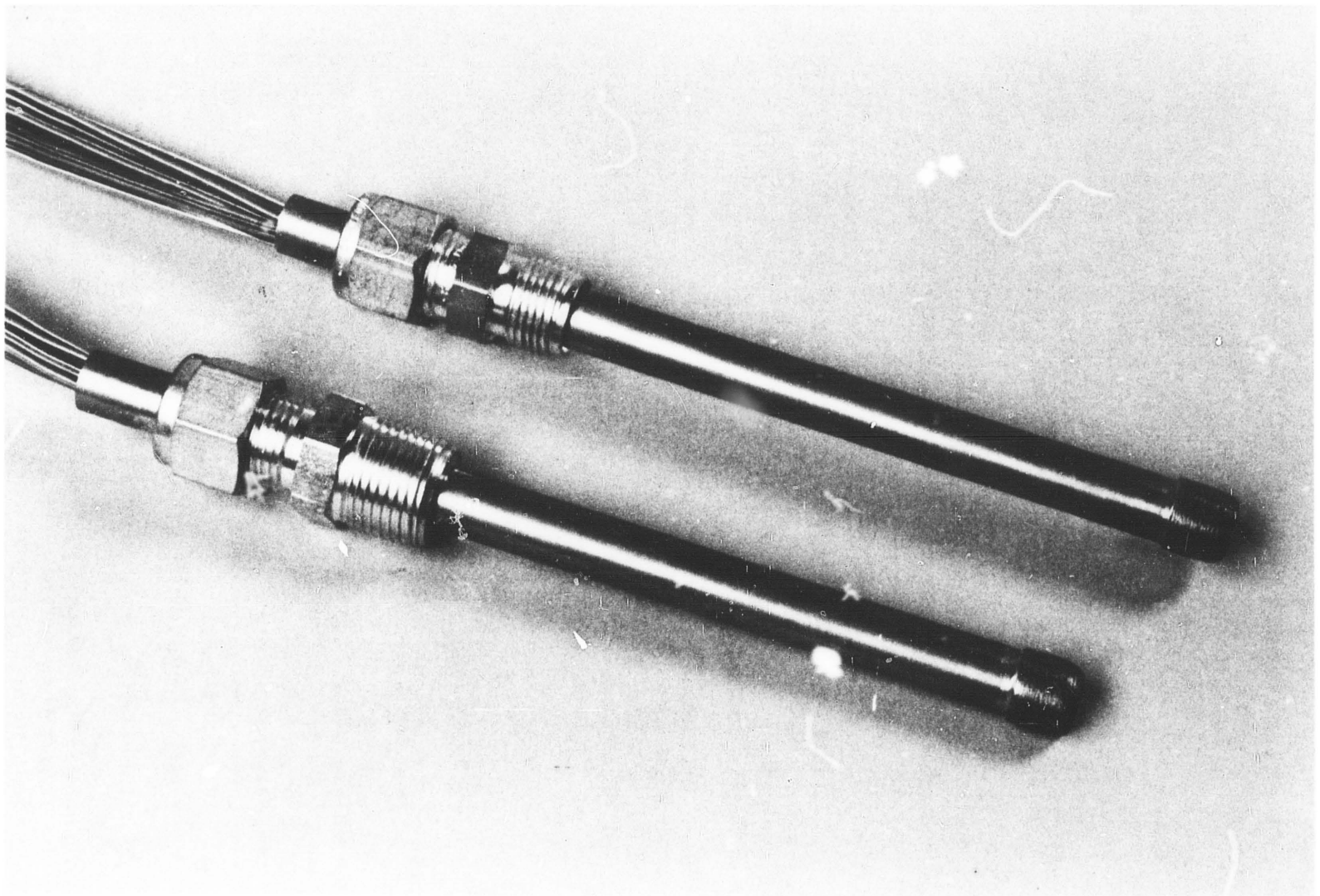

A six-junction thermopile used for temperature difference measurement

curve is shown in figure 19. In addition to the turbine flowmeter, a Brooks Model 1110 Full-View rotameter was used to monitor the flow rate.

The energy supplied to the heating element in the storage tank is measured using a General Electric 240 volt Type IW-70-S Watthour Meter equipped with a D-20-I contact closure device. Each contact closure is equivalent to 20 watthours. An electrical counter sums the number of contact closures. Connected in series with the watthour meter is a General Electric Type IB-10 Portable Watthour Meter Standard. Use of the watthour standard provides 0.12 watthour resolution. The use of both instruments provides two independent measurements. Instantaneous power consumption is measured with a Scientific Columbus XL5C5-A2-1-7 Watt Transducer. This instrument provides a 0 to 100-mV-output signal directly proportional to a 0 to 3500 watt power input. The output signal is fed to the data acquisition system. Specifications are given in Appendix C. Additionally, a 1.5 Vdc signal is fed to the data acquisition system whenever the heating element is energized.

Operation of the circulator pumps is monitored by a Cramer Elapsed-Time Meter. Resolution of 0.1 minutes is provided over a range of 0 to 9999.9 minutes. When the circulators are operating, a signal is sensed by the data acquisition system. This arrangement allows the operational status of the circulators to be continuously monitored.

A specified amount of energy is withdrawn from the solar storage tank during each test. An integrating volumetric water meter and weigh tank are used to measure the amount of water withdrawn from the storage tank. The water meter is a Model 15 Badger Recordall. Water withdrawn is collected in an insulated 0.114 m^3 tank which rests on a Fairbanks, Morse, and Co. balance scale. A thermometer suspended in the tank measures the mixed temperature of the withdrawn water. When a draw occurs, the three-junction thermopile signal is fed to an analog integrator. The integrator, manufactured by AGM Electronics, integrates the analog input signal with expired time and provides an analog output signal proportional to the accumulated integrated quantity. The input and output signals to the integrator are fed to the data acquisition system and to a Westronics MT-22 Strip Chart Recorder.

The instantaneous power supplied to the simulated solar collector array is measured during operation of the nonirradiated solar hot water system. This measurement is accomplished by using a Scientific Columbus watt transducer identical to the one described earlier. In addition, a Scientific Columbus Model 6335PF Digital Wattmeter is used. This wattmeter provides a visual digital readout of instantaneous power supplied to the simulated array. Specifications are given in Appendix C.

Outdoor meteorological conditions are measured during operation of the irradiated system. The net total global radiation is measured with an Eppley Model PSP Radiometer. The radiometer specifications are given in Appendix C. The longwave radiation, both indoors and outdoors, is measured using an Eppley Precision Infrared Radiometer (Pyrgeometer) whose specifications are given in Appendix C. Both instruments are located on the collector array support stand at a tilt angle of 39°. A Weather Measure W103/B three-cup anemometer is used

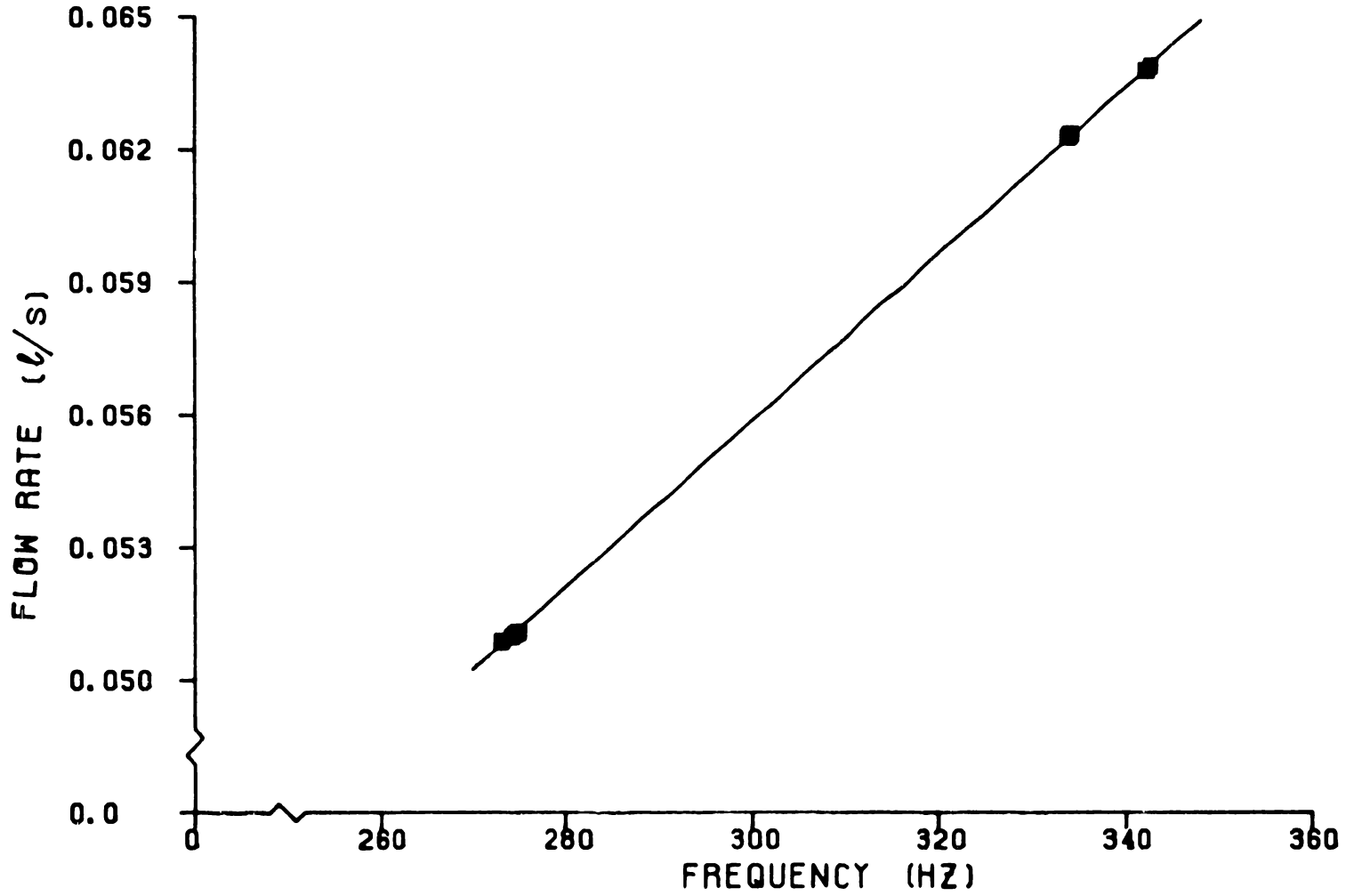

Figure 19. Typical calibration curve for volumetric flowmeter

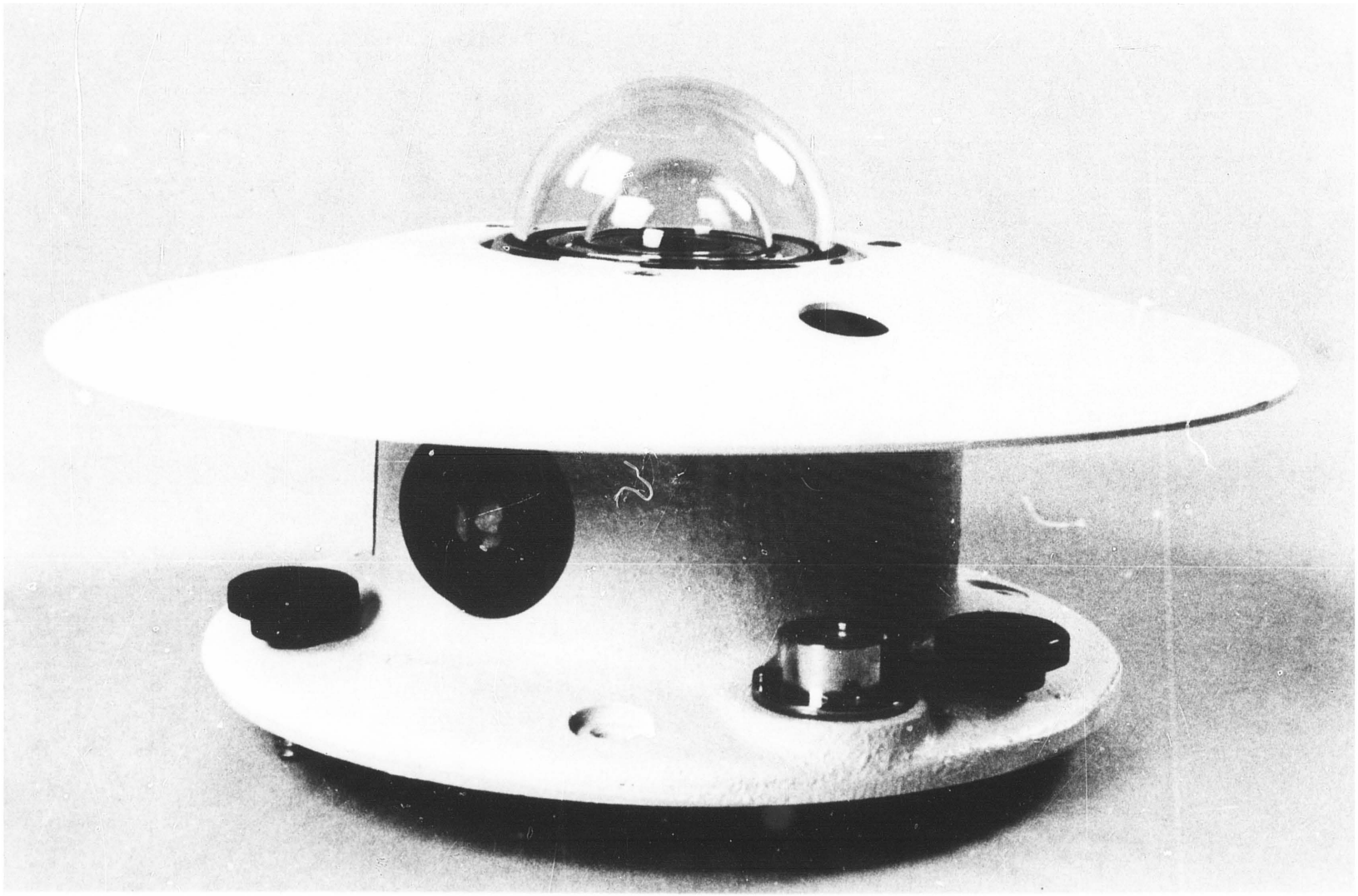

Epply Model PSP Radiometer used to measure net total global radiation

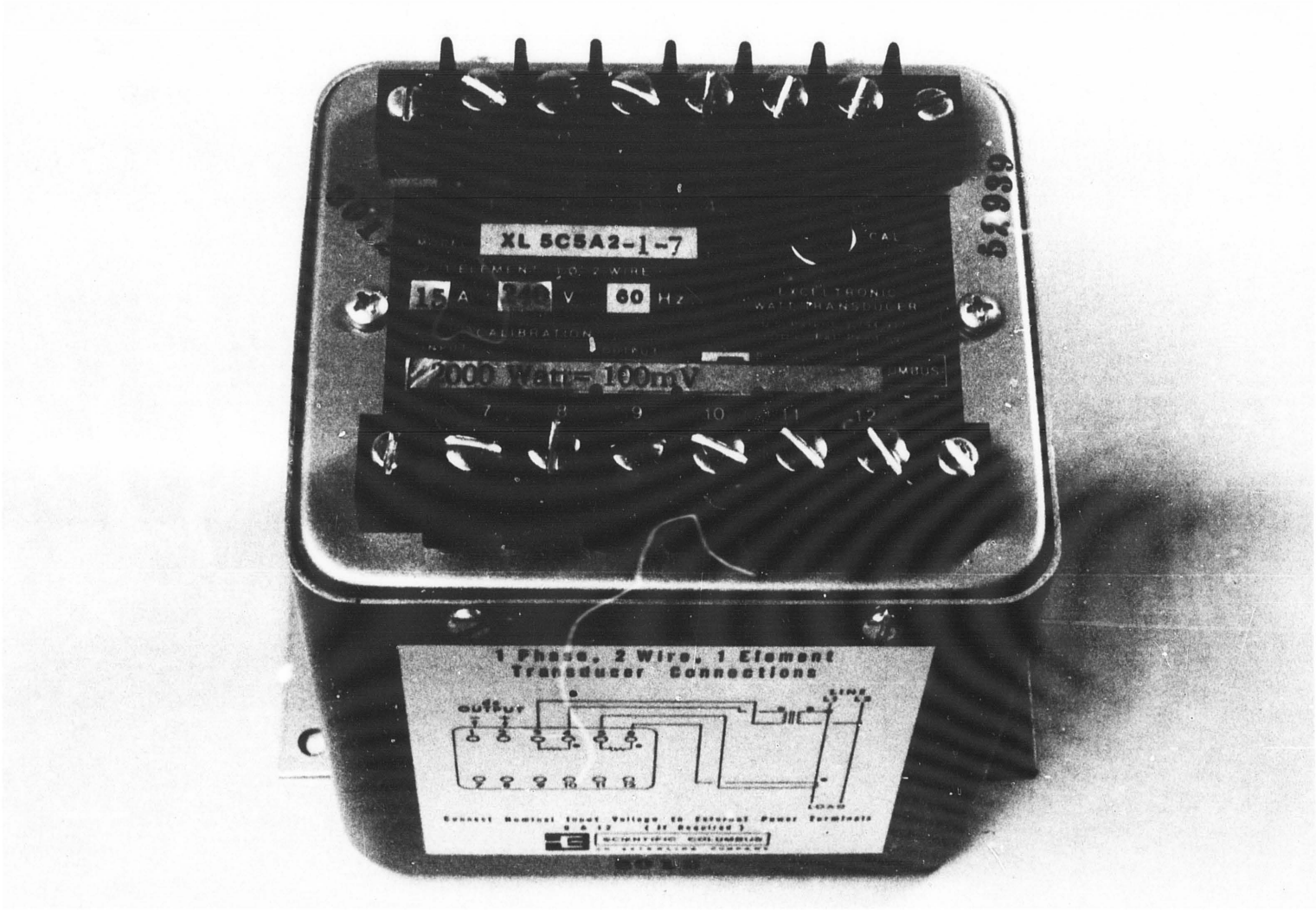

Watt transducer used to measure instantaneous power consumption

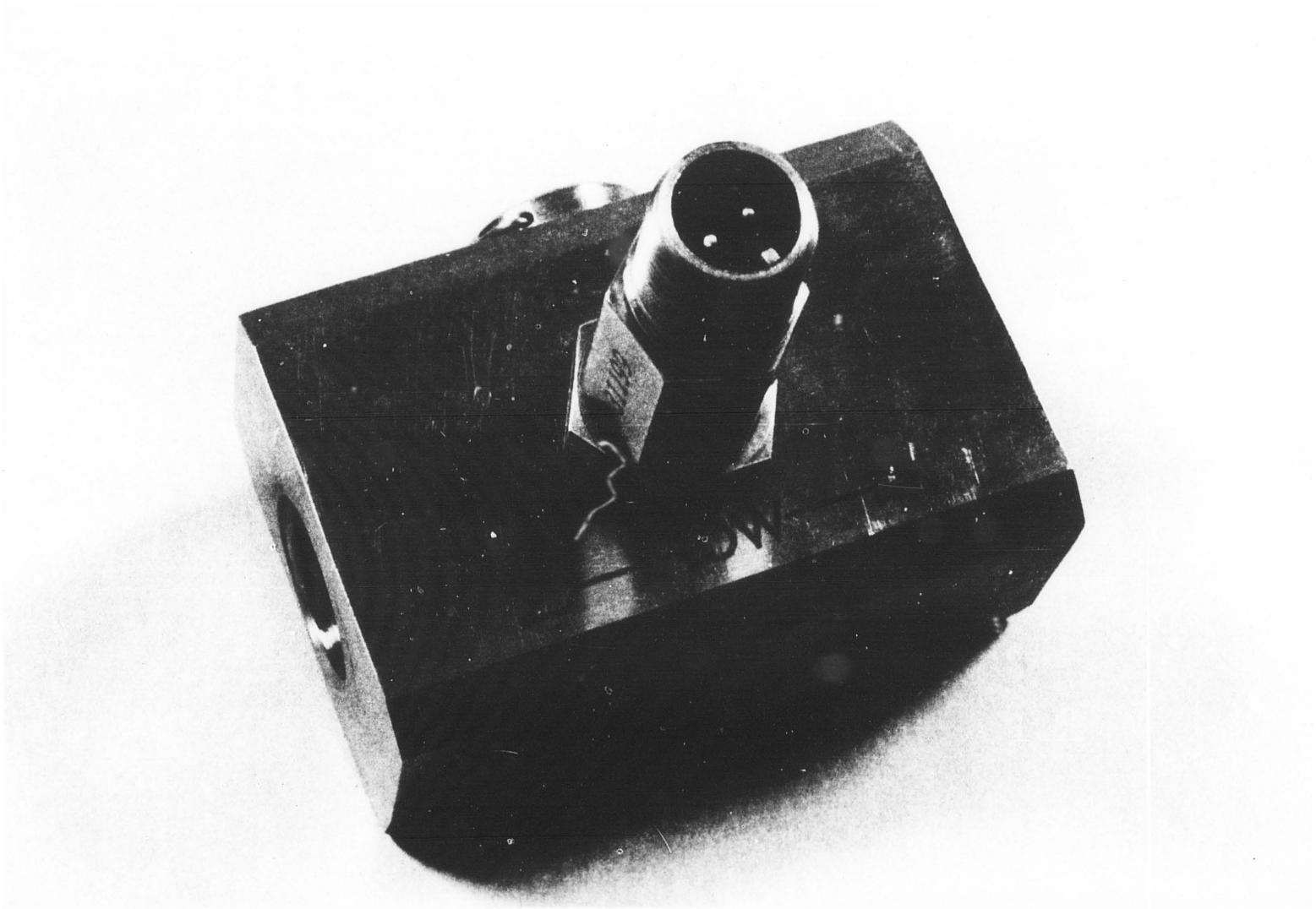

Turbine flowmeter used to monitor collector array flow rate

to measure the wind speed. Calibration was performed by the NBS Fluid Engineering Division. Outdoor ambient temperature is measured using a Type T thermocouple housed within a vented weather shelter.

Analog signals from various sensors are connected to a Leeds & Northrup Trendscan 1000 Data Acquisition System. This unit scans all instruments in one-minute intervals and is capable of accommodating 100 inputs. Appendix C shows the data recorded and channel assignments. The Trendscan 1000 has three ranges, which include a $\pm$ 400 mV range, a $\pm$ 10 V range and a -200 C to +400 C Type T thermocouple range. Any of the 100 input points may be addressed and assigned to any one of the three available ranges or omitted. The unit has an electronic discharge printer, and an internal clock provides real time display and initiates periodic logs at specified time intervals. Reference junction thermocouple compensation, using a bridge network, is located on the range input cards. Specifications are given in Appendix C for this data acquisition system.

A Kennedy Model 1642 Interface Unit interfaces the data acquisition system with a Kennedy Model 9832 Magnetic Tape Recorder. After recording the data, the magnetic tapes are read on the NBS UNIVAC 1108 Computer.

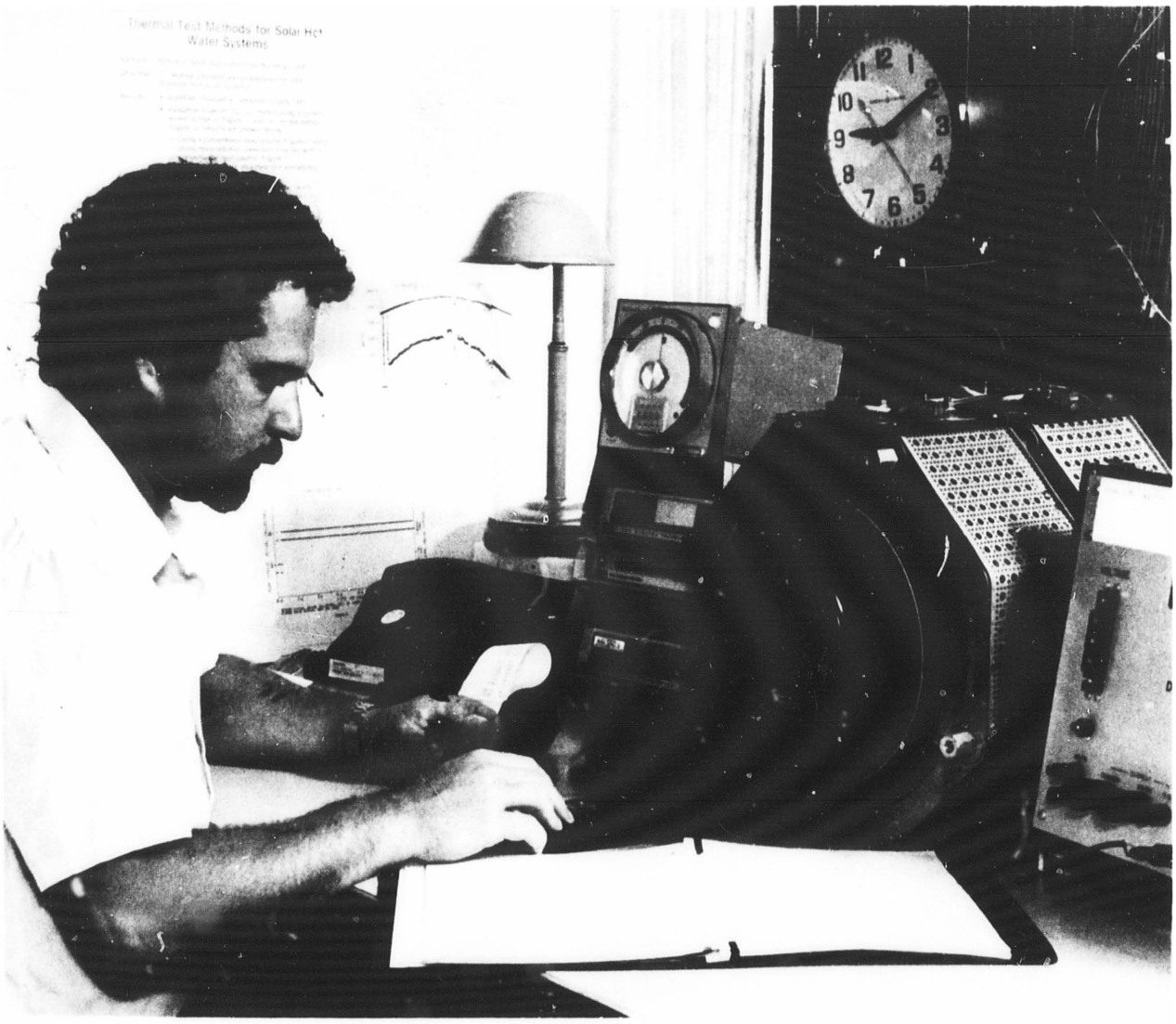

4. EXPERIMENTAL PROCEDURE, RESULTS, AND DISCUSSION

A number of experiments have been performed at the NBS to assess proposed test methods for solar domestic hot water systems. Three different experimental techniques of supplying the quantity of energy normally supplied by an outdoor irradiated array have been investigated. Tests were conducted to determine if the control functions of a system located entirely within a test facility are similar to those of a system subjected to outdoor meteorological conditions. An experimental study was performed to determine if one proposed test method (ASHRAE Standard 95) is sensitive to the amount of thermal stratification in the solar storage tank. Repeatability of test results was also investigated. A discussion of each experimental investigation follows.

4.1 REPLACEMENT OF THE IRRADIATED ARRAY WITH AN ELECTRIC HEAT SOURCE

An electric heat source is employed to supply the net energy gain of a solar collector array. The outdoor irradiated system was allowed to operate in a normal manner for several days in order to serve as a basis of comparison to the system performance using the electric heat source. During operation of the irradiated system, both clear and intermittently cloudy sky conditions existed. A description of the test sequence for the irradiated system follows.

At the beginning of each test day, the storage tank was filled with water at 20 C. The environment surrounding the tank was held at 20 C throughout the test. At 09:15 the heating element in the storage tank and differential controller were energized. Two hot water draws, one at 13:15 and one at 17:15, occurred during the test days. Each draw consisted of water entering the storage tank at 20 C at a flow rate of 2×10^{-4} m^3/s. During withdrawal periods, the incoming water temperature and temperature of the water withdrawn were measured. At the conclusion of each test day, water was withdrawn from the storage tank until the outlet temperature was within 1 C of the inlet temperature. The quantity of energy withdrawn was computed. Power consumed by the storage tank heating element was measured during each test day.

The testing procedure described for the irradiated system was followed by tests of the system which employed an electric heat source. Identical measurements were made. Using the incident irradiance and ambient temperature which were recorded during operation of the irradiated system, the power supplied to the heat source was determined using eq (2) and the flow rate correction procedure presented in Appendix A. The power supplied to the electric heat source was updated every five minutes.

Use of the identical test procedure for both systems allowed a direct comparison to be made between the performance of a solar domestic hot water system using irradiated collectors and one which employed an electric heat source. Figures 20 through 23 show the variation in solar irradiance for the four August test days. The test period included an almost clear day (August 10, figure 22) as well as intermittently cloudy days. The figures also show a comparison between the collector output for the irradiated array and the electric heat source. At the start of each test day for the irradiated system, the thermal output of the collector array is initially large and quickly decreases. This behavior is because the irradiated collectors experience stagnation conditions until the circulators are energized. The system using the electric heat source shows a rapidly increasing thermal output at the beginning of each test period. Outdoor stagnation conditions cannot be simulated accurately using an electric heat source only. Thus, the power output of the heat source is initially zero.

Large thermal output transients also occur during the hot water draw. During a hot water draw, cold makeup water enters the simulated and irradiated collector arrays. During the short time period between the time the cold water enters the arrays, but before the outlet temperature changes, the thermal output of the arrays suddenly increase. After the draw has terminated, water supplied from the storage tank enters the arrays causing the inlet temperature to increase sharply, resulting in a sudden decrease of thermal output.

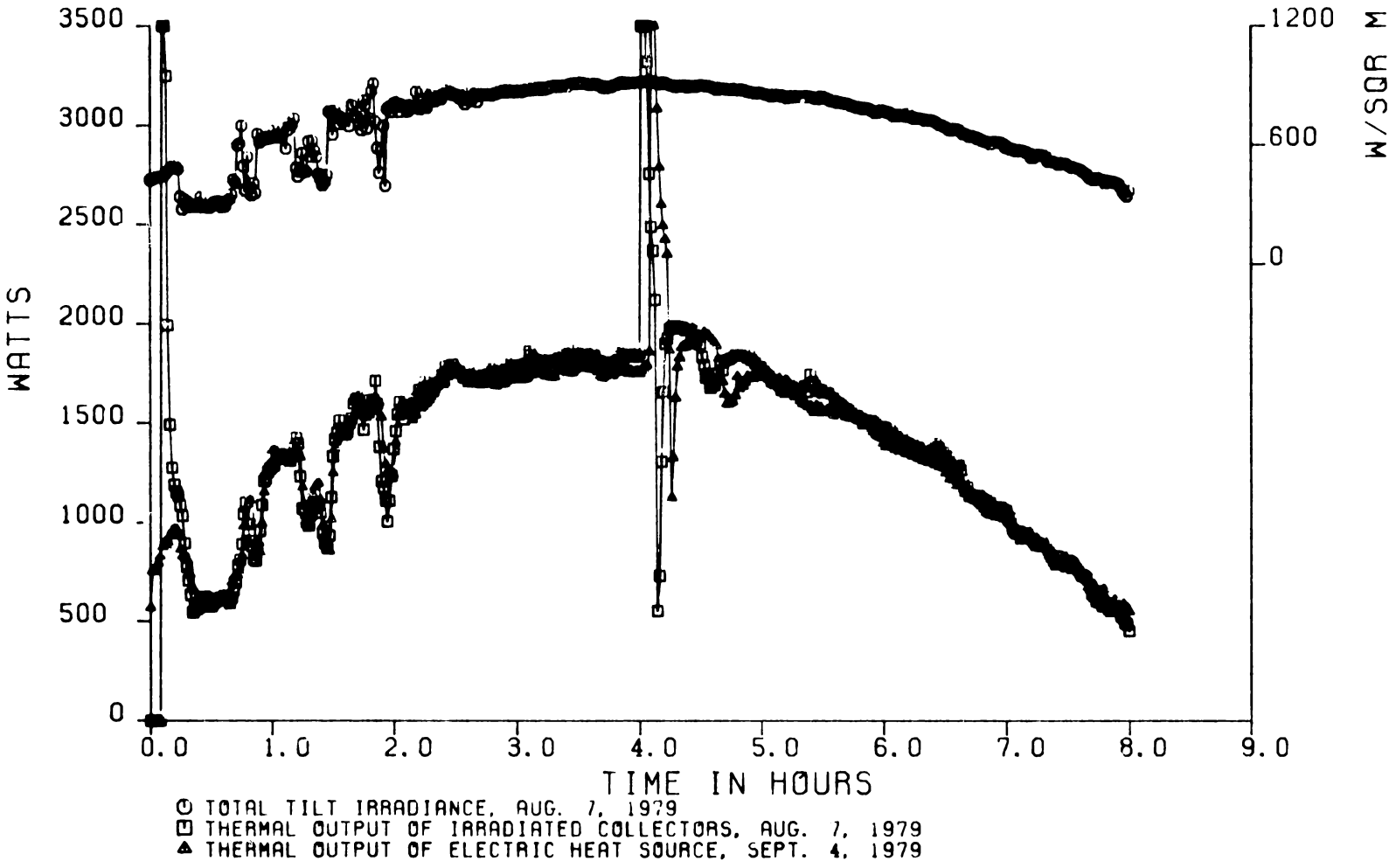

Figure 20. Thermal output comparison of irradiated collector array for August 7, 1979 and electric heat source for September 4, 1979

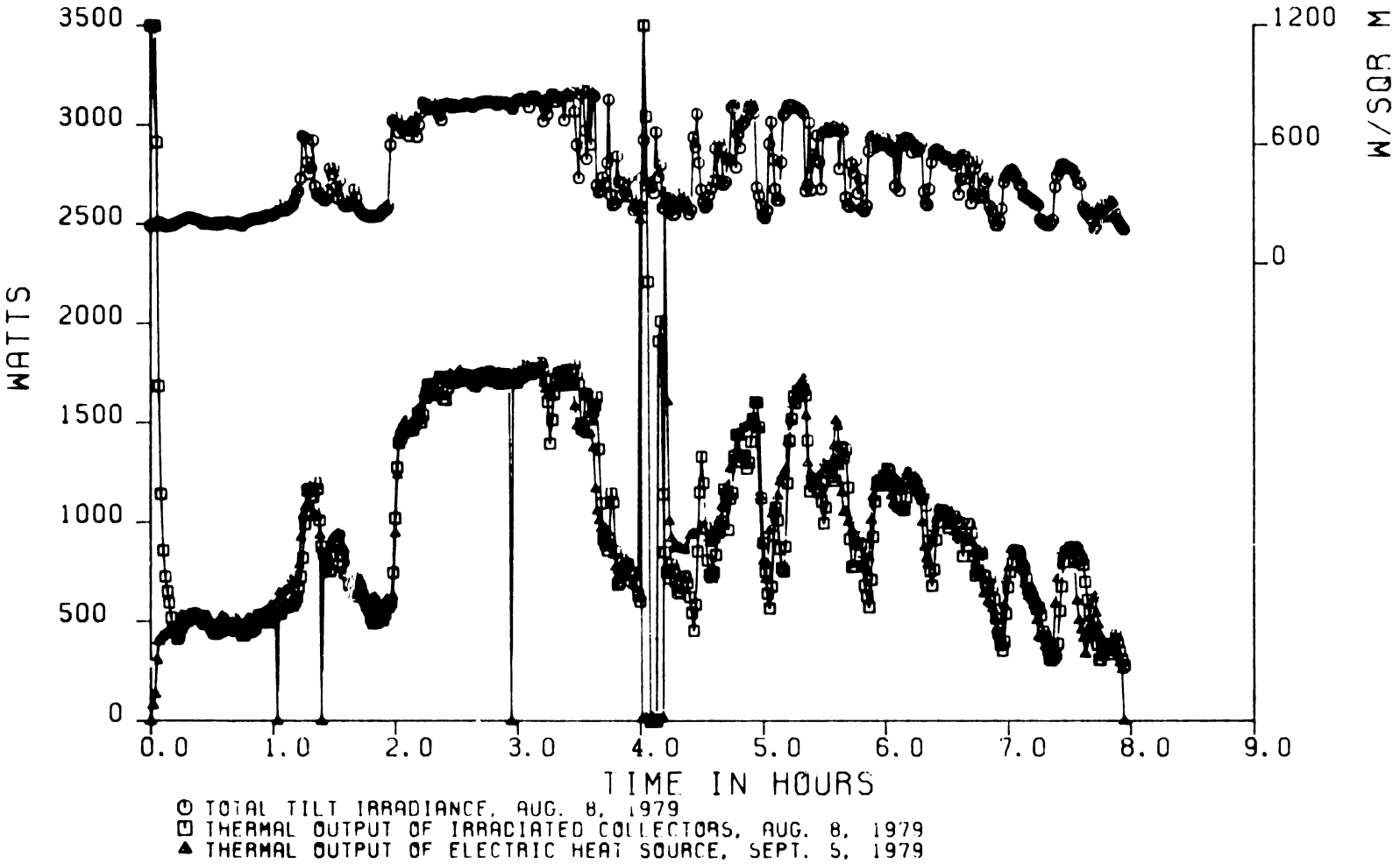

Figure 21. Thermal output comparison of irradiated collector array for August 8, 1979 and electric heat source for September 5, 1979

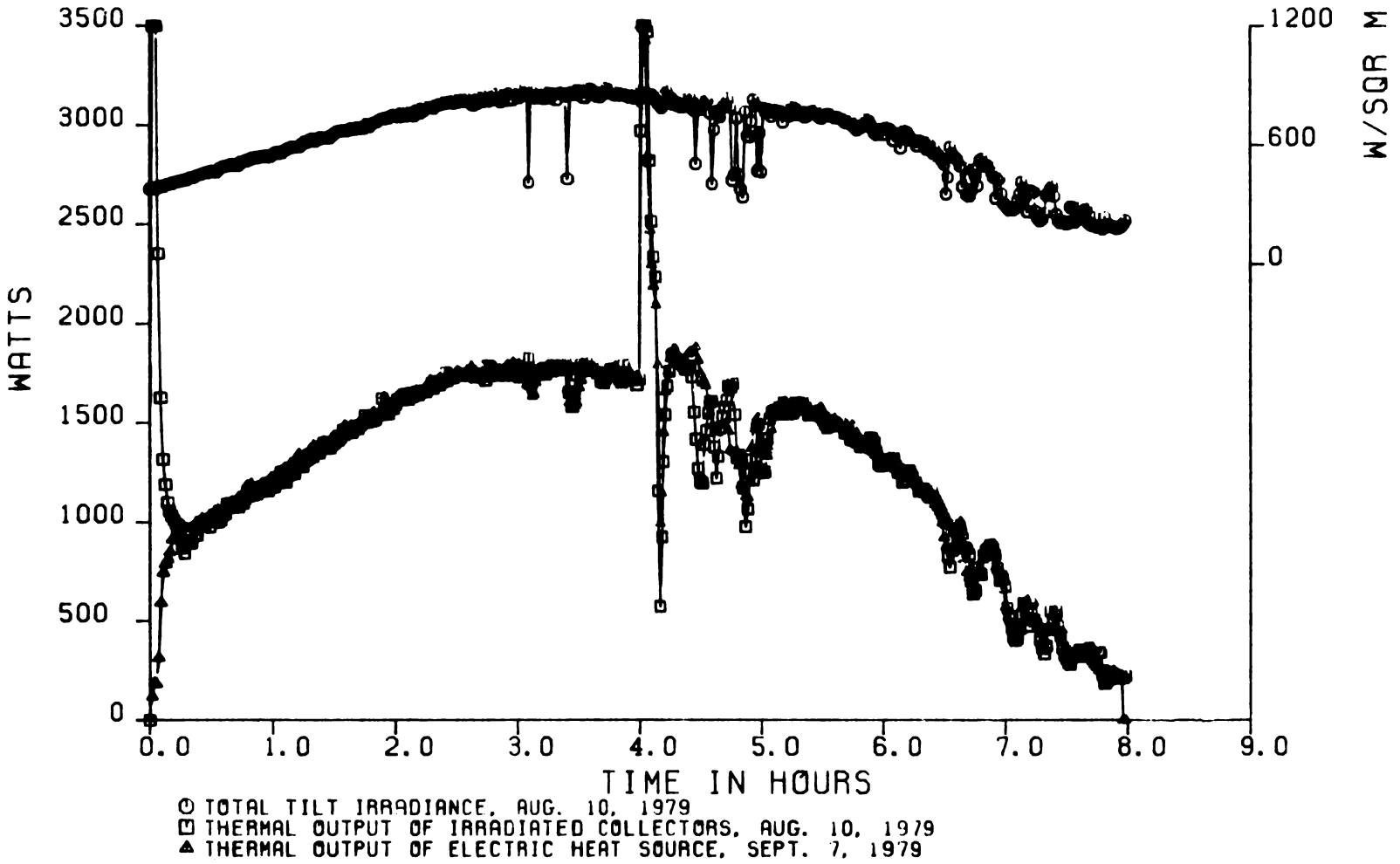

Figure 22. Thermal output comparison of irradiated collector array for August 10, 1979 and electric heat source for September 7, 1979

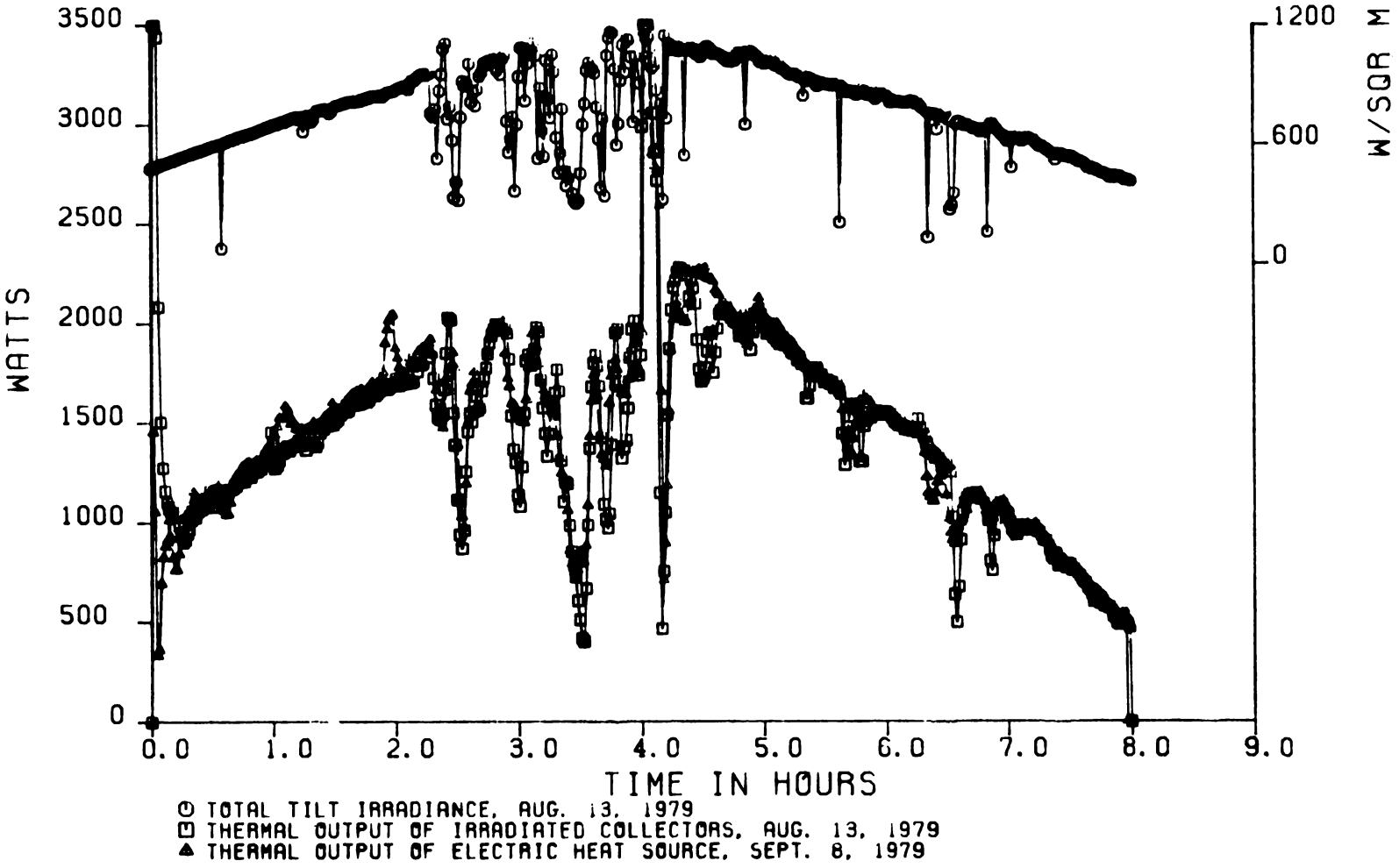

Figure 23. Thermal output comparison of irradiated collector array for August 13, 1979 and electric heat source for September 8, 1979

Table 1 shows the results of running the solar domestic hot water system with the irradiated array on four different days and repeating the tests for each day using the system with the electric heat source. It was possible to reproduce the outdoor daily collector output in the laboratory to within four percent even on the intermittently cloudy day of August 8 (figure 21). The daily fractional energy savings for the system with the electric heat source was within two percentage points for all the days tested. The fractional energy savings were calculated based on comparing the solar system with a 0.2 m^3 conventional electric water heater having thermal losses of 11,160 kJ per day.

The use of an electric heat source to simulate the thermal output of an irradiated array results in excellent agreement between outdoor and laboratory system performance. Additionally, a SDHW system may be tested with various numbers and types of collectors. These tests can be accomplished using corresponding values of $F_R(\tau\alpha)_n$, F_RU_L, and A_a without hardware changes. Outdoor stagnation conditions, however, cannot be accurately simulated using this technique. Thus, outdoor control functions cannot be duplicated indoors using an electric heat source only. A second disadvantage is the complexity of the calculation sequence. The calculation procedure requires that the real time measured quantities t_{fi} and $\dot{m}$ be used in addition to the simulated meteorological conditions.

4.2 REPLACEMENT OF THE IRRADIATED ARRAY WITH AN ELECTRIC HEAT SOURCE DOWNSTREAM OF A NONIRRADIATED ARRAY

An electric heat source downstream of a nonirradiated array is used to supply the net thermal output of an irradiated array. A fluid loop to bypass the storage tank allows stagnation conditions to be simulated within the laboratory.

The irradiated collector array system was allowed to operate in a normal manner for two days in October 1980 to provide a comparison basis for the system using an electric heat source downstream of a nonirradiated array. During the outdoor tests performed in August 1979, the pumps ran continuously during each test day except for a brief period on August 10. This continuous operation is attributed to the 20 C initial storage tank temperature. Initial storage tank temperatures of 35 C and 55 C were selected for October 6 and October 8, respectively, so that the controller would operate in a more typical manner. The test sequence for the irradiated system is identical to that followed in August 1979 until 17:15. Instead of deactivating the heating element and controller at 17:15, the system was allowed to operate until the controller cut the pumps off. At this time, water was withdrawn from the storage tank until the outlet temperature was within 1 C of the inlet temperature.

Tests were conducted in November 1980 using an electric heat source downstream of a nonirradiated array. The recorded incident irradiance during the comparison outdoor tests in conjunction with the mass flow rate correction procedure (Appendix A) allowed the quantity of power supplied to the electric heat source to be computed using eq (21). Input power was adjusted every three minutes throughout the test day. The ambient temperature surrounding the indoor nonirradiated collectors was controlled such that it was equivalent to the outdoor temperature during the irradiated system tests.

Table 1 Comparison of System Performance Using an Irradiated Collector Array to System Performance Using an Electric Heat Source

Variable	Aug 7/Sept 4		Aug 8/Sept 5		Aug 10/Sept 7		Aug 13/Sept 8	
Initial Storage Tank Temperature, C	21.7	23.7	20.2	21.9	20.2	20.2	21.2	19.6
Final Storage Tank Temperature, C	20.5	23.6	21.1	22.6	21.7	22.3	20.9	21.5
Daily Total Water Withdrawn, m	0.8203	0.8748	0.6416	0.8918	0.7423	1.053	0.6182	0.7635
Hot Water Energy Withdrawn at 13:15, kJ	12,610	12,190	11,930	12,500	12,060	12,250	12,380	12,630
Hot Water Energy Withdrawn at 17:15, kJ	12,080	11,140	12,190	12,470	12,000	12,130	12,170	12,210
Hot Water Energy Withdrawn at End of Day, kJ	28,750	24,890	18,440	15,290	24,410	20,270	27,590	25,090
Daily Energy Withdrawn From Storage Tank, kJ	53,440	48,220	42,560	40,260	48,470	44,650	52,140	49,930
Daily Total Solar Collector Array Output, kJ	41,740	41,020	29,410	28,360	38,720	37,630	42,370	42,360
Daily Solar Energy Delivered To Storage Tank, kJ	39,240	38,560	28,380	27,250	36,450	36,020	39,250	40,320
Daily Total Heat Loss from Collector Piping, kJ	2,500	2,460	1,030	1,110	2,270	1,610	3,120	2,040
Net Daily Increase in Stored Energy in Storage Tank, kJ	-1,570	-60	1,170	910	1,820	2,720	-390	2,460
Daily Energy Consumed by Heating Element, kJ	16,550	14,460	19,140	17,120	17,480	15,970	17,700	15,900
Daily Fractional Energy Savings, e, dimensionless	0.71	0.72	0.59	0.61	0.67	0.67	0.68	0.70

Table 2 compares the results obtained by running the irradiated system for the two selected days during October 1980 and repeating the tests using the system employing an electric heat source downstream of a nonirradiated array. The fractional energy savings was identical for the October 6 - November 17 comparison and within 3 percentage points for the October 8 - November 25 comparison. For both comparisons, the daily energy supplied by the electric heat source-nonirradiated array combination was higher than that delivered by the irradiated outdoor array, 2.8 percent for the October 6 - November 17 comparison and 3.4 percent for the October 8 - November 25 comparison. The combination of a higher effective sky temperature and a zero wind speed for the indoor system would tend to account for this difference.

Figures 24 and 25 show the incident tilt radiation for October 6 and 8, respectively. A comparison of the thermal output of the irradiated array with that of the nonirradiated array with downstream heat source is also shown. The large transients which occurred at the beginning of each test day resulted from the pumps cycling on and off. The pumps were initially energized when the systems were under stagnation conditions. When the incident irradiance on the outdoor collector system was not sufficient to maintain a 1.8 C temperature difference between the collector controller sensor and the storage tank sensor, the pumps were deactivated by the controller. Similarly, when the power input to the electric heat source was insufficient to maintain a 1.8 C temperature difference between the fluid leaving the heat source and the storage tank sensor, the controller deactivated the loop-bypass valves which stopped flow through the storage tank.

During the hot water draws, large transients in the thermal output occurred for both the irradiated collector system and the system using an electric heat source downstream of a nonirradiated array. The explanation for this behavior is identical to that given in the previous section. Figure 24 also shows an additional pump shutdown for both systems, shortly after the hot water draw, for the experiments with initial tank temperatures of 55 C. An explanation for this behavior for the irradiated collector array system follows. The reasoning is also valid for the nonirradiated collector array-heat source combination system. The pump restarted after the hot water draw and circulated the cold water in the bottom of the storage tank to the irradiated array. The water returning to the storage tank was at a lower temperature than the water in the upper portion of the tank. Mixing occurred within the storage tank. As the pump continued to operate, warm water reached the controller sensor location. The controller tank sensor temperature increased sufficiently to deactivate the pump. Under stagnation conditions, the temperature of the collector sensor increased and reactivated the pump. Due to the lower initial storage tank temperature during the October 8 - November 25 tests, this sequence of events did not occur after the hot water draw.

Figures 26 and 27 show the controller operation for October 6 and 8, respectively. There is good controller operation agreement between the irradiated system and the nonirradiated array with downstream heat source system. The total elapsed pump operation time for the irradiated system for October 6 was 424.6 minutes as compared to 427.5 minutes for the nonirradiated array-heat source system. On October 8, the circulators on the irradiated system operated

Table 2 Comparison of System Performance Using an Irradiated Array to System Performance Using a Nonirradiated Array With Downstream Heat Source

Variable	October 6/November 17 Irradiated Array	October 6/November 17 Nonirradiated Array With Downstream Heat Source	October 8/November 25 Irradiated Array	October 8/November 25 Nonirradiated Array With Downstream Heat Source
Initial Storage Tank Temperature, C	55.1	55.4	35.1	35.3
Final Storage Tank Temperature, C	20.0	19.4	20.6	19.9
Daily Total Water Withdrawn, m	0.8767	0.6987	0.8396	0.6884
Hot Water Energy Withdrawn at 13:00, kJ	13,902	14,806	12,120	13,034
Hot Water Energy Withdrawn at End of Day, kJ	53,256	52,368	49,790	47,947
Daily Energy Withdrawn From Storage Tank, kJ	67,158	67,174	61,910	60,981
Daily Total Solar Collector Array Output, kJ	34,098	35,065	37,160	38,434
Daily Solar Energy Delivered To Storage Tank, kJ	28,680	28,330	34,464	35,011
Daily Total Heat Loss from Collector Piping, kJ	5,418	6,735	2,696	3,423
Net Daily Increase in Stored Energy in Storage Tank, kJ	-44,595	-42,675	-17,326	-18,378
Daily Energy Consumed by Heating Element, kJ	3,520	3,384	14,634	12,636
Total Circulator Elapsed Running Time, min	424.6	427.5	479.4	489.7
Daily Fractional Energy Savings, e, dimensionless	.882	.882	.701	.731

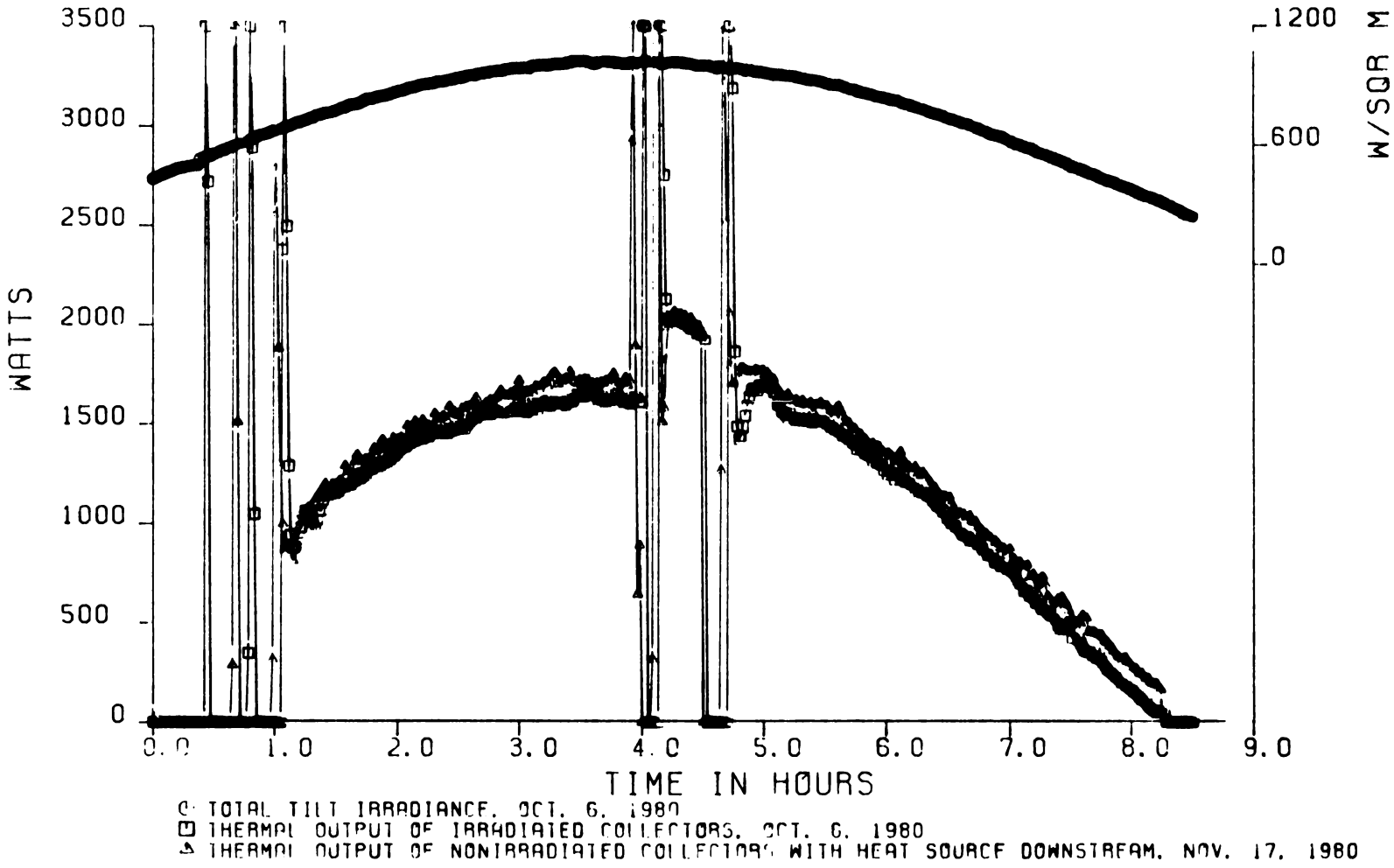

Figure 24. Thermal output comparison of irradiated collector array for October 6, 1980 and nonirradiated collector array with downstream heat source for November 17, 1980

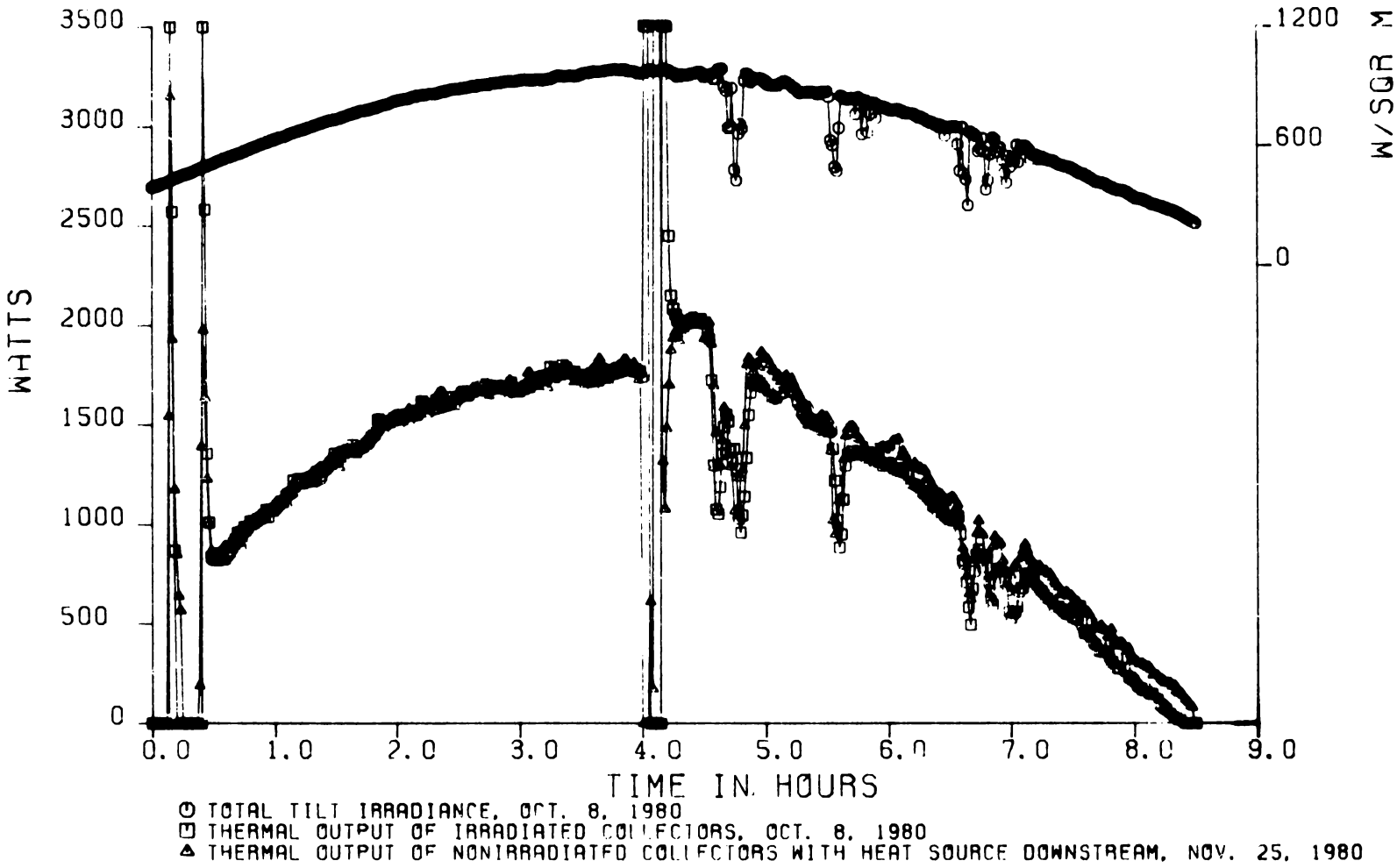

Figure 25. Thermal output comparison of irradiated collector array for October 8, 1980 and nonirradiated collector array with downstream heat source for November 25, 1980

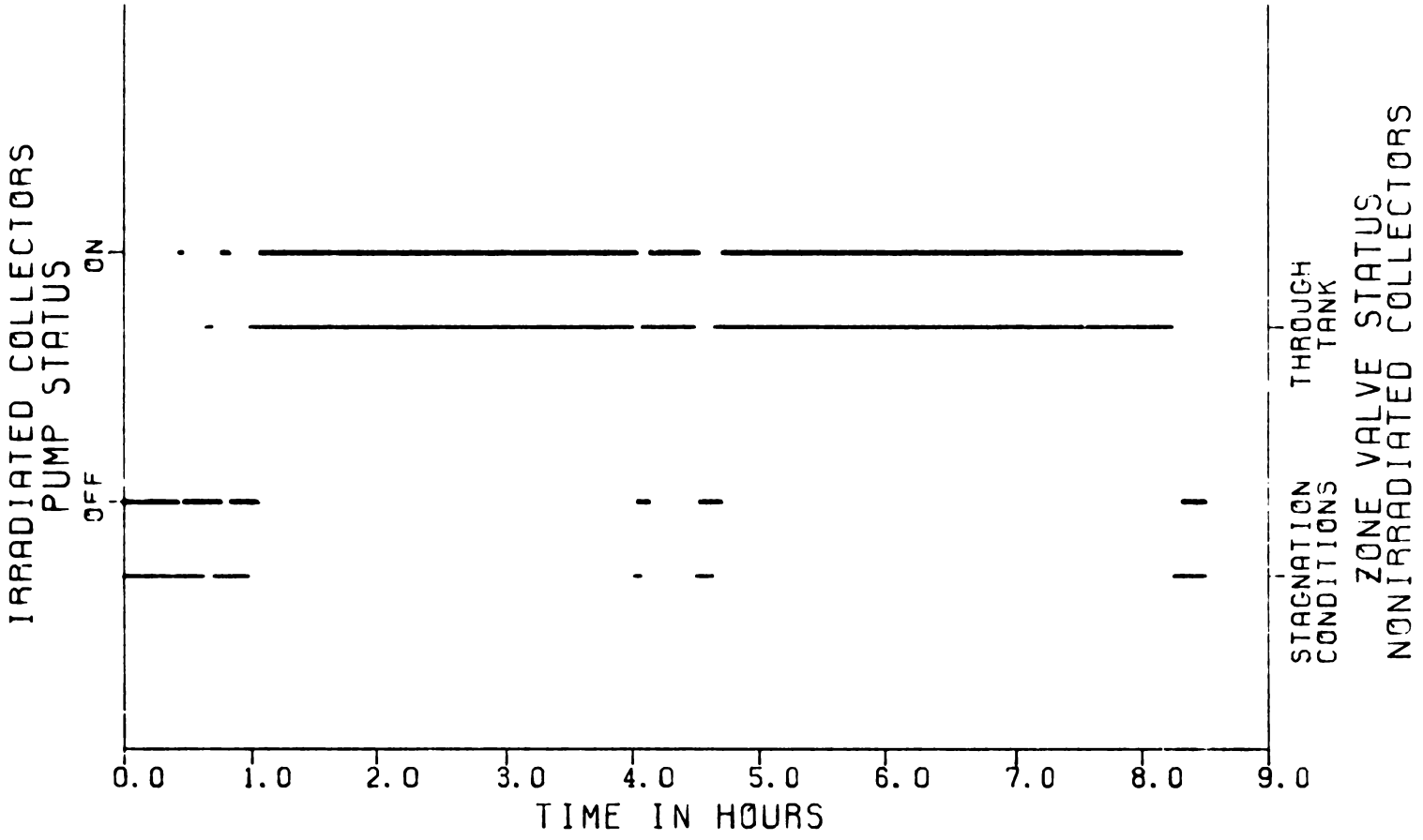

Figure 26. Controller operation comparison of irradiated collector array for October 6, 1980 and nonirradiated collector array with downstream heat source for November 17, 1980

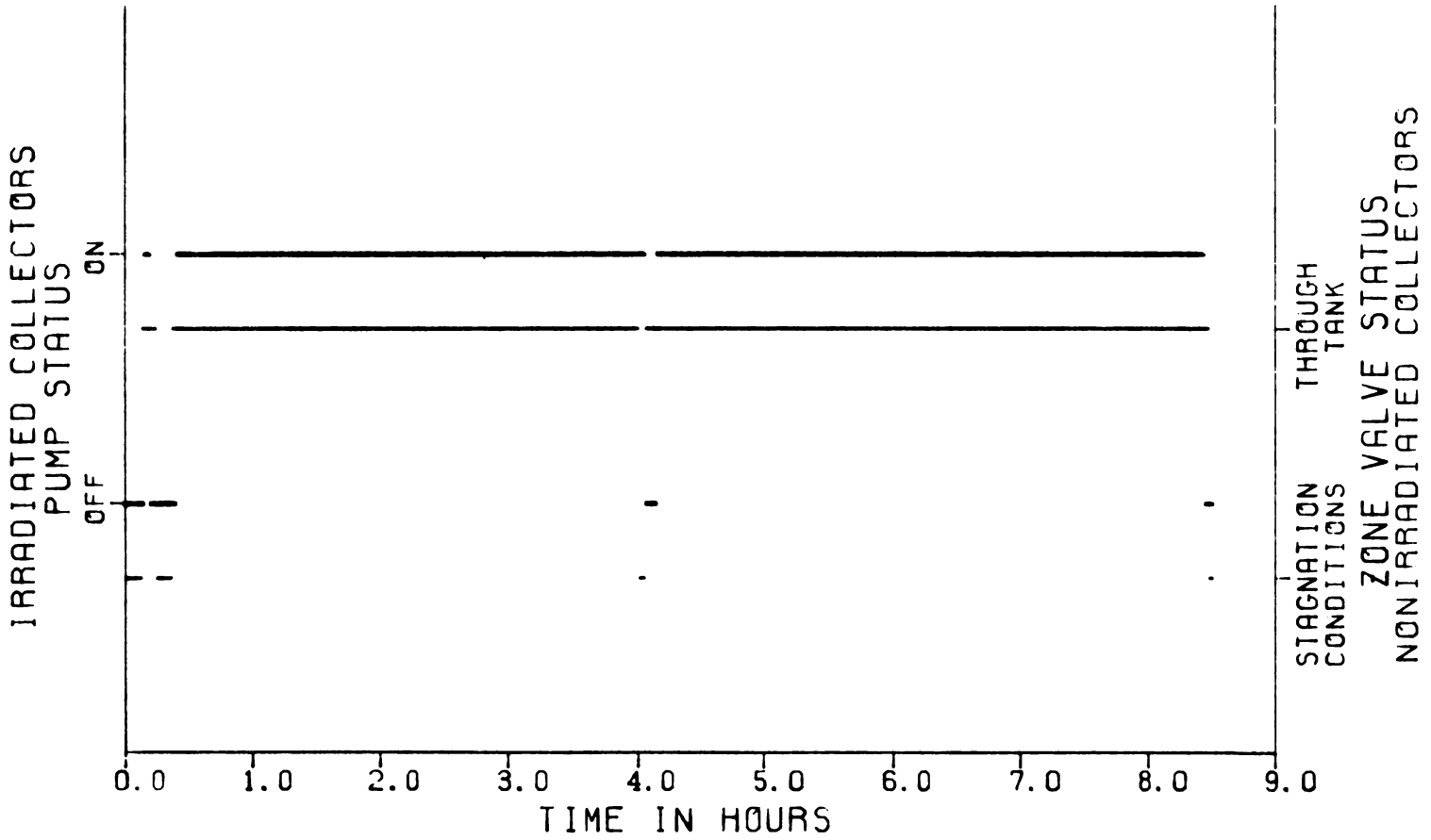

Figure 27. Controller operation comparison of irradiated collector array for October 8, 1980 and nonirradiated collector array with downstream heat source for November 25, 1980

for 479.4 minutes compared to 489.7 minutes for the nonirradiated array-heat source system. In addition to the good agreement between total circulator operation time, there is excellent agreement among the times when the circulator operated and the times at which stagnation conditions existed.

Using a nonirradiated collector array with a downstream heat source to supply the thermal output of an irradiated array results in excellent agreement between outdoor and laboratory system performance. Outdoor stagnation conditions can be simulated and thus outdoor control functions can be duplicated. With the heat source located downstream of a nonirradiated array, the calculation procedure is simpler than the calculation sequence for the electric heat source only. The ASHRAE 95 Committee extended this method to allow either an upstream or a downstream heat source, and incorporated it into the ASHRAE 95 Test Procedure. No experiments were performed at NBS using an upstream heat source.

4.3 REPLACEMENT OF AN IRRADIATED ARRAY USING STRIP HEATERS ATTACHED TO NONIRRADIATED SOLAR COLLECTORS

Solar energy absorbed by the irradiated absorber plates is replaced by energy supplied by electric strip heaters attached to the backside of nonirradiated absorber plates.

The irradiated collector array system operated on October 6 and 8, 1980 provided a basis for comparison with the system using electric strip heaters. These two test days have been described in the previous section.

Tests were conducted in April 1981 using electric strip heaters attached to the back of nonirradiated absorber plates. The recorded incident irradiance during the comparison outdoor tests allowed the quantity of power supplied to the strip heaters to be computed using eq (27). Power supplied to the strip heaters was updated every three minutes. The ambient temperature surrounding the indoor nonirradiated collectors was controlled such that it was equivalent to the outdoor temperature during the irradiated system tests. The test procedure was identical to that followed during the irradiated system tests in October 1980.

Table 3 compares the results of operating the solar domestic hot water system with an irradiated array and repeating the tests for each day using the system with electric strip heaters attached to the nonirradiated absorber plates. The daily fractional energy savings for the system using strip heaters was 2.4 percent higher than the irradiated array system for the October 6 - April 1 comparison, and 1.9 percent higher for the October 8 - April 2 comparison. For both comparisons, the daily quantity of energy supplied by the system using the nonirradiated array with attached strip heaters was within 0.9 percent of that supplied by the irradiated array. Figures 28 and 29 show the incident tilt radiation for October 6 and 8, respectively. A comparison between the thermal output of the irradiated array and that of the nonirradiated array with strip heaters is also shown. Examination of figures 28 and 29 reveals that the thermal output of the irradiated array is greater than the thermal output of the nonirradiated array with attached strip heaters before solar noon. After solar noon, the thermal output of the nonirradiated array with

Table 3 Comparison of System Performance Using an Irradiated Array to System Performance Using a Nonirradiated Array With Attached Strip Heaters

Variable	October 6/April 1 Irradiated Array	October 6/April 1 Nonirradiated Array With Attached Strip Heaters	October 8/April 2 Irradiated Array	October 8/April 2 Nonirradiated Array With Attached Strip Heaters
Initial Storage Tank Temperature, C	55.1	56.9	35.1	36.5
Final Storage Tank Temperature, C	20.0	20.0	20.6	19.9
Daily Total Water Withdrawn, m	0.8767	0.5784	0.8396	0.6681
Hot Water Energy Withdrawn at 13:00, kJ	13,902	13,103	12,120	13,103
Hot Water Energy Withdrawn at End of Day, kJ	53,256	53,784	49,790	45,296
Daily Energy Withdrawn From Storage Tank, kJ	67,158	66,887	61,910	54,919
Daily Total Solar Collector Array Output, kJ	34,098	33,816	37,160	36,945
Daily Solar Energy Delivered To Storage Tank, kJ	28,680	26,823	34,464	33,950
Daily Total Heat Loss from Collector Piping, kJ	5,418	6,992	2,696	2,994
Net Daily Increase in Stored Energy in Storage Tank, kJ	-44,595	-43,651	-17,326	-19,828
Daily Energy Consumed by Heating Element, kJ	3,520	2,597	14,634	12,024
Total Circulator Elapsed Running Time, min	424.6	436.1	479.4	501.8
Daily Fractional Energy Savings, e, dimensionless	.882	.906	.701	.720

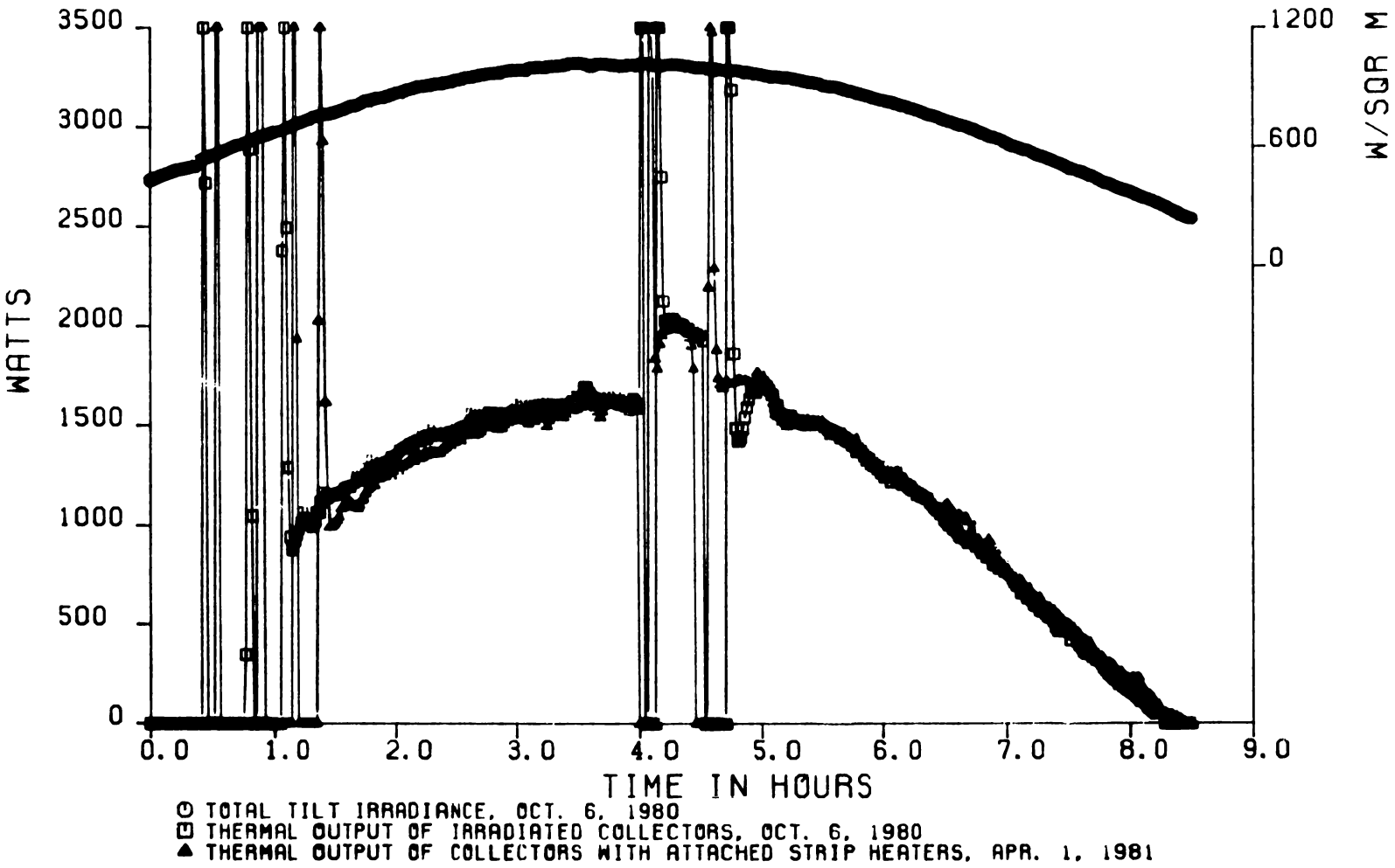

Figure 28. Thermal output comparison of irradiated collector array for October 6, 1980 and nonirradiated collector array with attached strip heaters for April 1, 1981

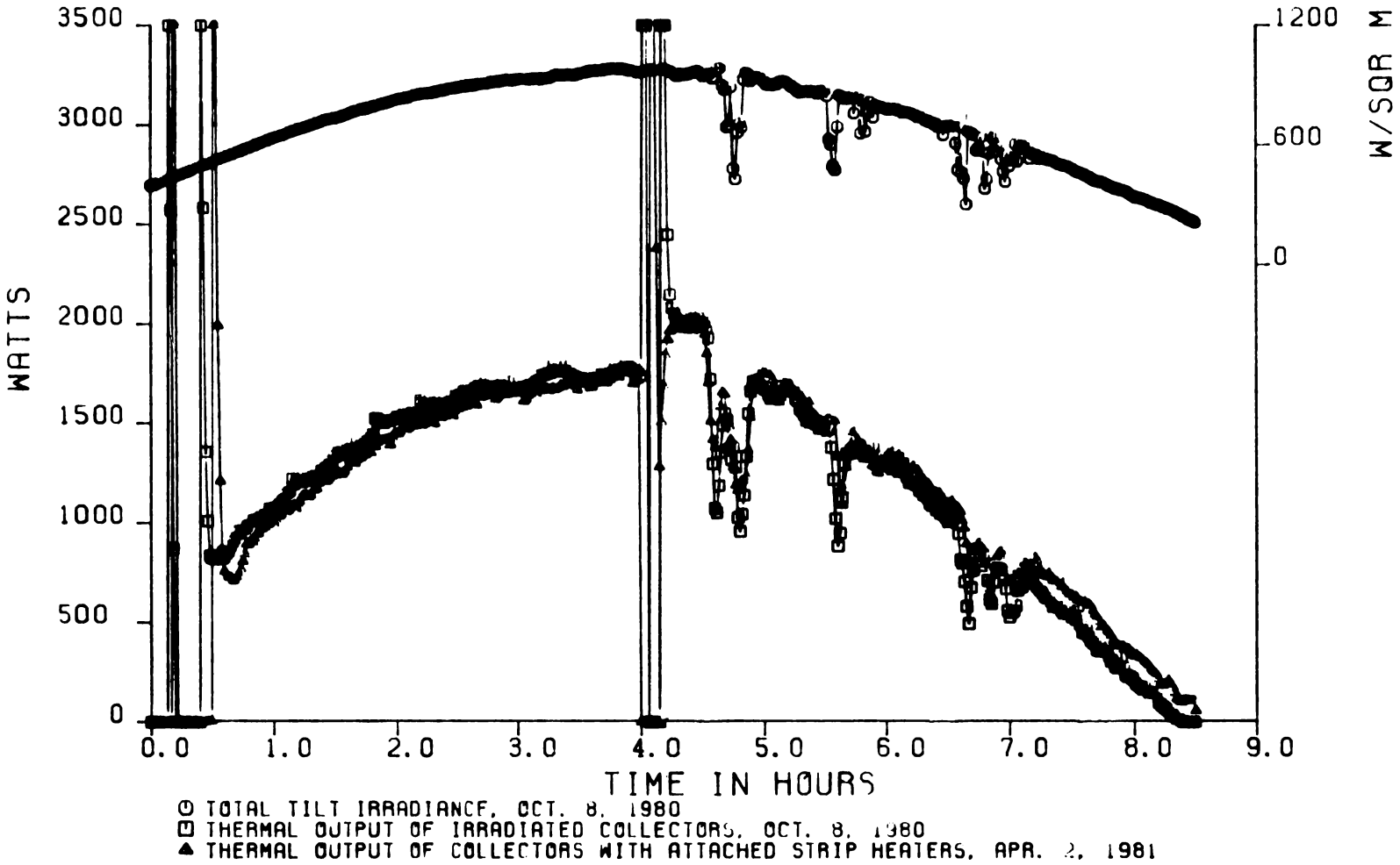

Figure 29. Thermal output comparison of irradiated collector array for October 8, 1980 and nonirradiated collector array with attached strip heaters for April 2, 1981

attached strip heaters is greater than the thermal output of the irradiated array. This behavior may be attributed to the increased effective thermal capacity of the collector array which results from attaching strip heaters to the absorber plates. The thermal capacity of an individual collector to which strip heaters have been added is approximately 50 percent greater than an unmodified collector.

Figure 30 shows the circulator pump status for October 6, 1980 and April 1, 1981. There is good agreement between the two test days among the times at which the circulators operated and the times at which stagnation conditions existed. The system using the electric strip heaters experienced one additional "off" period as compared to the irradiated system. The total elapsed pump operation time for the irradiated system was 424.6 minutes as compared to 436.1 minutes for the system using nonirradiated collectors with strip heaters attached to the absorber plates. The circulator pump status for October 8, 1980 and for April 2, 1981 is shown in figure 31. The circulators for the irradiated system operated for a total of 479.4 minutes as compared to 501.8 minutes for the system using nonirradiated collectors with attached strip heaters. Agreement between the times at which stagnation conditions existed and times at which the circulators operated is excellent.

Thermal performance agreement between the system using an irradiated array and the system which uses electric strip heaters attached to nonirradiated collector absorber plates is excellent. Outdoor stagnation conditions can be duplicated without the use of a storage tank bypass loop. The calculation procedure required to determine the amount of power supplied to the strip heaters is independent of mass flow rate and fluid type. Testing of an individual collector module, according to the ASHRAE 93-77 Test Procedure, is not necessary if the optical properties of the collector are known. Thermosyphon systems may be tested using this technique. This method, however, requires that the collectors be partially disassembled. Also, the absorber must be reasonably flat and sized to be compatible with commercially available strip heaters.

4.4 TEST PROCEDURE SENSITIVITY TO STORAGE TANK STRATIFICATION

Experiments have been conducted to determine if the ASHRAE 95 Test Procedure is sensitive to temperature stratification in the storage tank. Storage tank temperature stratification is influenced by the design and dimensions of the storage tank, velocity at which fluids enter the tank, and the manner in which fluids are introduced into the storage tank. During this experimental investigation, several designs of return tubes, which introduce the solar heated water into the storage tank, were fabricated and tested. The storage tank was not altered and the mass flow rate thrcugh all return tubes was maintained at 0.055 kg/s.

An electric heat source downstream of a nonirradiated array was used in the studies to determine the influence of each return tube on storage tank stratification. The recorded outdoor irradiance and associated incident angle for October 6, 1980 were used to calculate the quantity of power supplied to the electric heat source. The input power was updated every five minutes. Ambient temperature surrounding the nonirradiated array was maintained at 20 C. Each test began with an initial 20 C storage tank temperature. The circulator pumps

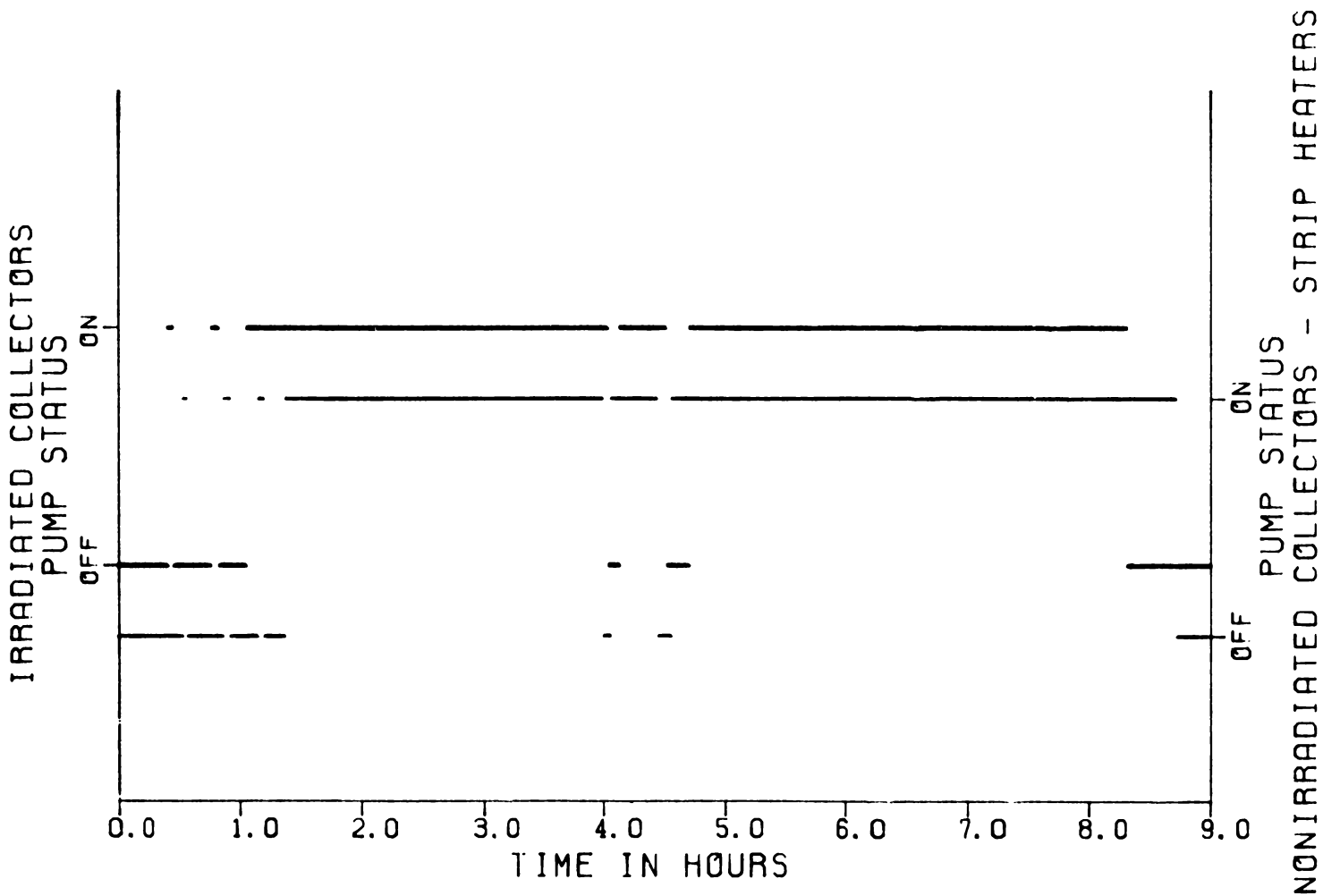

Figure 30. Controller operation comparison of irradiated collector array for October 6, 1980 and nonirradiated collector array with attached strip heaters for April 1, 1981

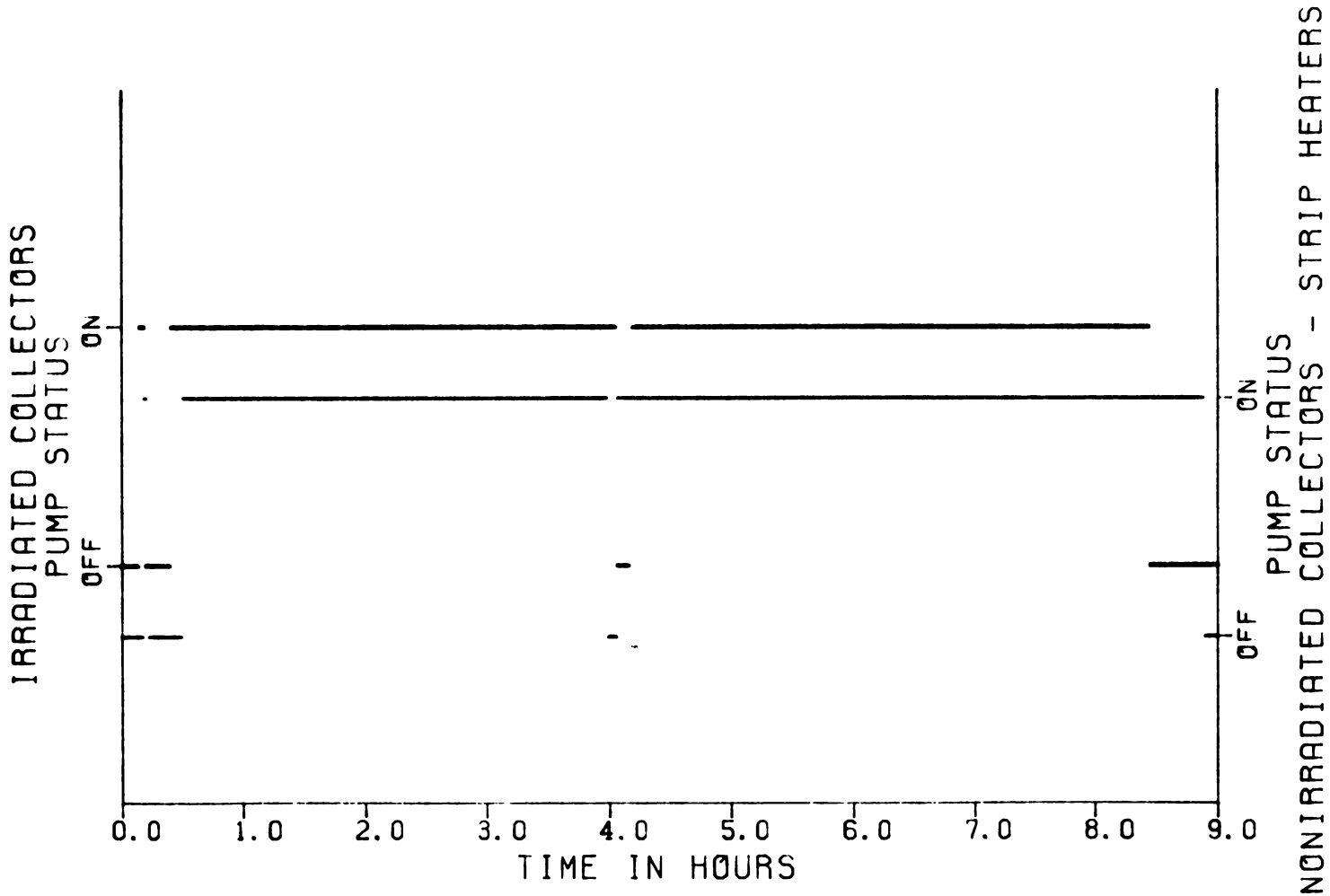

Figure 31. Controller operation comparison of irradiated collector array for October 8, 1980 and nonirradiated collector array with attached strip heaters for April 2, 1981

and storage tank heating element were energized at 09:00. Power was supplied to the electric heat source from 09:00 to 11:30.

Construction details for each return tube and the resulting storage tank temperature distributions are shown in figures 32 through 45. Details of the return tube which was used in the previously described experiments are given in figure 32. Figure 33 shows the resulting storage tank temperature distribution. The upper thermocouple shows the influence of the heating element. The temperature of this thermocouple increases rapidly until the thermostat deactivates the heating element. The upper thermocouple temperature subsequently decreases as a result of heat loss from the storage tank and mixing within the tank. The second thermocouple from the top, located 25.4 mm below the heating element, is also influenced by the heating element. The bottom portion of the storage tank is well mixed as shown by the temperatures of the bottom seven thermocouples. Figure 34 shows a return tube which redirects the downward axial fluid flow into a number of radially directed fluid streams. Two concentric tubes were used in an effort to eliminate any downward momentum. The resulting temperature distribution, figure 35, shows improved stratification as compared with figure 33. Figure 36 shows a commercially available return tube which also redirects the downward axial fluid flow. Only one tube, with holes drilled in the radial direction, is used. The resulting temperature distribution is displayed in figure 37. Stratification in the lower portion of the tank is almost identical to that displayed in figure 35. The temperature decay in the upper portion of the tank is slightly greater than that shown in figure 35.

Three return tubes, as shown in figures 38, 39, and 40, were constructed such that fluid enters the storage tank in a single radially directed fluid stream. The corresponding temperature profiles, as shown in figures 41, 42, and 43, are essentially identical. The bottom seven thermocouples display a temperature profile equivalent to the profile shown in figures 35 and 37. The temperature decay rate for the two uppermost thermocouples is greater than the decay rate displayed in figures 35 and 37 but less than the decay rate exhibited in figure 33.

A return tube consisting of a number of radially directed openings at a fixed elevation is shown in figure 44. The temperature decay rate for the two uppermost thermocouples, shown in figure 45, is less than the rate displayed in figures 33, 41, 42, and 43 but greater than that exhibited in figures 35 and 37.

The return tube shown in figure 34 was selected as the best among those considered for promoting stratification within the storage tank. Figure 32 shows the return tube which provided virtually no stratification in the storage tank and a rapid temperature decay rate for the two uppermost thermocouples.

All-day tests were performed using each return tube to determine if the ASHRAE 95 Test Procedure is sensitive to temperature stratification in the storage tank. The recorded outdoor irradiance and associated incident angle of October 6, 1980 were used to calculate the quantity of power supplied to the electric heat source. Input power was updated every three minutes. Ambient temperature surrounding the nonirradiated collectors was maintained at 20 C. Storage tank initial temperature was 35 C. The controller and heating element were energized

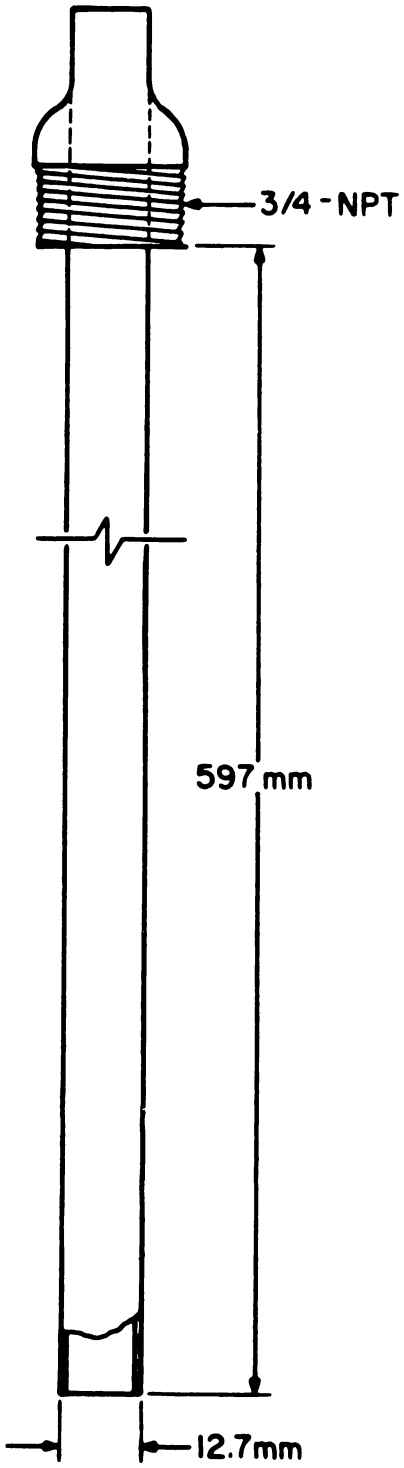

Figure 32. Return tube construction details

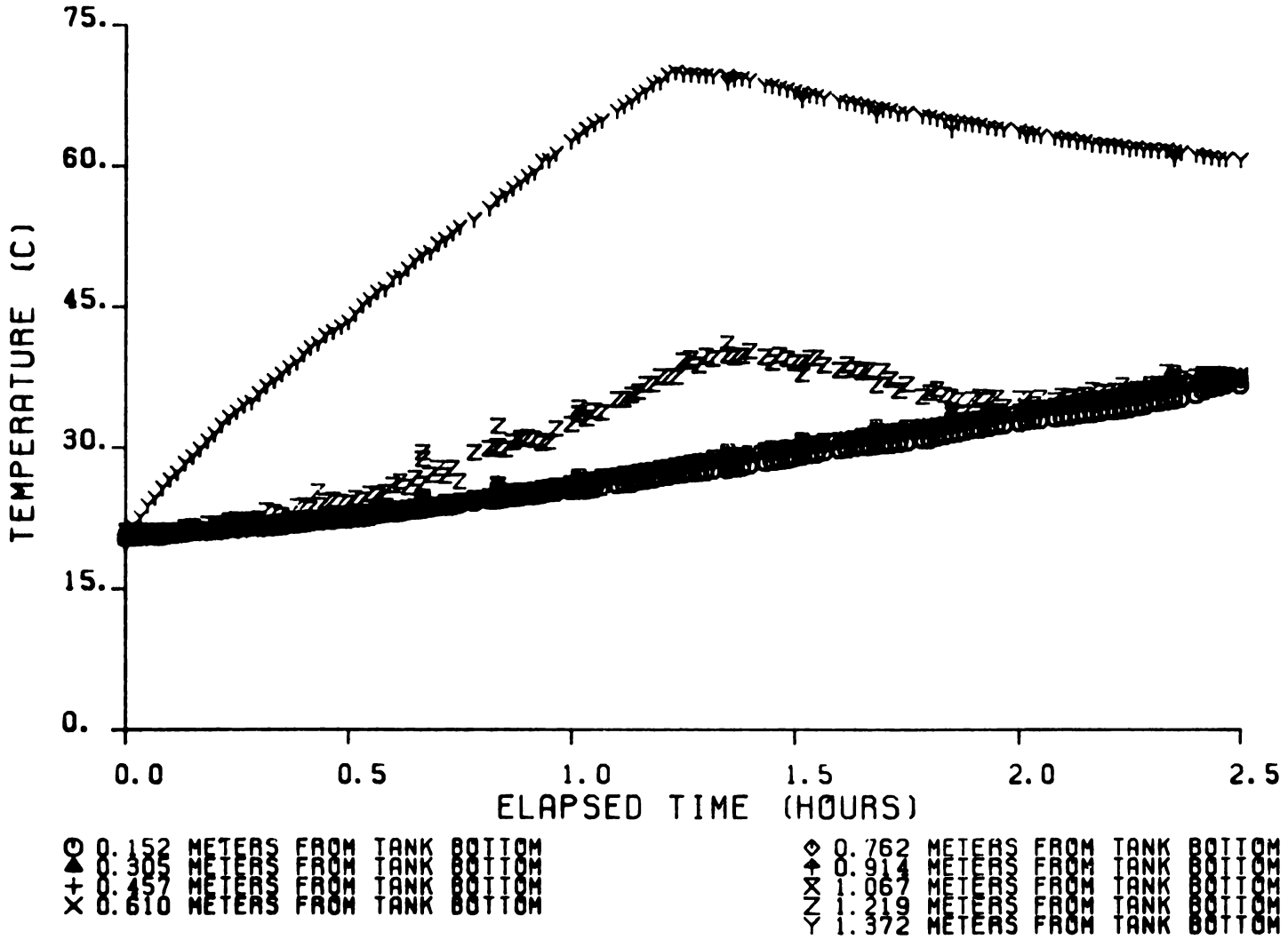

Figure 33. Storage tank temperature distribution for the return tube shown in figure 32

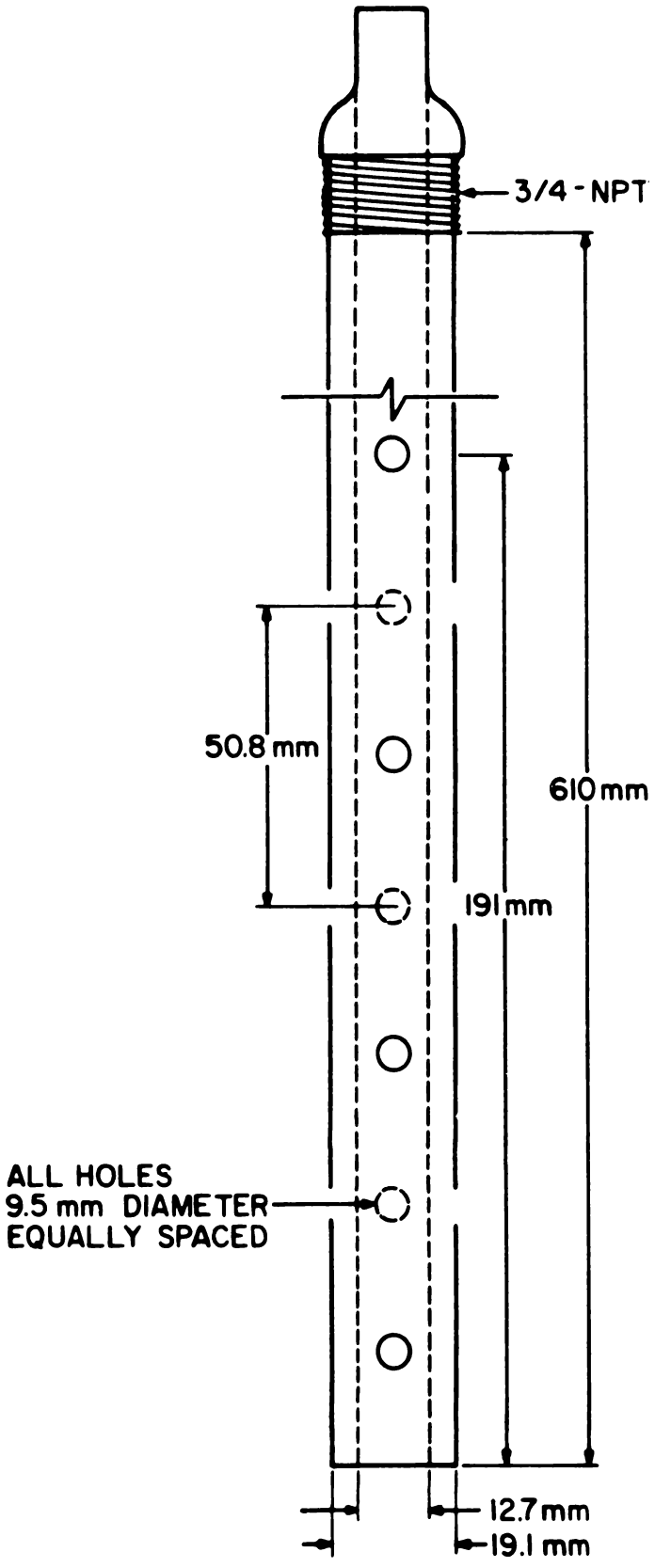

Figure 34. Return tube construction details

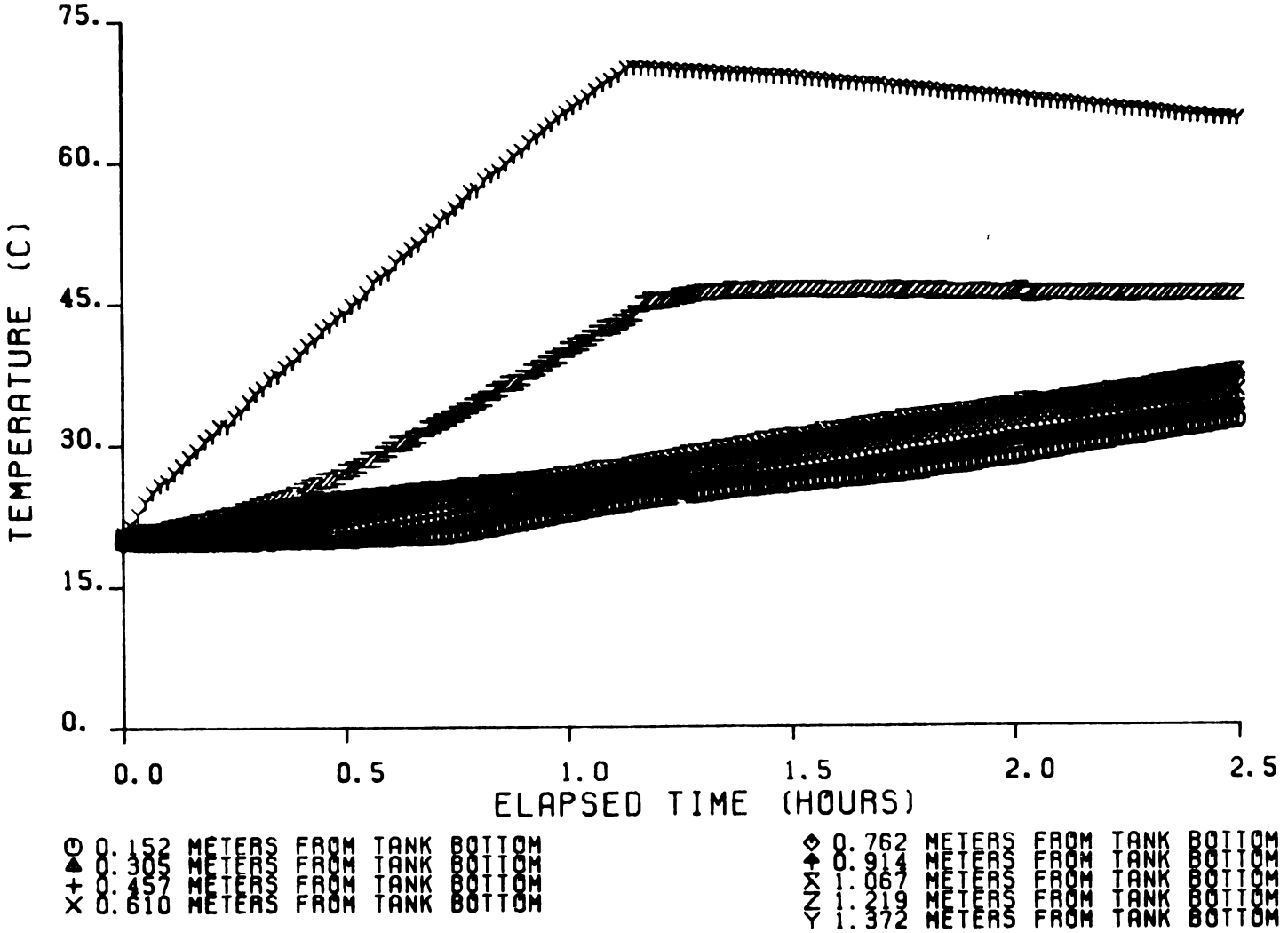

Figure 35. Storage tank temperature distribution for the return tube shown in figure 34

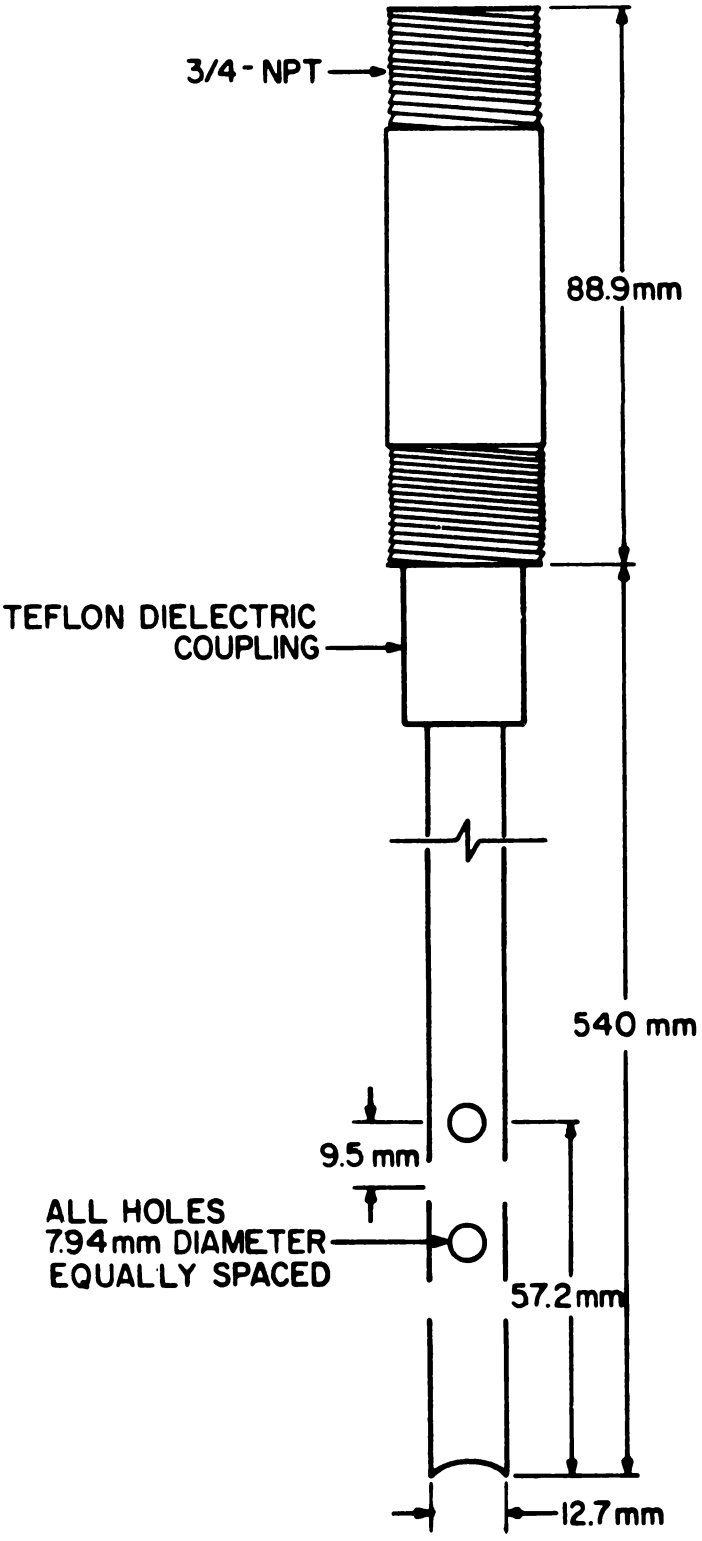

Figure 36. Construction details of a commercially available return tube

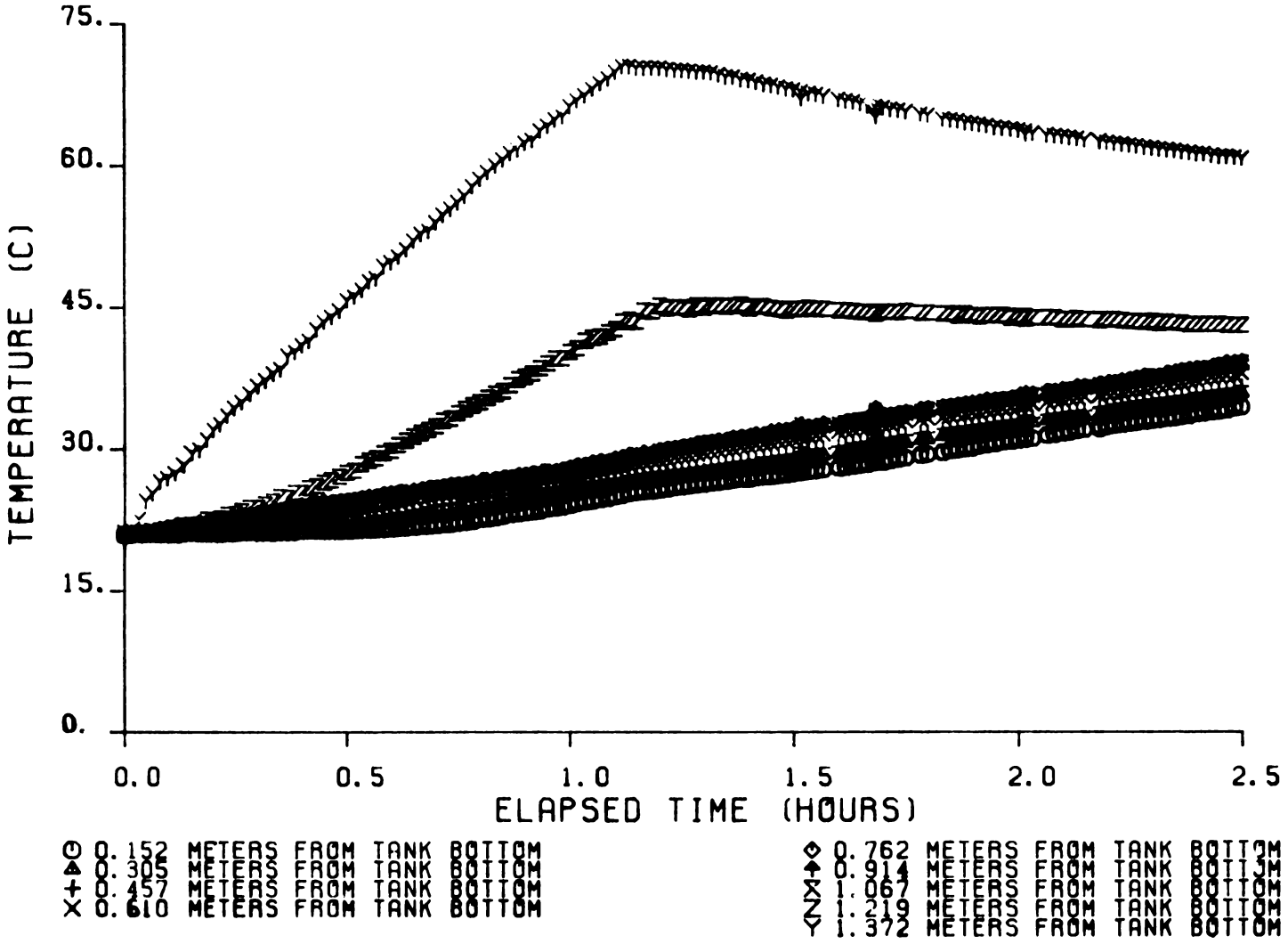

Figure 37. Storage tank temperature distribution for the commercially available return tube

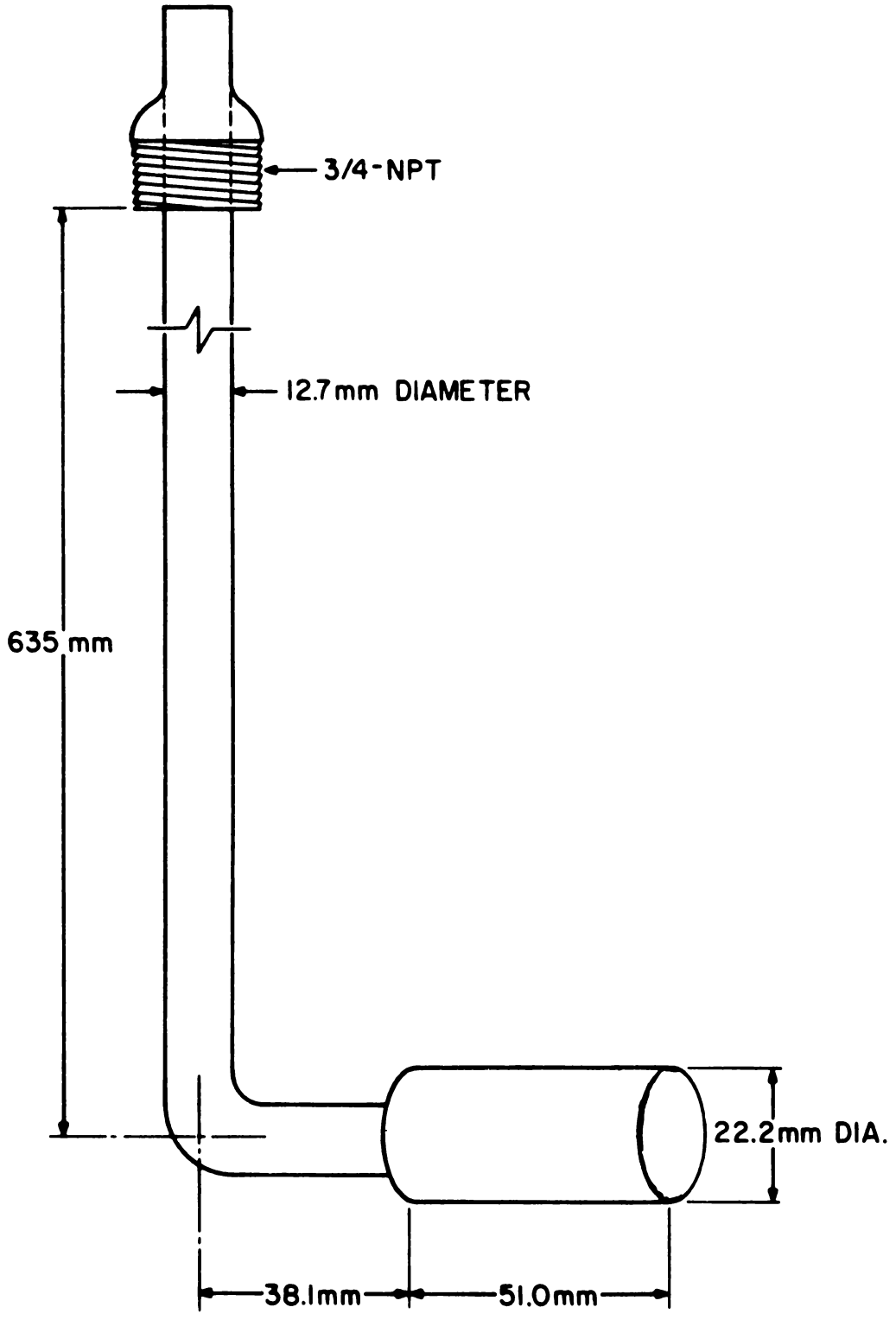

Figure 38. Return tube construction details

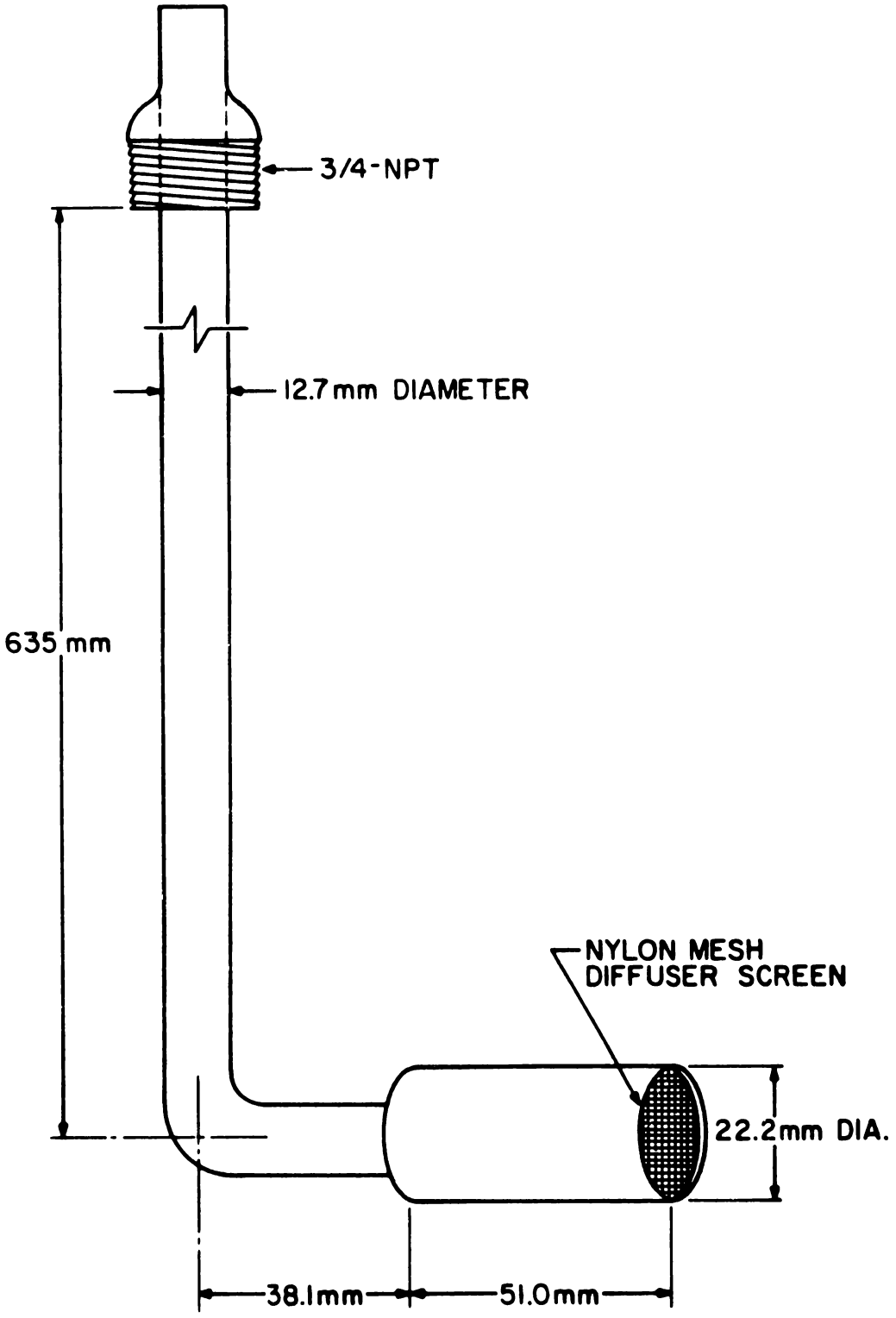

Figure 39. Return tube construction details

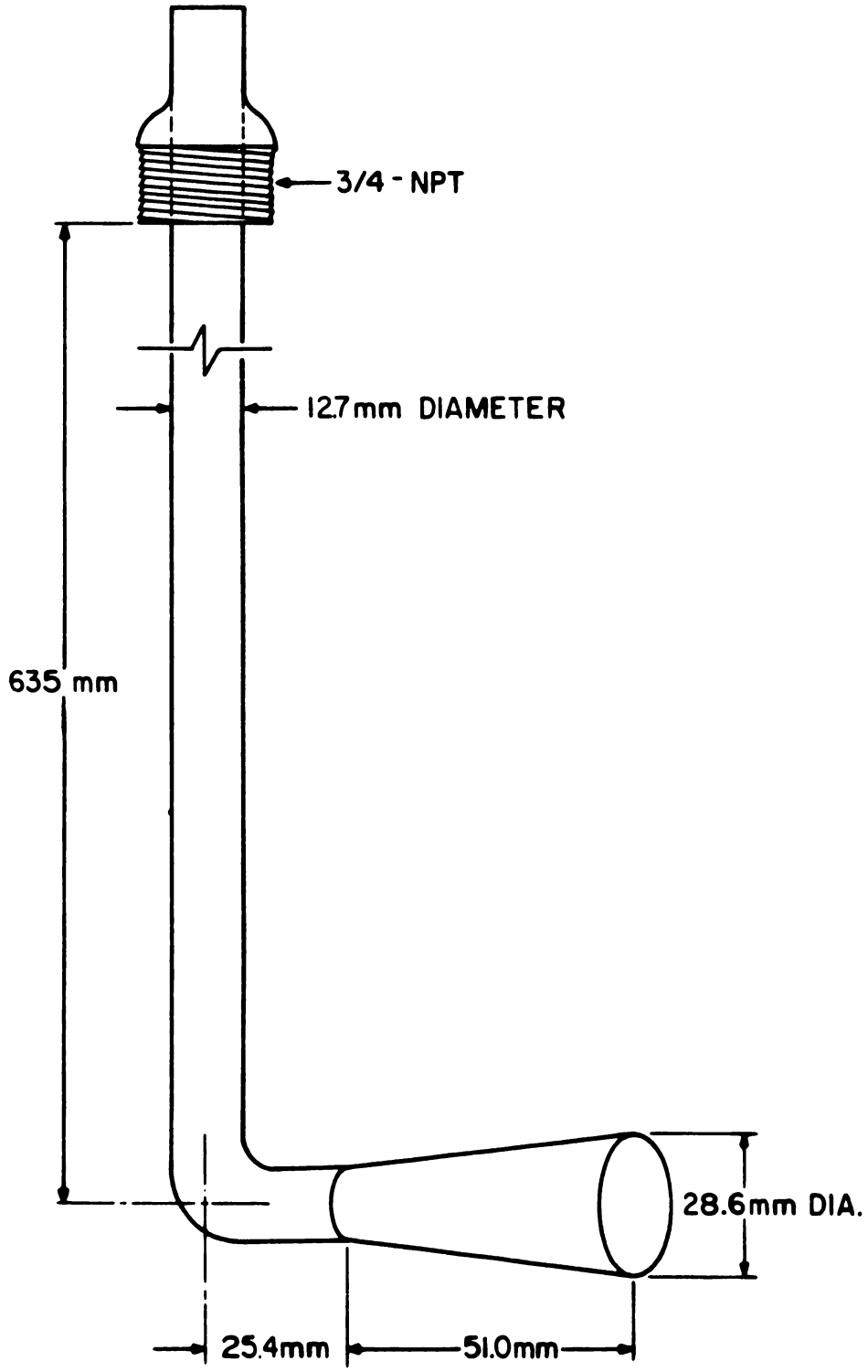

Figure 40. Return tube construction details

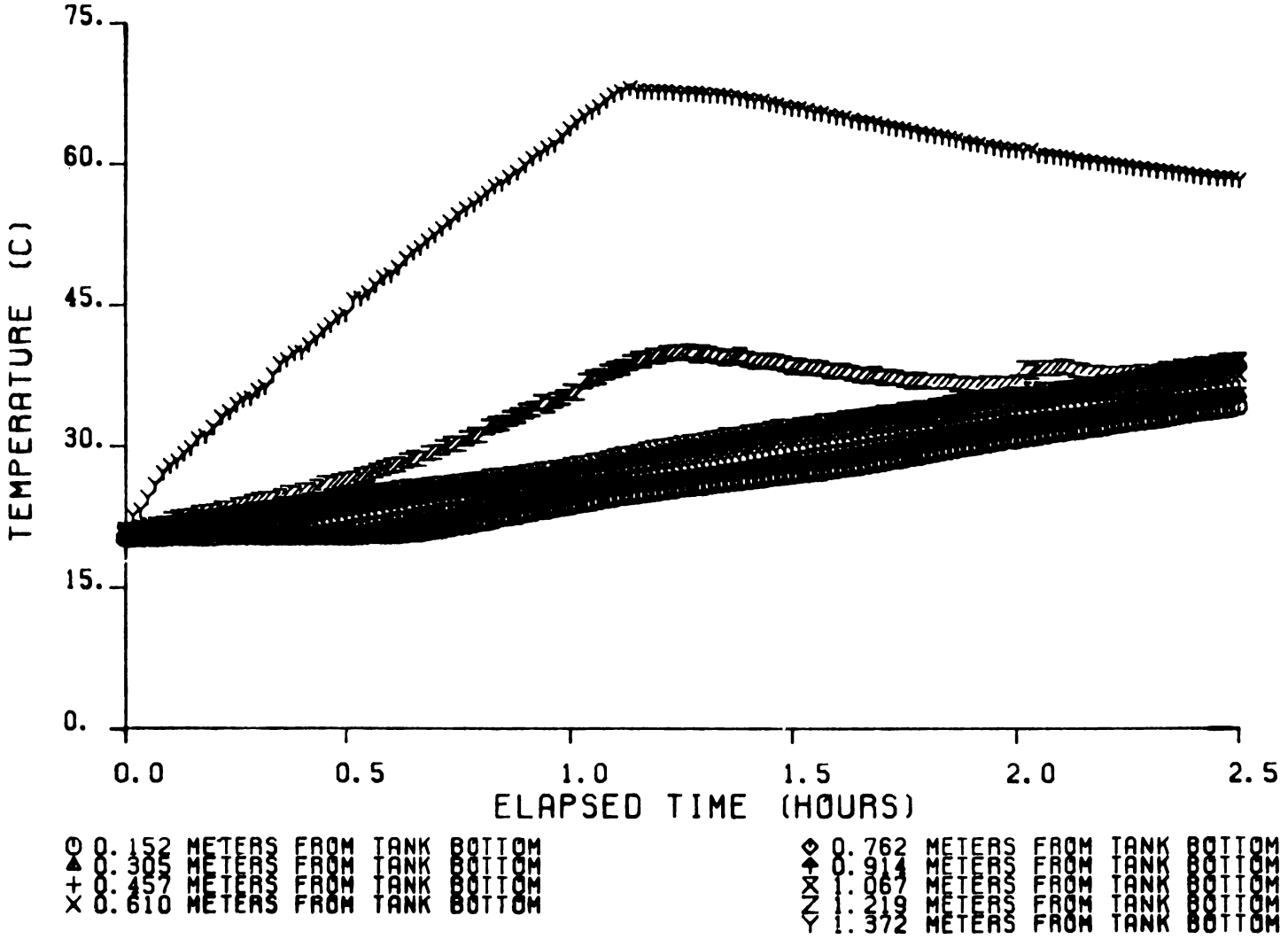

Figure 41. Storage tank temperature distribution for the return tube shown in figure 38

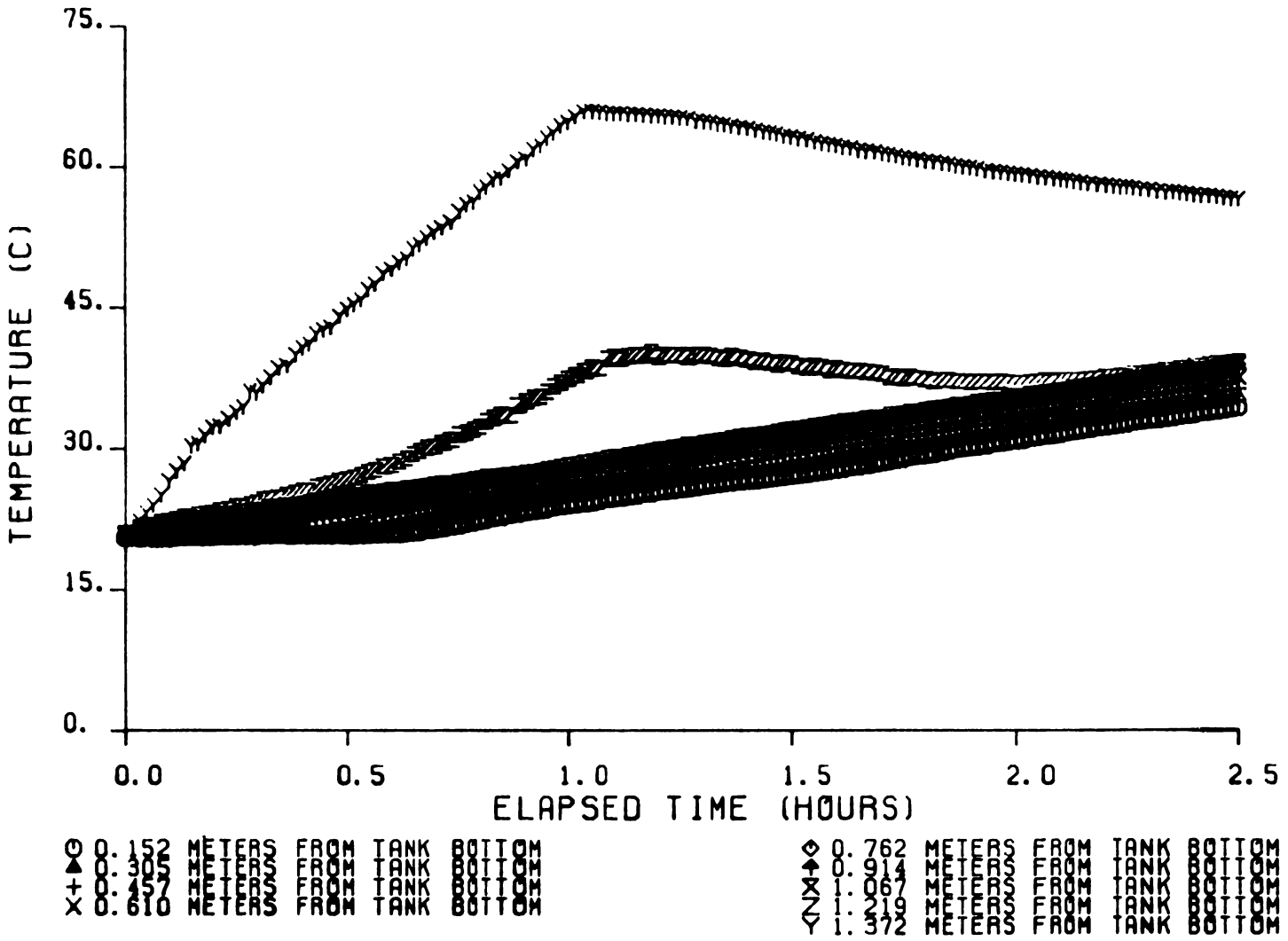

Figure 42. Storage tank temperature distribution for the return tube shown in figure 39

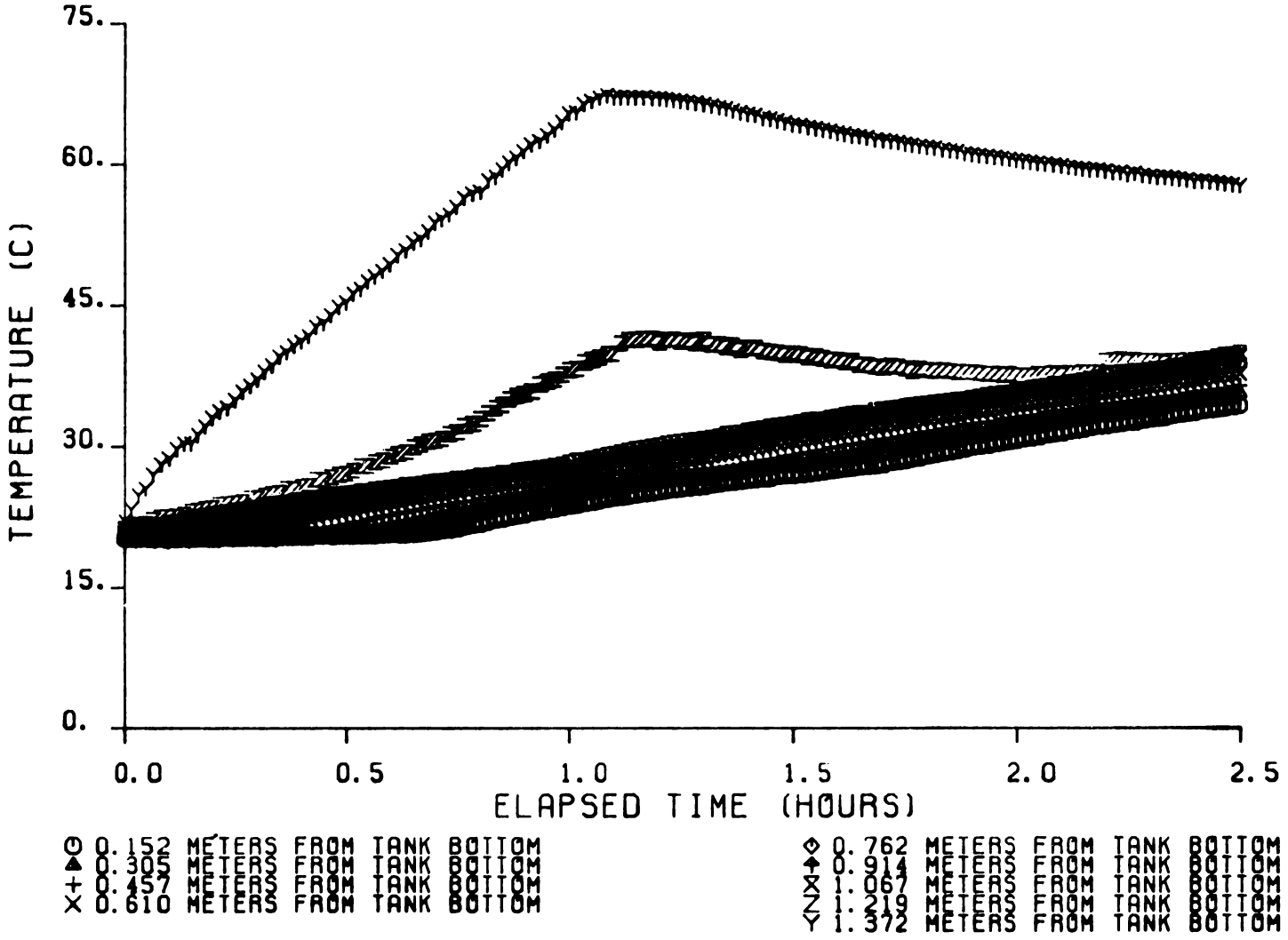

Figure 43. Storage tank temperature distribution for the return tube shown in figure 40

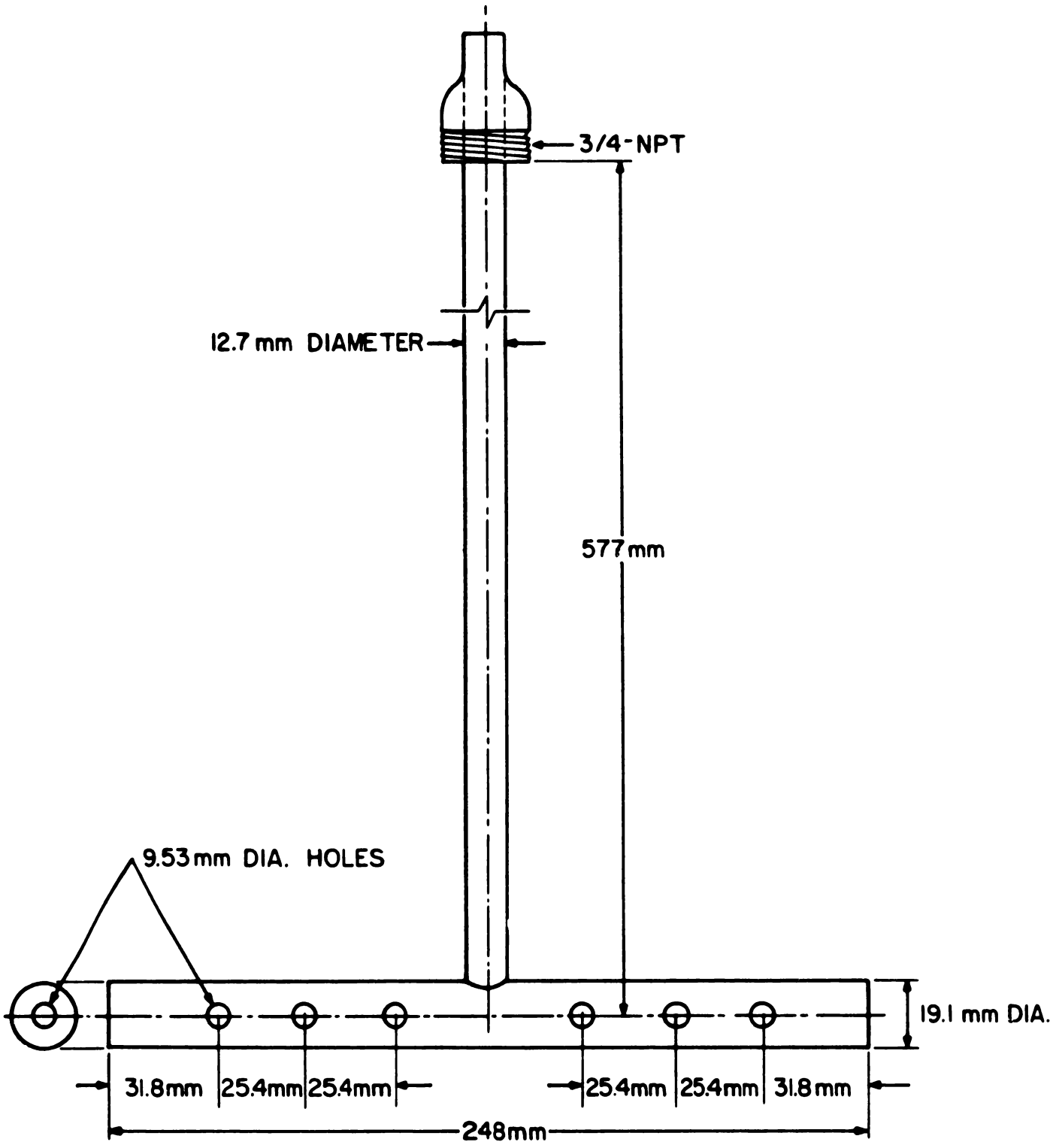

Figure 44. Return tube construction details

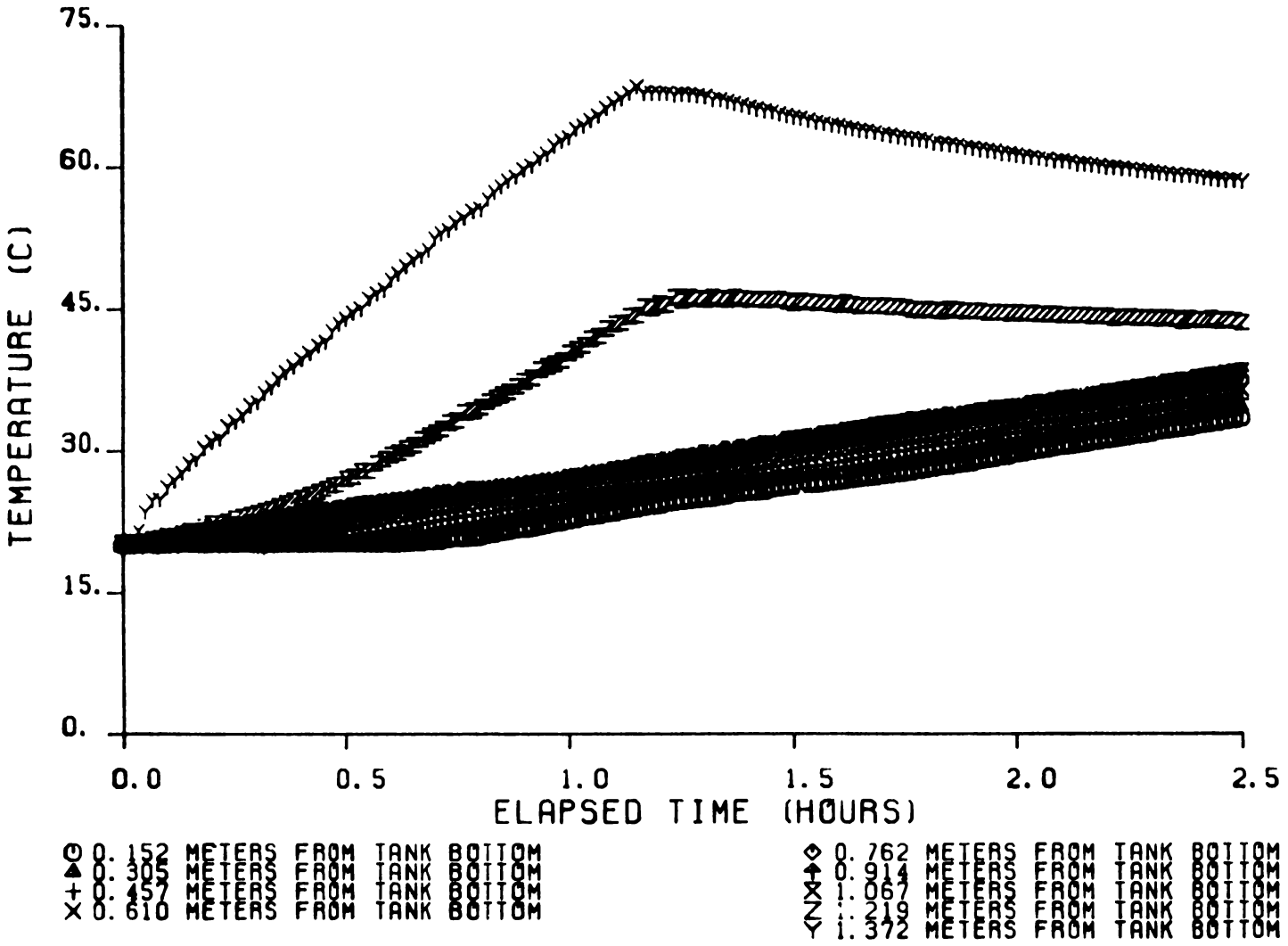

Figure 45. Storage tank temperature distribution for the return tube shown in figure 44

were used to calculate the quantity of power supplied to the electric heat source. Input power was updated every three minutes. Ambient temperature surrounding the nonirradiated collectors was maintained at 20 C. Storage tank initial temperature was 35 C. The controller and heating element were energized at 09:00. One hot water draw occurred during each test day at 13:00. The draw consisted of water entering the storage tank at 20 C at a flow rate of 2×10^{-4} m^3/s. During withdrawal periods, the incoming water temperature and water temperature leaving the tank were measured. Near the end of the test day, the system was allowed to operate until the controller deactivated the circulator pumps. At the conclusion of each test day, water was withdrawn from the storage tank until the outlet temperature was within 1 C of the inlet temperature. The quantity of energy withdrawn was then computed. The power used by the storage tank heating element was measured during each test.

Figure 46 displays the tank temperature distribution for February 3, 1981, during which, the return tube which best promoted stratification was used. The tank temperature distribution for January 29, 1981, as shown in figure 47, resulted when the return tube shown in figure 32 was used. Table 4 gives the results of running the hot water system for January 29, 1981 and February 3, 1981. The fractional energy savings which results from a stratified tank is 8.7 percent higher than the fractional energy savings which occurs using a tank which exhibits minimal stratification. The slower temperature decay rate in the upper portion of the tank results in lower auxiliary energy usage for the system where the tank is stratified. The stratified storage tank temperature profile also results in a lower inlet fluid temperature to the collector array as compared to the mixed storage tank temperature profile. The lower inlet fluid temperature allows the collector array to operate at a higher efficiency and thus a greater quantity of energy is delivered to the storage tank.

Based on these results, it is concluded that the ASHRAE 95 Test Procedure is sensitive to the degree of temperature stratification which occurs in the storage tank.

4.5 REPEATABILITY OF TEST RESULTS

The test conducted on January 29, 1981 was repeated on February 4, 1981 to determine the repeatability of the ASHRAE 95 Test Procedure. The same return tube, as shown in figure 32, was used in both tests. Table 5 gives the test results for January 29, 1981 and February 4, 1981. The daily fractional energy savings was within 0.1 percent for the two test days.

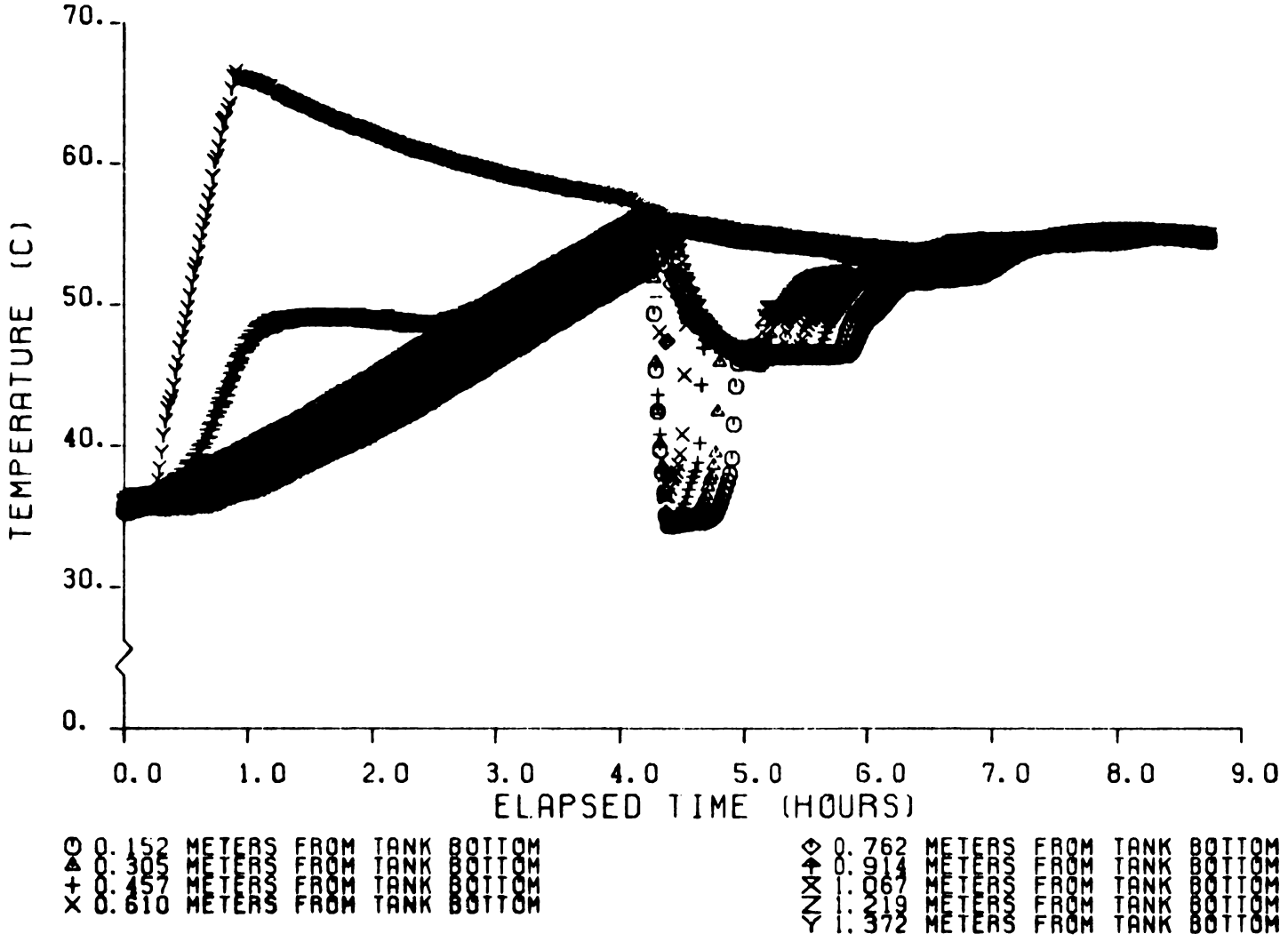

Figure 46. Storage tank temperature distribution for stratification sensitivity test, February 3, 1981

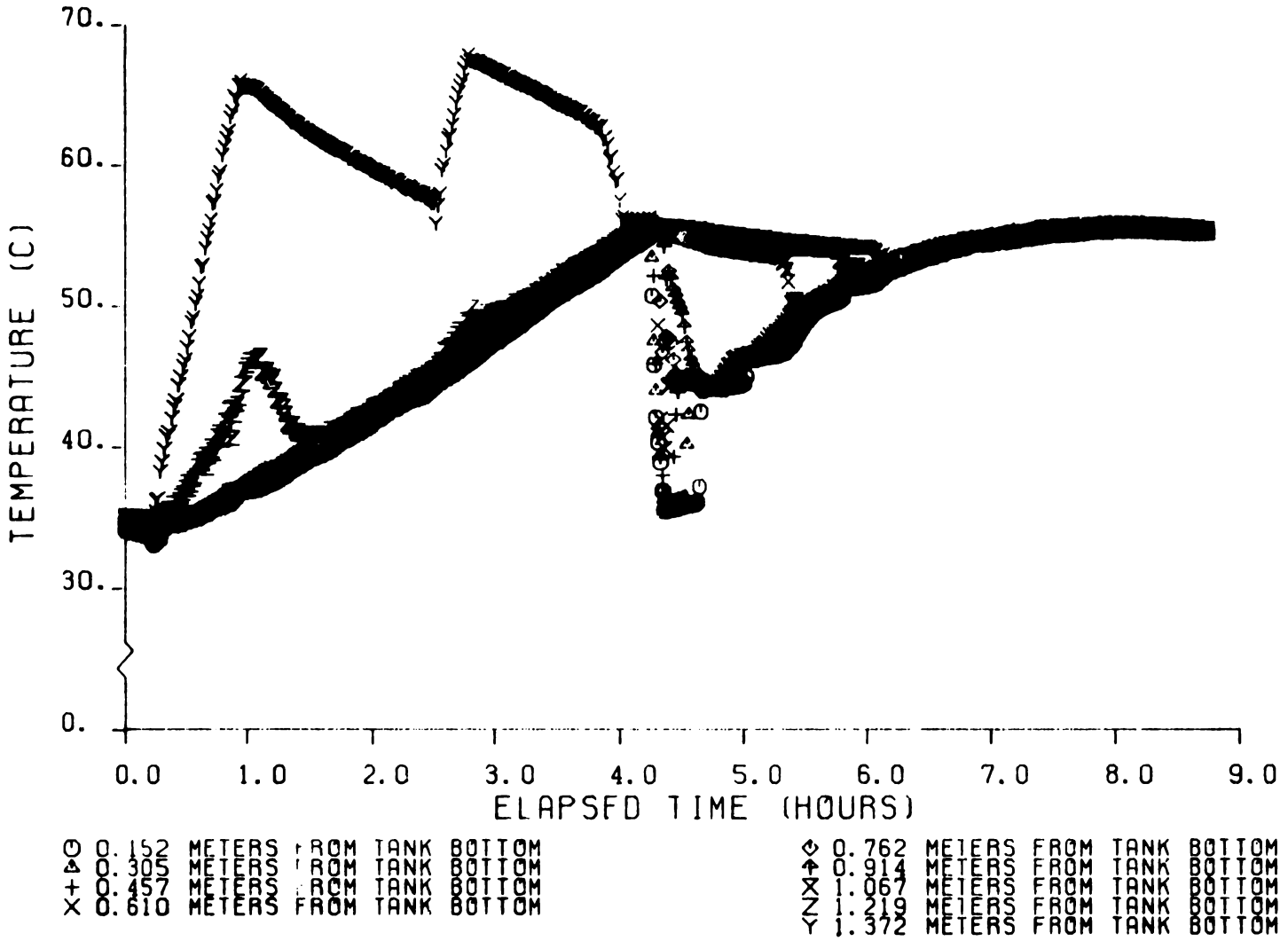

Figure 47. Storage tank temperature distribution for stratification sensitivity test, January 29, 1981

Table 4 Comparison of System Performance for Two Return Tube Designs

Variable	January 29, 1981 MIXED Tank Temperature Profile	February 3, 1981 STRATIFIED Tank Temperature Profile
Initial Storage Tank Temperature, C	34.7	35.9
Final Storage Tank Temperature, C	19.4	19.5
Daily Total Water Withdrawn, m	0.6299	0.6102
Hot Water Energy Withdrawn at 13:00, kJ	12,975	13,442
Hot Water Energy Withdrawn at End of Day, kJ	44,292	43,152
Daily Energy Withdrawn From Storage Tank, kJ	57,267	56,594
Daily Total Thermal Output of Heat Source Downstream of Nonirradiated Array, kJ	37,722	38,519
Daily Solar Energy Delivered To Storage Tank, kJ	34,091	35,650
Daily Total Heat Loss from Collector Piping, kJ	3,631	2,869
Net Daily Increase in Stored Energy in Storage Tank, kJ	-18,302	-19,512
Daily Energy Consumed by Heating Element, kJ	11,160	7,052
Total Circulator Elapsed Running Time, min	513.6	516.7
Daily Fractional Energy Savings, e, dimensionless	.743	.830

Table 5 Repeatability of Test Results Using ASHRAE STANDARD 95

Variable	January 29, 1981	February 4, 1981
Initial Storage Tank Temperature, C	34.7	34.8
Final Storage Tank Temperature, C	19.4	19.8
Daily Total Water Withdrawn, m	0.6299	0.5001
Hot Water Energy Withdrawn at 13:00, kJ	12,975	13,318
Hot Water Energy Withdrawn at End of Day, kJ	44,292	44,142
Daily Energy Withdrawn From Storage Tank, kJ	57,267	57,460
Daily Total Thermal Output of Heat Source Downstream of Nonirradiated Array, kJ	37,722	38,008
Daily Solar Energy Delivered To Storage Tank, kJ	34,091	34,511
Daily Total Heat Loss from Collector Piping, kJ	3,631	3,497
Net Daily Increase in Stored Energy in Storage Tank, kJ	-18,302	-17,929
Daily Energy Consumed by Heating Element, kJ	11,160	11,318
Total Circulator Elapsed Running Time, min	513.6	517.3
Daily Fractional Energy Savings, e, dimensionless	.743	.742

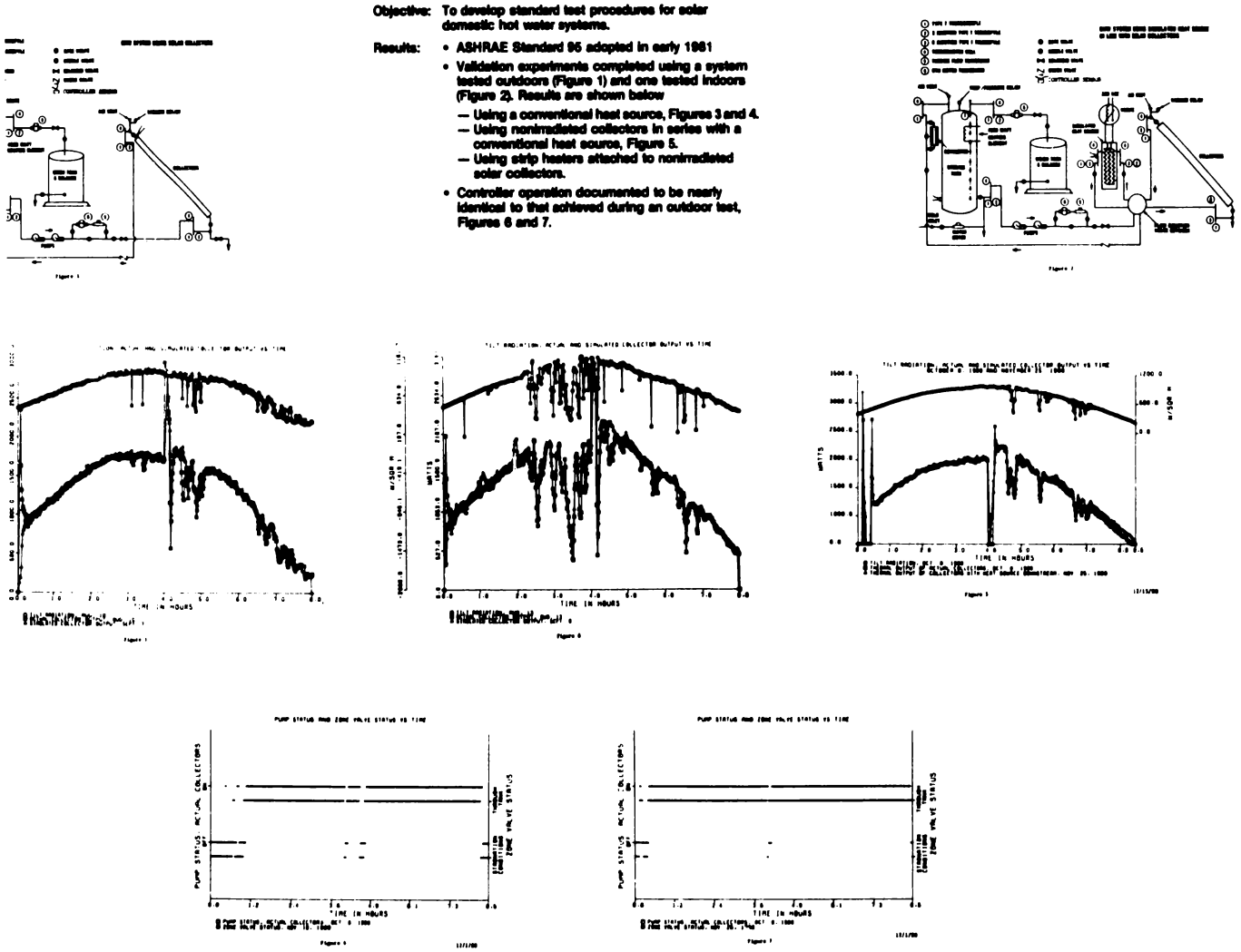

5. ANALYTICAL RESULTS AND DISCUSSION

Effects on solar hot water system performance resulting from the use of various test methods and different environmental conditions are considered. Results are presented for a system having normally irradiated solar collectors, nonirradiated collectors in series with an electric heat source, and nonirradiated collectors with strip heaters attached to the absorber plates.

5.1 SDHW SYSTEM ANALYTICAL MODEL VALIDATION

The thermal performance of a solar hot water system is predicted using the analytical model. The predicted performance is compared to the measured performance of the single-tank direct system for four selected test days.

The first step in validation of the total system model is to verify the routine used to predict the thermal performance of the solar collector modules. Figure 48 shows the solar collector efficiency curve which was predicted using the analytical model. The absorptance of the absorber plate and the edge heat loss coefficient were selected such that the linearized calculated efficiency curve for the solar collector was identical to the measured efficiency curve. Both of these parameters, however, are well within the range of those expected from handbook tabulations of property data. Following reference 7, the linearization is based on least-squares fits to the points shown which are at approximately 10, 30, 50 and 70 percent of the absorber stagnation temperature rise above ambient. The linearized efficiency curve slightly overestimates the ordinate intercept. Also, the negative slope of the linear curve is somewhat greater than that of the corresponding nonlinear curve over the range of practical importance for domestic water heating.

Experimental data collected during operation of the single-tank direct SDHW system during August 7 and 13, 1979 and October 6 and 8, 1980 provide a comparison basis for the predicted results of the analytical model. The initial tank temperature for the analytical model is set equal to the measured value for each test day. The meteorological data required for the analytical model are the values recorded during operation of the SDHW system for each test day. As discussed previously, the analytical model can simulate a storage tank which is composed of N volume segments or "nodes." Selection of a single-temperature tank corresponds to a "well mixed" condition and neglects any thermal stratification occurring within the storage tank. Increasing the number of nodes in the storage tank model corresponds to increasing the degree of temperature stratification within the tank. In order to determine the number of temperature nodes which would provide the closest agreement between analytical and experimental results, three computer simulations were made for each test day. These three computer simulations are based on

(a) taking the tank to be completely mixed (one nodal temperature),

(b) considering partial stratification with two tank volume elements (two nodal temperatures), and

(c) considering more complete thermal stratification with five tank volume elements (five nodal temperatures).

The upper volume element for the two- and five-node storage tanks corresponds to the volume of water between the storage tank heating element and the upper surface of the tank. The four bottom elements of the five-node tank contain equal volumes of water.

Tables 6 through 9 show the results of the analytical SDHW system model using a one-node, two-node, and five-node storage tank for August 7, August 13, October 6, and October 8, respectively. The fractional energy savings predicted by the analytical model using a one-node storage tank is significantly less than the fractional energy savings predicted when a two- or five-node storage tank is used. This large difference in predicted performance can be explained as follows. The storage tank heating element maintains the upper node (in which

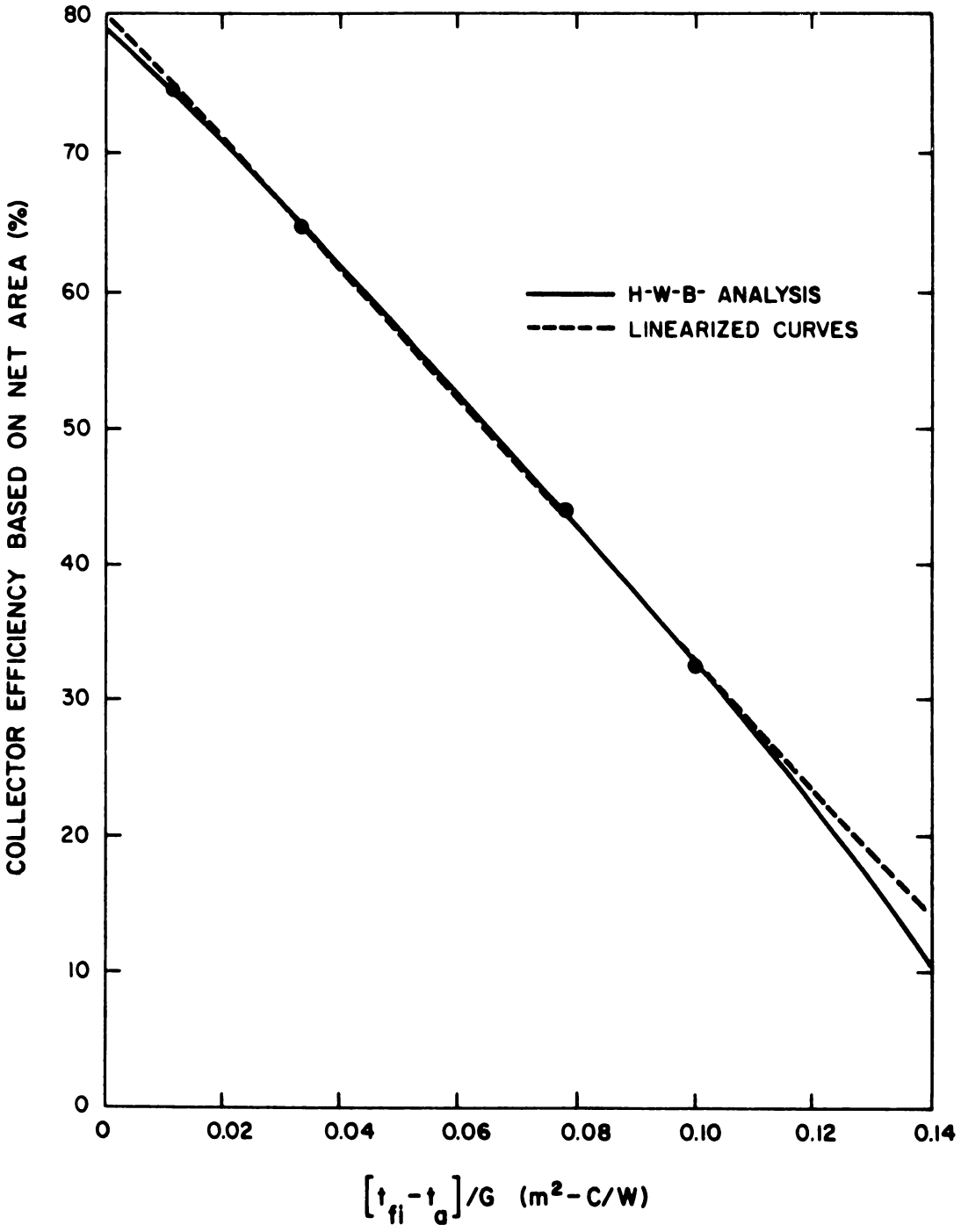

Figure 48. Solar collector efficiency curve

Table 6 Comparison of Experimental Results With Analytical Model Predicted Results for August 7, 1979

Variable	Experimental	Analytical Model Single Node Storage Tank	Analytical Model Two Node Storage Tank	Analytical Model Five Node Storage Tank
Initial Storage Tank Temperature, C	21.7	21.7	21.7	21.7
Energy Withdrawn at 13:00, kJ	12,610	12,606	12,602	12,604
Daily Total Solar Collector Array Output, kJ	41,740	34,284	41,564	42,350
Daily Solar Energy Delivered To Storage Tank, kJ	39,240	25,111	37,735	39,504
Daily Total Heat Loss from Collector Piping, kJ	2,500	9,173	3,829	2,846
Net Daily Increase in Stored Energy in Storage Tank, kJ	39,260	62,828	39,711	39,867
Daily Energy Consumed by Heating Element, kJ	16,550	55,228	17,330	15,997
Daily Fractional Energy Savings, e, dimensionless	0.71	0.302	0.690	0.715

Table 7 Comparison of Experimental Results With Analytical Model Predicted Results for August 13, 1979

Variable	Experimental	Analytical Model Single Node Storage Tank	Analytical Model Two Node Storage Tank	Analytical Model Five Node Storage Tank
Initial Storage Tank Temperature, C	21.2	21.2	21.2	21.2
Energy Withdrawn at 13:00, kJ	12,380	12,382	12,380	12,377
Daily Total Solar Collector Array Output, kJ	42,370	35,771	43,352	44,179
Daily Solar Energy Delivered To Storage Tank, kJ	39,250	25,297	38,609	40,528
Daily Total Heat Loss from Collector Piping, kJ	3,120	10,475	4,743	3,651
Net Daily Increase in Stored Energy in Storage Tank, kJ	39,370	63,291	40,500	40,905
Daily Energy Consumed by Heating Element, kJ	17,700	55,609	17,330	15,997
Daily Fractional Energy Savings, e, dimensionless	0.68	0.300	0.694	0.719

Table 8 Comparison of Experimental Results With Analytical Model Predicted Results for October 6, 1980

Variable	Experimental	Analytical Model Single Node Storage Tank	Analytical Model Two Node Storage Tank	Analytical Model Five Node Storage Tank
Initial Storage Tank Temperature, C	55.1	55.1	55.1	55.1
Energy Withdrawn at 13:00, kJ	13,902	13,898	13,900	13,901
Daily Total Solar Collector Array Output, kJ	34,098	29,499	32,768	33,690
Daily Solar Energy Delivered To Storage Tank, kJ	28,680	20,268	25,220	26,849
Daily Total Heat Loss from Collector Piping, kJ	5,418	9,231	7,547	6,842
Net Daily Increase in Stored Energy in Storage Tank, kJ	8,661	16,835	8,317	9,836
Daily Energy Consumed by Heating Element, kJ	3,520	18,092	3,428	3,428
Daily Fractional Energy Savings, e, dimensionless	0.882	0.477	0.869	0.876

Table 9 Comparison of Experimental Results With Analytical Model Predicted Results for October 8, 1980

Variable	Experimental	Analytical Model Single Node Storage Tank	Analytical Model Two Node Storage Tank	Analytical Model Five Node Storage Tank
Initial Storage Tank Temperature, C	35.1	35.1	35.1	35.1
Energy Withdrawn at 13:00, kJ	12,120	12,119	12,117	12,116
Daily Total Solar Collector Array Output, kJ	37,160	32,270	37,794	38,643
Daily Solar Energy Delivered To Storage Tank, kJ	34,464	23,215	32,013	33,648
Daily Total Heat Loss from Collector Piping, kJ	2,696	9,054	5,781	4,996
Net Daily Increase in Stored Energy in Storage Tank, kJ	32,464	39,425	27,616	27,784
Daily Energy Consumed by Heating Element, kJ	14,634	34,470	12,188	10,855
Daily Fractional Energy Savings, e, dimensionless	0.701	0.379	0.721	0.752

it is located) within a specified temperature range. A single-node storage tank requires that the heating element supply a quantity of energy sufficient to maintain the entire storage tank within this temperature range. Thus, the electrical energy used by the heating element is greatly increased over the amount required for only the upper node of a two- or five-segment tank. The predicted system performance using a five-node tank is slightly greater than the predicted performance when a two-node tank is used. The fluid which enters the solar collector array is supplied from the bottom volume element. As the number of storage tank nodes increases, the average fluid temperature entering the collector array decreases. The lower fluid temperature results in a higher collector efficiency, so the higher system performance is expected.

Analytical model results for both the two-node and five-node storage tank are in close agreement with the experimental results for all four test days. However, whereas the analytical model predicted a small increase in system performance from increased storage tank stratification (five-node as compared to two-node), the experimental results indicated a significant increase in fractional energy savings (see Table 4). This discrepancy is due to the internal mixing within the storage tank which the analytical model fails to take into account.

Figures 49 and 50 show a comparison of the experimental and the analytically predicted storage tank temperature distributions for October 8, 1980. Figure 49 shows the storage tank distribution for a two-node storage tank, while figure 50 shows the distribution for a five-node storage tank. The other three test days exhibited similar temperature profile comparisons. In the experimental tank, the top thermocouple displays a greater temperature decay than predicted by the analytical model, while the lower seven thermocouples show a greater increase in temperature than predicted. The second thermocouple from the top of the experimental storage tank is influenced, although to a lesser degree than the upper thermocouple, by the operation of the heating element. This thermocouple, located 25.4 mm below the heating element, increases rapidly in temperature until the heating element is de-energized by the thermostat. Then, the temperature of this thermocouple decreases rapidly because of internal mixing. Internal mixing also affects the bottom seven thermocouples, which show no stratification in the portion of the tank they monitor. The numerical results show that the five-node tank model slightly overestimates the effects of thermal stratification, while the two-node tank gives results which agree more consistently with experimental results. Due to this lack of stratification in the experimental storage tank, a two-node storage tank model was used in all subsequent simulations. Thus, the upper node represents the region which contains the heating element, and the lower node represents the remaining "well mixed" lower portion of the tank.

5.2 TEST METHOD INFLUENCE ON SYSTEM PERFORMANCE

The thermal performance of a SDHW system may be influenced by the technique used to supply the net thermal output of an irradiated array. In order to quantitatively determine the effect of various test methods, the SDHW system model was used to predict the performance of a system using an irradiated collector array, a nonirradiated array with a downstream heat source, a nonirradiated array with an upstream heat source, and strip heaters attached to

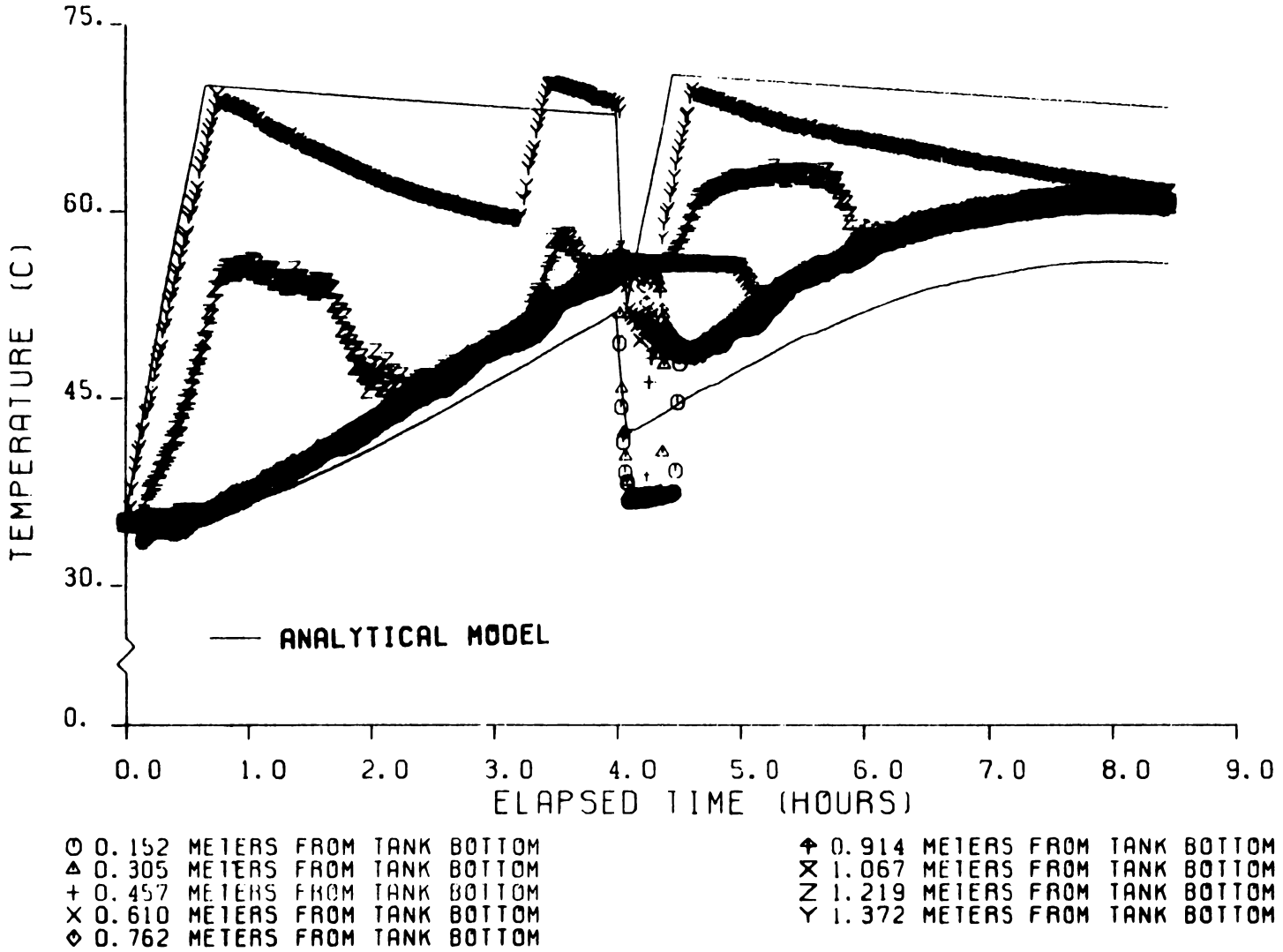

Figure 49. Experimental and two-node analytical model predicted storage tank temperature distribution for October 8, 1980

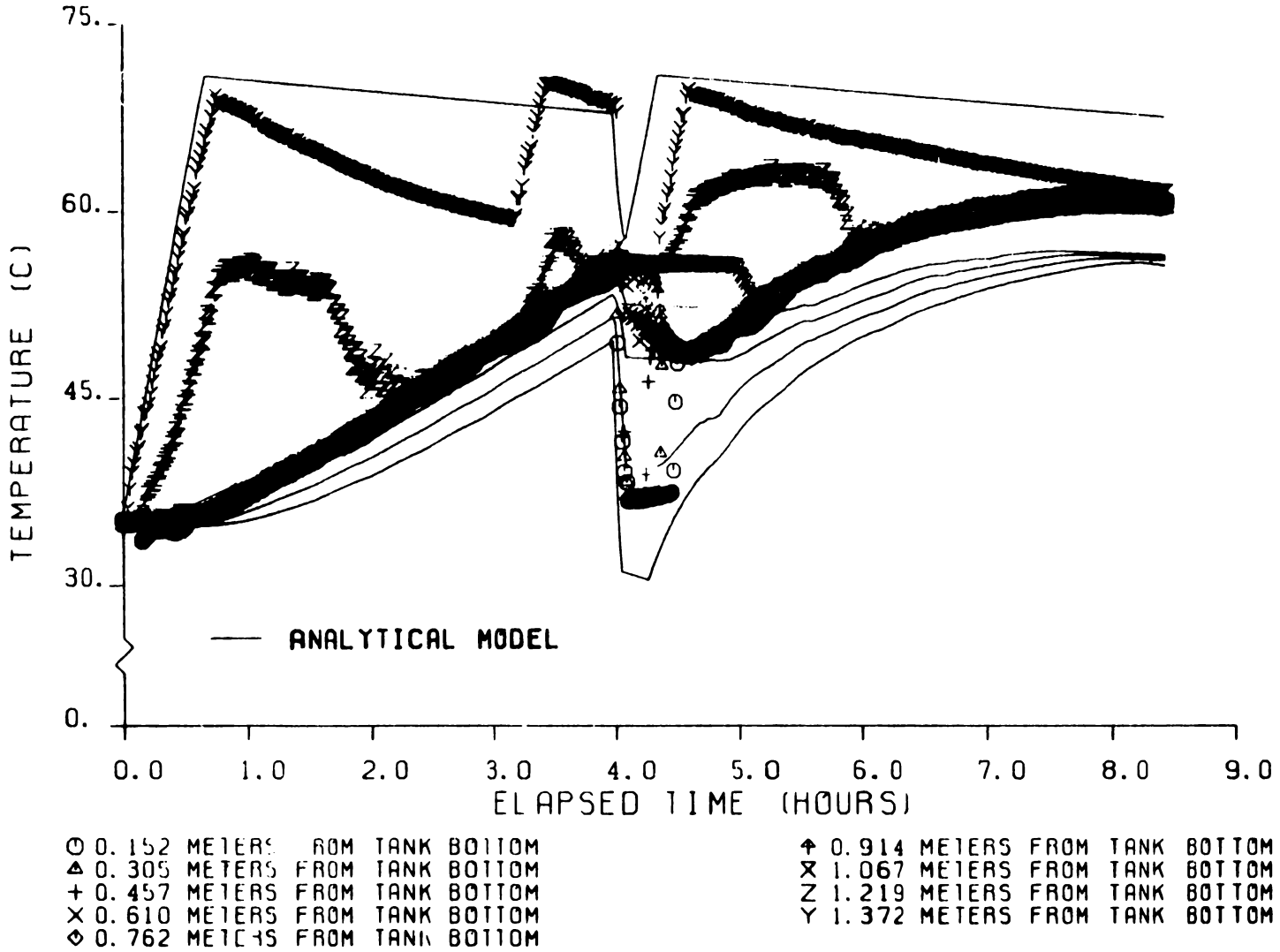

Figure 50. Experimental and five-node analytical model predicted storage tank temperature distribution for October 8, 1980

nonirradiated absorber plates. The recorded environmental and initial conditions for October 6 and 8, 1980 provided the required input parameters. The use of the same ambient temperature, effective sky temperature, and wind velocity for the simulation of each test method allowed the effect of various test methods (as opposed to different environmental conditions) on system performance to be determined.

Tables 10 and 11 summarize the results of the test method comparison. The values of $F_R(\tau\alpha)_n$ and F_RU_L used in the expressions for calculating the power input to the heat source are based on the linearized efficiency curve shown in figure 48. Use of the various test methods resulted in almost identical fractional energy savings. For the October 6, 1980 comparisons, the daily thermal output of the nonirradiated array with downstream heat source and the nonirradiated array with strip heaters attached to the absorber plates are 1.3 percent less than the daily thermal output of the irradiated array. Using the environmental conditions for October 8, 1980, the daily thermal output of the nonirradiated array with downstream heat source and the nonirradiated array with strip heaters attached to the absorber plates are 1.4 percent and 1.1 percent less, respectively, than that for the irradiated array. The lower net thermal output is attributed to the lack of solar absorption and the resulting heating in the cover which has also been analyzed by Gillett [13]. The lower cover temperature under nonirradiated conditions results in a higher value of F_RU_L as compared to irradiated conditions. The higher value of F_RU_L results in greater thermal losses for the nonirradiated collectors and thus a decrease in the net thermal output. The daily thermal output of the nonirradiated array with upstream heat source is 0.1 percent and 0.3 percent less than that of the irradiated array for October 6 and October 8, 1980, respectively. This close agreement is attributed to two phenomena. The nonirradiated conditions result in a higher value of F_RU_L than for irradiated conditions, thereby decreasing the net thermal output of the nonirradiated array with an upstream heat source. The other contributing factor can be explained by considering the denominator in eq (20). This term accounts for the incremental heat loss resulting from the higher inlet temperature to the downstream nonirradiated collector array. Since F_RU_L is based on the linearized measured efficiency curve and is larger than the F_RU_L value for both the nonirradiated collector and the irradiated collector, at the inlet temperature conditions encountered during October 6 and 8, 1980, the denominator term in eq (20) allows for a greater heat loss than is actually dissipated from the downstream nonirradiated collector array. For example, for an irradiance of 900 W/m^2, a 25 C ambient temperature, an effective sky temperature of 11 C, a 2.0 m/s wind velocity and an inlet temperature of 40 C, the F_RU_L value is 4.19 W/(m^{2}C). For an irradiance of zero, all other conditions identical, the F_RU_L value increases to 4.31 W/(m^{2}C) due to the decreased cover temperature, thus accounting for the higher heat loss from the nonirradiated collector. However, the 4.31 W/(m^{2}C) value of F_RU_L is still considerably less than the value of 4.73 W/(m^{2}C) obtained from the linear efficiency curve. This condition results in a greater power input to the upstream heat source than is actually required. Thus, the greater thermal input to the heat source tends to compensate for the greater thermal loss from the nonirradiated array.

Table 10 Effect of Test Method on SDHW System Performance; Analytical Model Results Using October 6, 1980 Meteorological Conditions

Variable	Irradiated Array	Nonirradiated Array With Downstream Heat Source	Nonirradiated Array With Upstream Heat Source	Nonirradiated Array With Strip Heaters Attached to Back of Absorber Plates
Initial Storage Tank Temperature, C	55.1	55.1	55.1	55.1
Energy Withdrawn at 13:00, kJ	13,900	13,907	13,900	13,897
Daily Total Solar Collector Array Output, kJ	32,768	32,344	32,738	32,350
Daily Solar Energy Delivered To Storage Tank, kJ	25,220	24,830	25,194	24,836
Daily Total Heat Loss from Collector Piping, kJ	7,547	7,513	7,546	7,515
Net Daily Increase in Stored Energy in Storage Tank, kJ	8,317	7,943	8,293	7,958
Daily Energy Consumed by Heating Element, kJ	3,428	3,428	3,428	3,428
Daily Fractional Energy Savings, e, dimensionless	0.869	0.867	0.868	0.867

Table 11 Effect of Test Method on SDHW System Performance; Analytical Model Results Using October 8, 1980 Meteorological Conditions

Variable	Irradiated Array	Nonirradiated Array With Downstream Heat Source	Nonirradiated Array With Upstream Heat Source	Nonirradiated Array With Strip Heaters Attached to Back of Absorber Plates
Initial Storage Tank Temperature, C	35.1	35.1	35.1	35.1
Energy Withdrawn at 13:00, kJ	12,118	12,120	12,124	12,125
Daily Total Solar Collector Array Output, kJ	37,794	37,254	37,665	37,412
Daily Solar Energy Delivered To Storage Tank, kJ	32,013	31,533	31,904	31,671
Daily Total Heat Loss from Collector Piping, kJ	5,781	5,721	5,761	5,741
Net Daily Increase in Stored Energy in Storage Tank, kJ	27,616	27,168	27,511	27,290
Daily Energy Consumed by Heating Element, kJ	12,188	12,188	12,188	12,188
Daily Fractional Energy Savings, e, dimensionless	0.721	0.718	0.720	0.719

5.3 INFLUENCE OF ENVIRONMENTAL CONDITIONS ON SYSTEM PERFORMANCE

Environmental conditions surrounding the nonirradiated array located in the laboratory influence the performance of the SDHW system. The analytical model is used to predict the performance of a SDHW system subjected to zero wind speed and an effective sky temperature equivalent to ambient temperature using each indoor test method. The results are compared to an outdoor system experiencing the environmental conditions recorded during October 6 and 8, 1980. The indoor ambient temperature was set equivalent to the recorded outdoor ambient temperature. By this approach, the combined effects of testing the system indoors and the use of various test methods can be simulated.

Figure 51 displays the recorded wind speed for October 6, 1980, and the ambient temperature and effective sky temperature recorded for October 6, 1980 are shown in figure 52. Table 12 gives the results for each test method for the October 6, 1980 comparison. As expected, the fractional energy savings increased for all test methods as compared to the results given in Table 10. This result is due to a lower heat loss from the nonirradiated collector array because of a zero wind speed and higher effective sky temperature. The increase in fractional energy savings is less than 0.5 percent for all methods. Under indoor environmental conditions, the daily thermal output of a nonirradiated array with downstream heat source best matches the daily thermal output of an irradiated array subjected to outdoor environmental conditions. The daily thermal output of the nonirradiated array with an upstream heat source exceeds the outdoor irradiated array by 1.8 percent. The daily thermal output of the nonirradiated array with a downstream heat source and the nonirradiated array with attached strip heaters exceeds the daily thermal output of the irradiated array by 1.1 percent and 1.6 percent, respectively.

Figure 53 displays the wind speed and figure 54 shows the ambient temperature and effective sky temperature recorded for October 8, 1980. Table 13 gives the results for each test method for the October 8, 1980 comparison. The increase in fractional energy savings is less than 0.8 percent for all methods. The test method using the nonirradiated collector array with a downstream heat source matches the performance of the irradiated system better than the two other test methods. The thermal output of the nonirradiated array with an upstream heat source and the nonirradiated array with attached strip heaters are almost identical; both are approximately 1.4 percent higher than the thermal output of the normally irradiated array.

5.4 INFLUENCE OF THERMAL LOSSES FROM HEAT SOURCE

The electric heat source, even when highly insulated, will experience some heat transfer to the surrounding environment. The numerical SDHW system model, in conjunction with the heat source efficiency curve shown in figure 55, allows the effect of a nonadiabatic heat source to be determined.

The test method using a nonirradiated collector array with a downstream heat source is used to generate the results shown in Tables 14 and 15. Each table includes the predicted performance results of a system using an irradiated

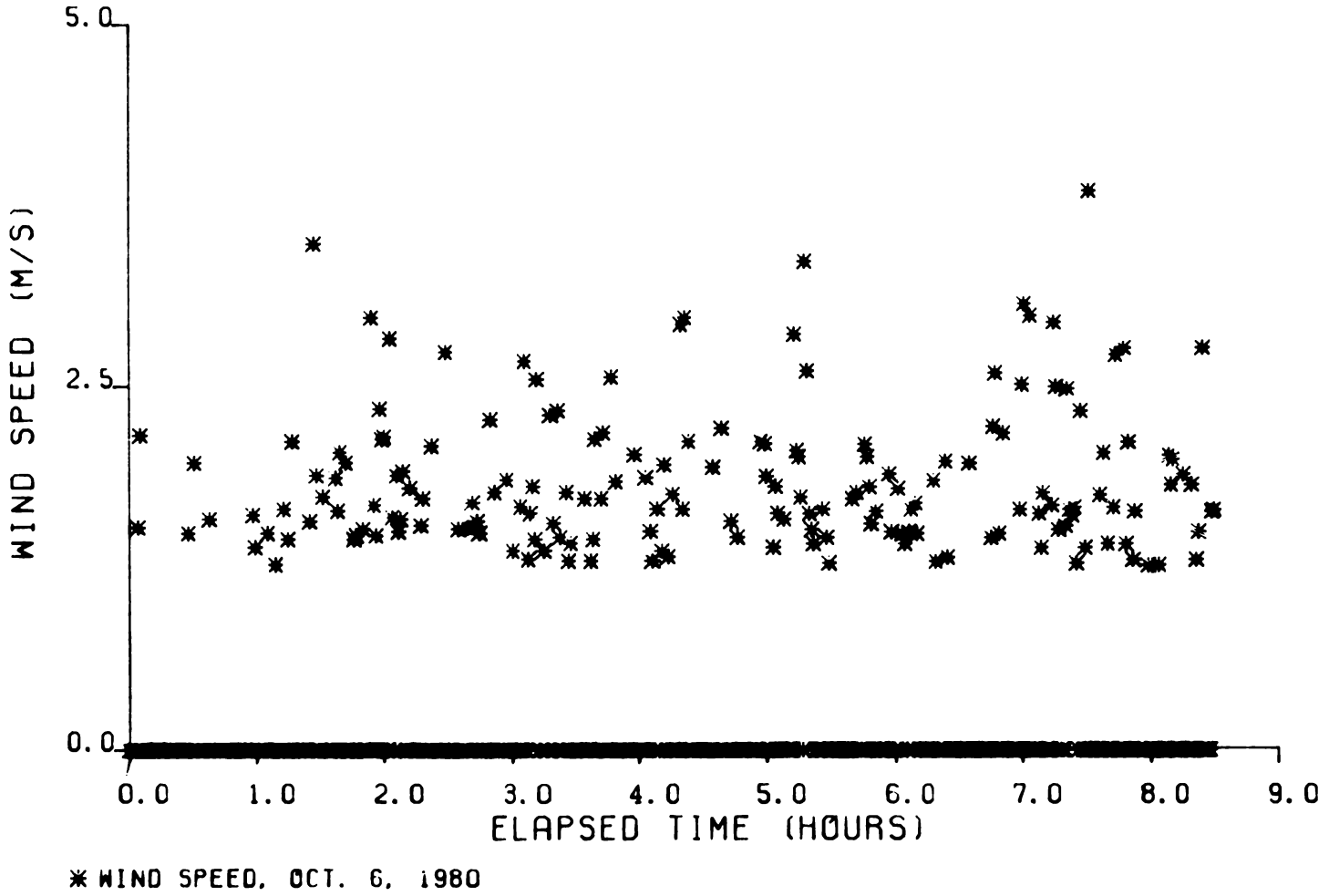

Figure 51. Recorded wind speed for October 6, 1980

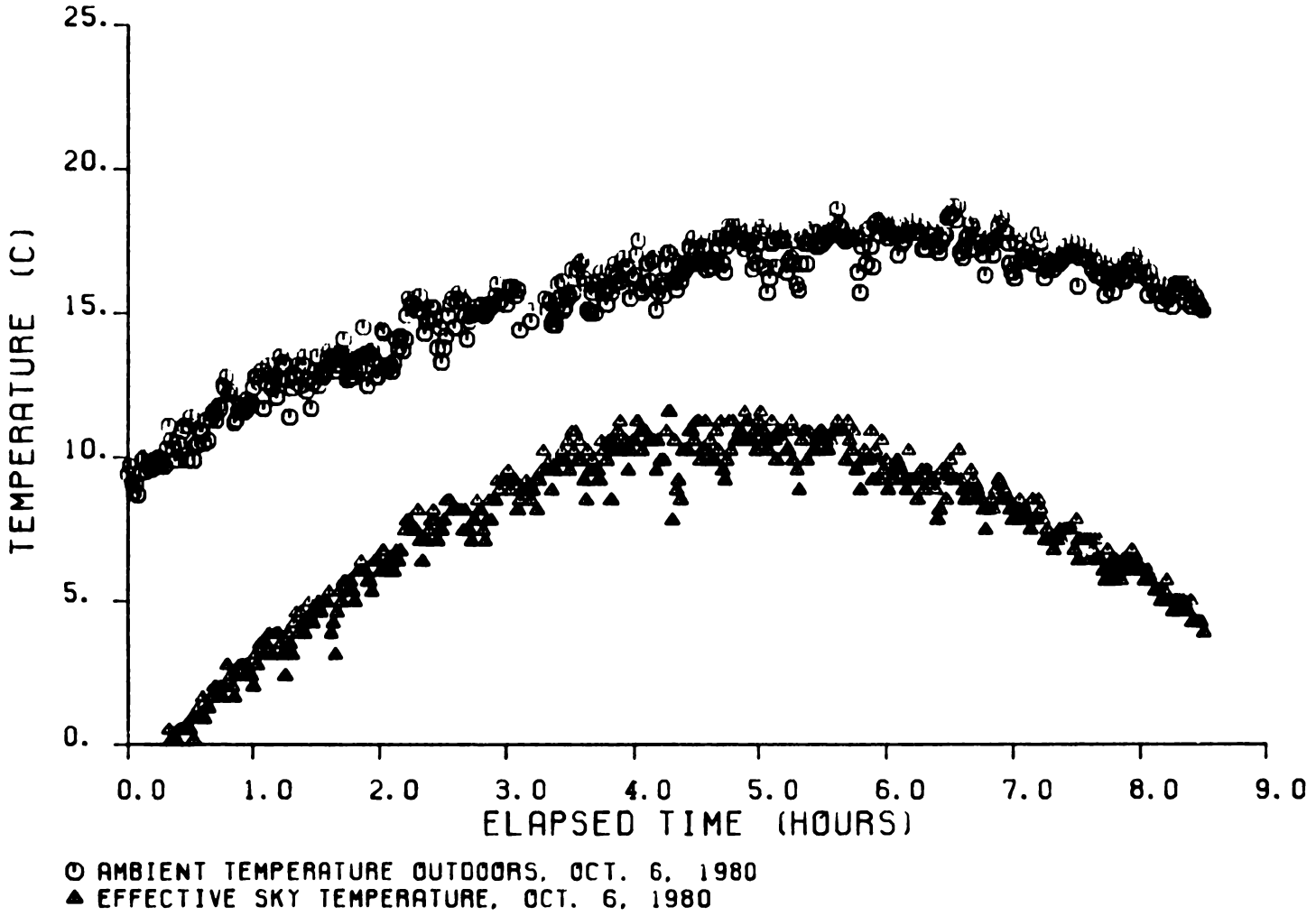

Figure 52. Recorded ambient temperature and effective sky temperature for October 6, 1980

Table 12 Effect of Wind Speed and Effective Sky Temperature on SDHW System Performance; Analytical Model Results For Various Test Methods, October 6, 1980 Meteorological Conditions

Variable	Irradiated Array Outdoor Conditions	Nonirradiated Array With Downstream Heat Source Vw=0, Tsky=Ta	Nonirradiated Array With Upstream Heat Source Vw=0, Tsky=Ta	Nonirradiated Array With Strip Heaters Attached to Back of Absorber Plates Vw=0, Tsky=Ta
Initial Storage Tank Temperature, C	55.1	55.1	55.1	55.1
Energy Withdrawn at 13:00, kJ	13,900	13,903	13,903	13,898
Daily Total Solar Collector Array Output, kJ	32,768	33,125	33,340	33,288
Daily Solar Energy Delivered To Storage Tank, kJ	25,220	25,556	25,754	25,706
Daily Total Heat Loss from Collector Piping, kJ	7,547	7,569	7,586	7,582
Net Daily Increase in Stored Energy in Storage Tank, kJ	8,317	8,636	8,822	8,781
Daily Energy Consumed by Heating Element, kJ	3,428	3,428	3,428	3,428
Daily Fractional Energy Savings, e, dimensionless	0.869	0.870	0.871	0.871

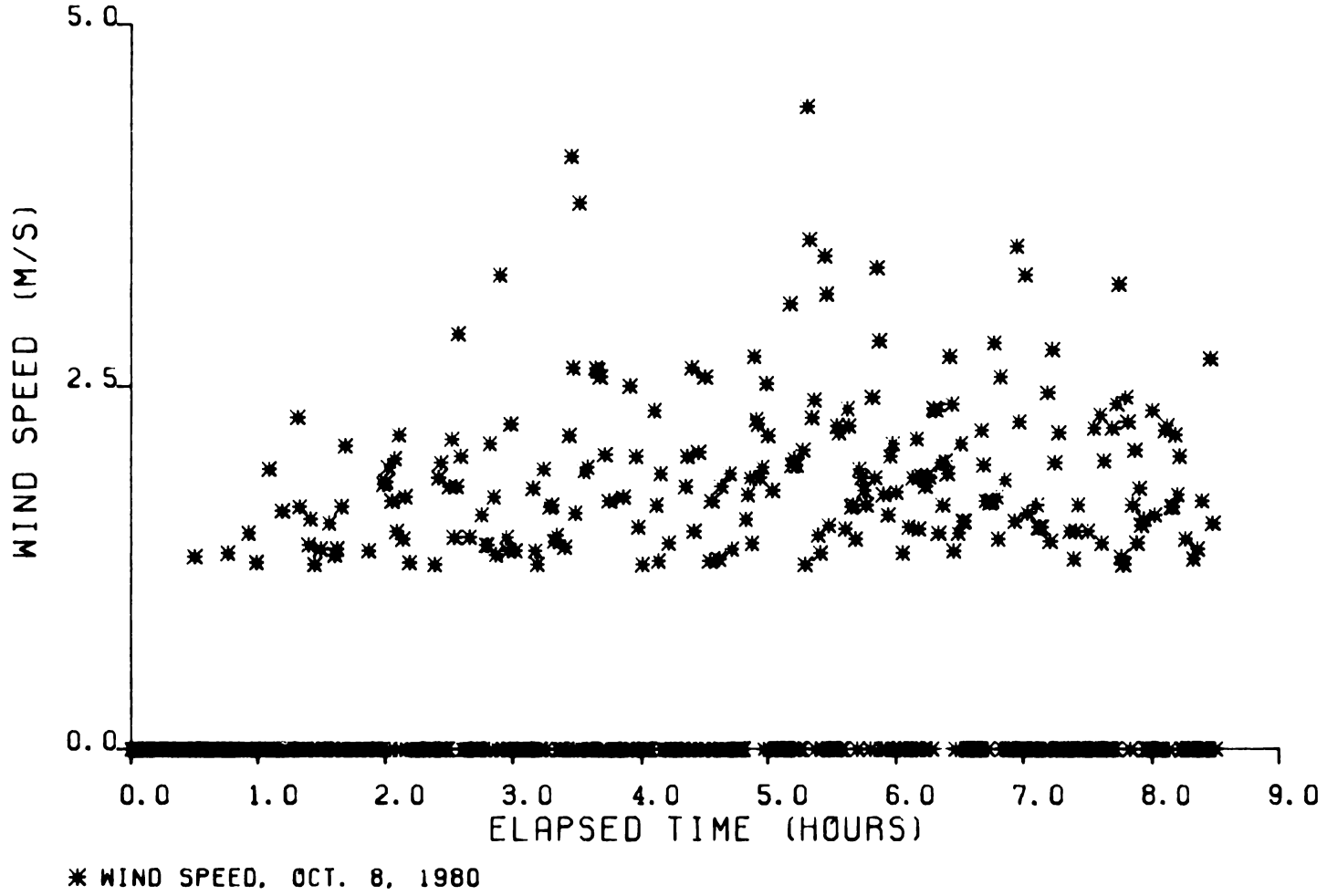

Figure 53. Recorded wind speed for October 8, 1980

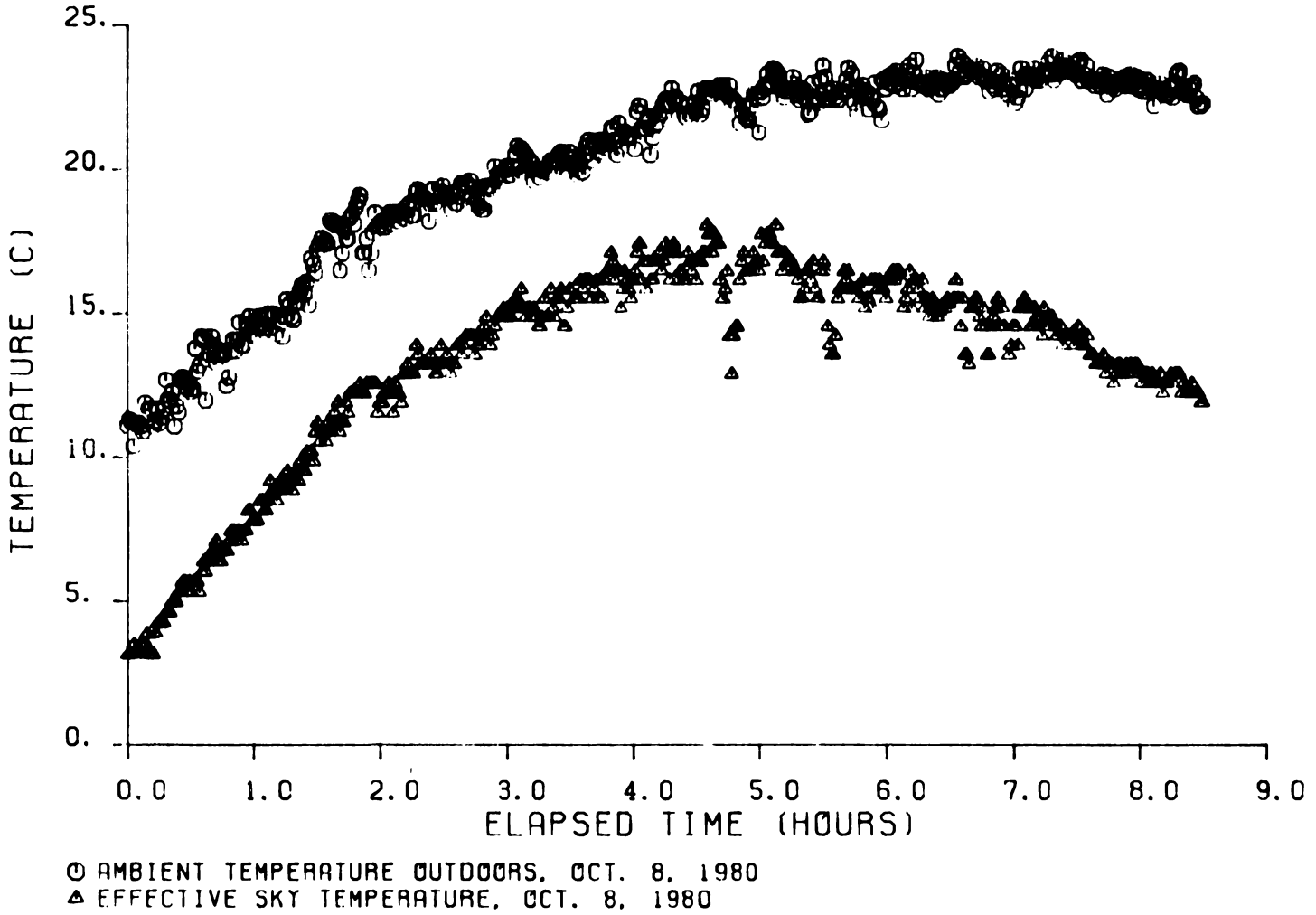

Figure 54. Recorded ambient temperature effective sky temperature for October 8, 1980

Table 13 Effect of Wind Speed and Effective Sky Temperature on SDHW System Performance: Analytical Model Results For Various Test Methods, October 8, 1980 Meteorological Conditions

Variable	Irradiated Array Outdoor Conditions	Nonirradiated Array With Downstream Heat Source Vw=0, Tsky=Ta	Nonirradiated Array With Upstream Heat Source Vw=0, Tsky=Ta	Nonirradiated Array With Strip Heaters Attached to Back of Absorber Plates Vw=0, Tsky=Ta
Initial Storage Tank Temperature, C	35.1	35.1	35.1	35.1
Energy Withdrawn at 13:00, kJ	12,118	12,121	12,116	12,116
Daily Total Solar Collector Array Output, kJ	37,794	37,928	38,243	38,268
Daily Solar Energy Delivered To Storage Tank, kJ	32,013	32,152	32,433	32,455
Daily Total Heat Loss from Collector Piping, kJ	5,781	5,776	5,810	5,813
Net Daily Increase in Stored Energy in Storage Tank, kJ	27,616	27,754	27,841	27,861
Daily Energy Consumed by Heating Element, kJ	12,188	12,188	11,998	11,998
Daily Fractional Energy Savings, e, dimensionless	0.721	0.722	0.727	0.727

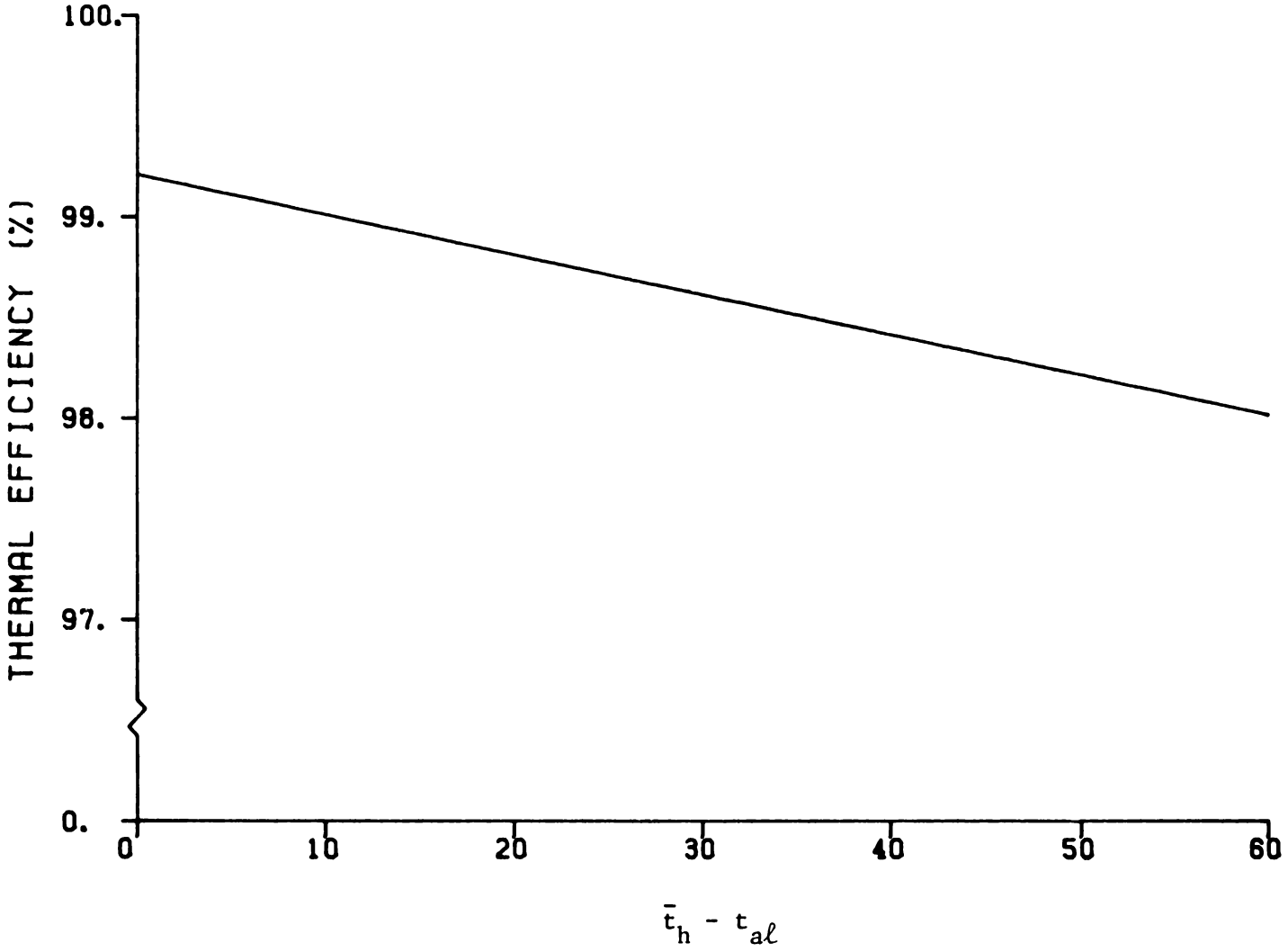

Figure 55. Thermal efficiency of electric heat source

array, a system using a nonirradiated collector array with an adiabatic downstream heat source, and a system using a nonirradiated array with a nonadiabatic downstream heat source. Inclusion of the thermal losses based on the measured heat source effficiency curve resulted in a fractional energy savings decrease of 0.3 percent for both test days. The net thermal output of the nonirradiated collector array with a downstream heat source decreased by 2.0 percent for November 17 conditions and 1.5 percent for November 25 conditions.

5.5 COMPARISON OF ANALYTICAL MODEL RESULTS WITH EXPERIMENTALLY MEASURED RESULTS

The analytical model results can be compared to the experimental results for the irradiated system and the system which uses a nonirradiated collector array with a nonadiabatic downstream heat source. As shown in Table 14, the analytical model predicts identical fractional energy savings for the irradiated system using October 6, 1980 environmental conditions, and for the system which employs a nonirradiated collector array with a nonadiabatic downstream heat source using November 17, 1980 environmental conditions. Identical fractional energy savings were measured experimentally for the outdoor irradiated system on October 6, 1980 and the indoor nonirradiated collector array with downstream heat source on November 17, 1980 (see Table 2). However, the measured fractional energy savings is 1.4 percent higher than that predicted by the analytical model. The measured thermal output of the nonirradiated array with the downstream heat source was 2.8 percent higher than the measured thermal output of the irradiated array. However, Table 14 shows that the analytical model predicts a decrease of 0.2 percent, assuming a nonadiabatic heat source.

The analytically predicted fractional energy savings (Table 15) for the system which uses a nonirradiated collector array with a downstream nonadiabatic heat source subjected to November 25, 1980 environmental conditions is 0.1 percent less than the predicted fractional energy savings for the irradiated system subjected to October 8, 1980 environmental conditions. However, an increase of 3.0 percent in fractional energy savings was observed experimentally. Table 2 shows that the measured thermal output of the nonirradiated array with a downstream heat source was 1.6 percent higher than the measured thermal output of the irradiated array. However, the analytical model predicts a decrease of 0.6 percent, as shown in Table 15.

Table 14 Effect of Heat Source Thermal Loss on SDHW System Performance For Nonirradiated Array With Downstream Heat Source; Analytical Model Results Using Two-Node Storage Tank For October 6, 1980

Variable	Irradiated Array October 6, 1980 Environmental Conditions	Nonirradiated Array With Downstream Heat Source November 17, 1980 Environmental Conditions Adiabatic Heat Source	Nonirradiated Array With Downstream Heat Source November 17, 1980 Environmental Conditions Nonadiabatic Heat Source
Initial Storage Tank Temperature, C	55.1	55.1	55.1
Energy Withdrawn at 13:00, kJ	13,900	13,898	13,899
Daily Total Solar Collector Array Output, kJ	32,768	33,375	32,709
Daily Solar Energy Delivered To Storage Tank, kJ	25,220	25,791	25,180
Daily Total Heat Loss from Collector Piping, kJ	7,547	7,584	7,530
Net Daily Increase in Stored Energy in Storage Tank, kJ	8,317	8,867	8,291
Daily Energy Consumed by Heating Element, kJ	3,428	3,428	3,428
Daily Fractional Energy Savings, e, dimensionless	0.869	0.871	0.868

Table 15 Effect of Heat Source Thermal Loss on SDHW System Performance For Nonirradiated Array With Downstream Heat Source; Analytical Model Results Using Two-Node Storage Tank for October 8, 1980

Variable	Irradiated Array October 8, 1980 Environmental Conditions	Nonirradiated Array With Downstream Heat Source November 25, 1980 Environmental Conditions Adiabatic Heat Source	Nonirradiated Array With Downstream Heat Source November 25, 1980 Environmental Conditions Nonadiabatic Heat Source
Initial Storage Tank Temperature, C	35.1	35.1	35.1
Energy Withdrawn at 13:00, kJ	12,118	12,119	12,120
Daily Total Solar Collector Array Output, kJ	37,794	38,087	37,548
Daily Solar Energy Delivered To Storage Tank, kJ	32,013	32,299	31,814
Daily Total Heat Loss from Collector Piping, kJ	5,781	5,789	5,734
Net Daily Increase in Stored Energy in Storage Tank, kJ	27,616	27,897	27,442
Daily Energy Consumed by Heating Element, kJ	12,188	12,188	12,188
Daily Fractional Energy Savings, e, dimensionless	0.721	0.723	0.720

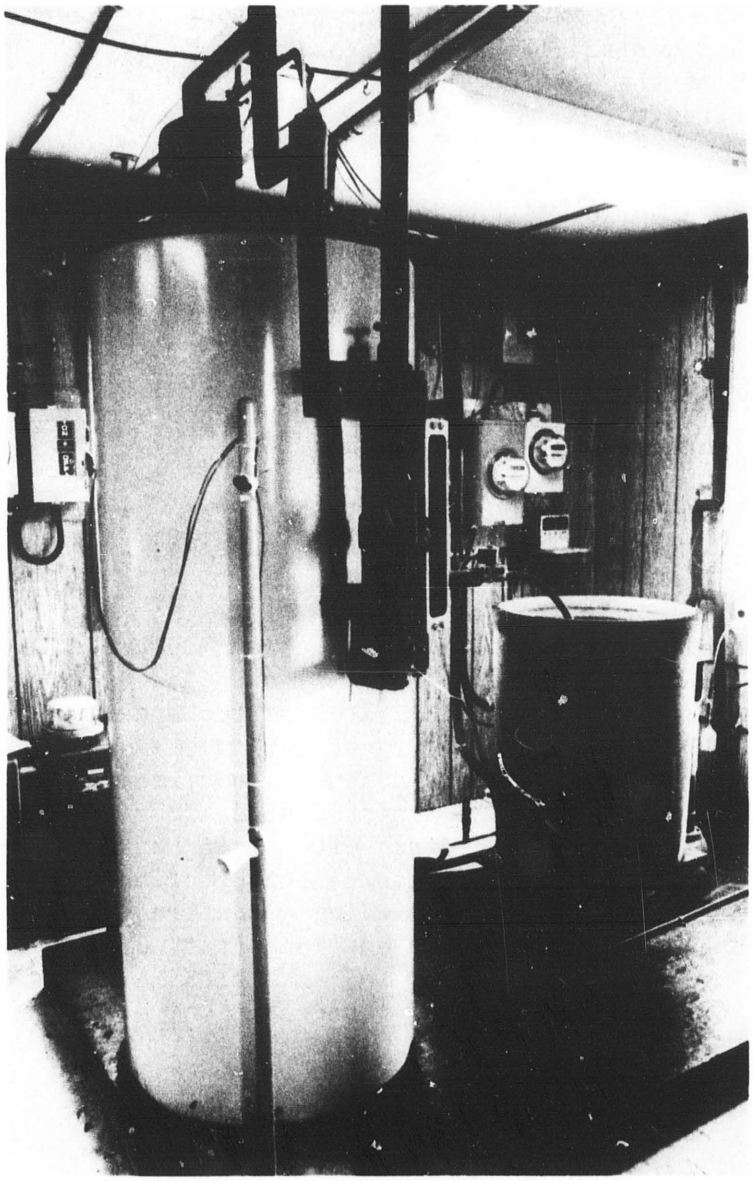

6. CONCLUSIONS AND RECOMMENDATIONS

Conclusions which may be drawn from this analytical and experimental investigation of test methods for SDHW systems are as follows:

(1) The thermal performance of a SDHW system can be duplicated indoors, without the use of a solar simulator, by replacing the irradiated array with an electric heat source alone, an electric heat source in series with a nonirradiated collector array, or by attaching electric strip heaters to the back of nonirradiated absorber plates. All three indoor test techniques reproduced the outdoor daily collector array thermal output within 4 percent.

(2) Outdoor stagnation conditions cannot be duplicated in the laboratory using an electric heat source only. Stagnation conditions and outdoor pump controller actions can be reproduced indoors using an electric heat source in series with a nonirradiated collector array or by attaching strip heaters to the back of the absorber plates contained within a nonirradiated collector array.

(3) The ASHRAE Proposed Standard 95, which specifies the use of an electric heat source in series with a nonirradiated collector array, is sensitive to temperature stratification in the storage tank. The use of a return tube which reduced internal mixing in the storage tank increased, for a selected test day, the fractional energy savings 74 percent to 83 percent. The analytical model predicted a smaller increase in fractional energy savings, approximately three percent. The analytical tank model does not accurately simulate internal mixing within the storage tank, which accounts for this discrepancy.

(4) Test result repeatability is excellent for the experimental technique of using a nonirradiated collector array in series with a downstream heat source.

(5) Computer simulations indicate that the particular technique used to supply the quantity of energy normally supplied by an irradiated array has an insignificant effect on system performance for the SDHW system used during this experimental investigation. Techniques considered during this analytical investigation included a nonirradiated collector array with upstream heat source, a nonirradiated array with downstream heat source, and a nonirradiated array with strip heaters attached to the back of the absorber plates. The thermal output of an irradiated collector array can best be reproduced by using a nonirradiated collector array with upstream heat source if outdoor environmental conditions are duplicated indoors. For easily obtainable indoor environmental conditions, $V_w = 0$ and $T_{sky} = t_{al}$, the use of a nonirradiated collector array with a downstream heat source gave the best agreement with the irradiated collector array thermal output.

(6) The electric heat source should be constructed such that thermal losses to the surrounding environment are minimized.

The following recommendations should be considered for future research:

(1) Correlations should be developed which relate ASHRAE Standard 95 test results to the input meteorological conditions. These correlations would enable the thermal performance of a SDHW system to be predicted for environmental conditions which differ from the prescribed test conditions.

(2) Experiments should be conducted to validate the suggested test method for SDHW systems which rely on thermosyphoning action for circulating fluid through the collector array. The thermal performance of such systems, using normally irradiated collector arrays, should be compared to an identical system where the array consists of collectors equipped with electric strip heaters attached to the absorber plates.

(3) Further investigations should be undertaken to improve the currently proposed method of accounting for the effects of liquid flow rate and composition of the absorber plate efficiency factor. An improved method would eliminate the requirement that the same test fluid be used in testing the collector and the entire SDHW system.

REFERENCES

1. "TRNSYS, A Transient Simulation Program," Engineering Experiment Station Report 38-10, University of Wisconsin-Madison, Solar Energy Laboratory, June, 1979.

2. Beckman, W. A., and Duffie, J. A., Solar Heating Design by the f-CHART Method, John Wiley & Sons Inc., 1977.

3. Connolly, M., Giellis, R., Jensen, C., and McMordie, R., "Solar Heating and Cooling Computer Analysis - A Simplified Design Method for Non-Thermal Specialists," Proceedings of the Joint Conference of the American Section of the International Solar Energy Society and the Solar Energy Society of Canada, held in Winnipeg, Canada, August 15-20, 1976.

4. Fanney, A. H., and Liu, S. T., "Comparison of Experimental and Computer-Predicted Performance for Six Solar Domestic Hot Water Systems," ASHRAE Transactions, Vol. 86, Part I, 1980, pp. 823-835.

5. Chandra, Subrato, and Khatter, Mukesh K., "Analytical Investigations of the Relative Solar Rating Concept," Draft Final Report, Florida Solar Energy Center, Report No. FSEC-TT-80-6, June 20, 1980.

6. "Method of Testing to Determine Thermal Performance of Solar Domestic Water Heating Systems," ASHRAE Proposed Standard 95-P, February, 1981.

7. "Methods of Testing to Determine the Thermal Performance of Solar Collectors," ASHRAE Standard 93-77, 1977.

8. Hill, J. E., and Fanney, A. H., "A Proposed Procedure of Testing for Rating Solar Domestic Hot Water Systems," ASHRAE Transactions, Vol. 86, Part 1, 1980, pp. 805-822.

9. Kotas, J. F., and Wood, B. D., "Design and Evaluation of a Computer Controlled Solar Collector Simulator," ASME Paper 80-WA/Sol-6, November, 1980.

10. Fanney, A. H., and Thomas, W. C., "Simulation of Thermal Performance of Solar Collector Arrays," ASME Transactions, Journal of Solar Energy Engineering, submitted for publication, 1981.

11. Thomas, W. C., "Solar Collector Test Procedures: Development of a Method to Refer Measured Efficiencies to Standardized Test Conditions," Report VPI-E-80.23, Virginia Polytechnic Institute and State University, November, 1980.

12. Duffie, J. A., and Beckman, W. A., Solar Engineering of Thermal Processes, John Wiley & Sons Inc., 1980.

13. Gillett, W. B., "The Equivalence of Outdoor and Mixed Indoor/Outdoor Solar Collector Testing," Solar Energy, Vol. 25, No. 6, 1980, pp. 543-548.

14. Buchberg, H. I., Catton, I., and Edwards, D. K., "Natural Convection in Enclosed Spaces -- A Review of Application to Solar Energy Collection," Trans., ASME, Vol. 98C, May, 1976, pp. 184-188.

15. U.S. Standard Atmosphere, 1962, U.S. Government Printing Office, Washington, D.C., December, 1962, p. 14-15.

16. Streed, E. R., Thomas, W. C., Dawson, A. G., III, Wood, B. D., and Hill, J. E., "Results and Analysis of a Round-Robin Test Program for Liquid-Heating Flat-Plate Solar Collectors," NBS TN 975, August, 1978.

17. Thomas, W. C., "Effects of Test Fluid, Flow Rate, and Flow Regime on Solar Collector Thermal Performance Measurements," Modeling, Simulation, Testing, and Measurements Symposum, Vol. H00138, ASME, 1978, pp. 85-89.

18. Thomas, W. C., "Effects of Test Fluid Composition and Flow Rates on the Thermal Efficiency of Solar Collectors," Report ENG 80-03, Virginia Polytechnic Institute and State University, Blacksburg, Virginia 24061.

19. Eckert, E. R. G., and Drake, R. M., Analysis of Heat and Mass Transfer, McGraw-Hill, 1972, p. 351.

20. Seider, E. N., and Tate, C. E., "Heat Transfer and Pressure Drop of Liquids in Tubes," Industrial Engineering Chemistry, Vol. 28, 1936, p. 1429.

21. Kreith, F., Principles of Heat Transfer, Third Edition, International Textbook Co., 1973, p. 433.

APPENDIX A

ASHRAE STANDARD 95-P COLLECTOR HEAT REMOVAL FACTOR MODIFICATION PROCEDURE

The value of F_R is dependent upon mass flow rate and the specific heat of the transfer fluid. Therefore, if the flow rate of transfer fluid through the collector in the operation of the solar hot water system is different from the value used during the ASHRAE 93-77 tests on the collector, then the value of F_R must be modified from the value obtained from the ASHRAE 93-77 tests. This can be done utilizing the following procedure:

1. Calculate $(\tau\alpha)_n$ for the solar collector. For an ordinary flat-plate collector

$$(\tau\alpha)_n = \frac{t_n \alpha_p}{1-(1 - \tau_n)\rho_d} \tag{A.1}$$

where

ρ_d = 0.16 for a one-cover glass system
= 0.24 for a two-cover glass system
= 0.29 for a three-cover glass system

For concentrating or other types of collectors, the value of $(\tau\alpha)_n$ must be determined based on the geometrical and optical properties of the collector.

2. Calculate the value of F_R from the ASHRAE 93-77 tests by

$$F_R = \frac{\frac{A_a}{A_g} F_R (\tau\alpha)_n}{\frac{A_a}{A_g} (\tau\alpha)_n} \tag{A.2}$$

3. Calculate the value of the U_L from the ASHRAE 93-77 tests by

$$U_L = \frac{\frac{A_a}{A_g} F_R U_L}{\frac{A_a}{A_g} F_R} \tag{A.3}$$

where $F_R U_L$ is the absolute value of the slope of the efficiency curve at a value of $t_{set_G} - t_a$ at solar noon during the system test.

4. Calculate the collector efficiency factor, F' by

$$F' = \frac{-\dot{m}_c C_{p,c}}{A_a U_L} \ln \left[1 - \frac{F_R A_a U_L}{m_c C_{p,c}} \right] \qquad (A.4)$$

5. Once F' is determined, F_R can be calculated for any system's transfer fluid, flow rate and specific heat by using

$$F_R = \frac{\dot{m}_s C_{p,s}}{MA_a U_L} \left[1 - \exp\left(- \frac{MA_a U_L F'}{m_s C_{p,s}} \right) \right] \qquad (A.5)$$

It should be noted that the above correction technique is based on the assumption that the collector absorber plate efficiency factor, F', is not a function of flow rate.

APPENDIX B

TOP HEAT LOSS ANALYSIS

The purpose of this analysis, taken directly from reference 11, is to develop mathematical expressions for heat loss through the absorber-cover assembly and to define a top loss coefficient. The conventional analysis summarized in reference 12 applies only to materials with vanishingly small transmittance for longwave (infrared) radiation. The limitation is a result of the expression used for radiation heat transfer between a cover and either a parallel absorber plate or another cover. The present analysis for the heat loss through the cover assembly accounts for strong (as well as weak) infrared transmittance. A two-step iterative approach is used. The distribution of nodal (infrared) radiosities is determined for specified absorber, ambient, and sky temperatures and an estimated set of cover temperatures. Energy balances on the covers are then used to calculate improved estimates of the cover temperature distribution. The analysis is developed for a one-cover collector.

Referring to figure 56, the top heat loss and loss coefficients are

$$\dot{Q}''_t = h_{pc1} [t_p - t_{c1}] + [J_1 - J_2] \tag{B.1}$$

$$U_t = \dot{Q}''_t / [t_p - t_a] \tag{B.2}$$

The usefulness of the latter coefficient is limited since it varies strongly with temperature and includes the effect of radiant interchange with the sky at an effective temperature generally different from t_a. Nevertheless, U_t (and U_L) are convenient concepts and widely used in simplified, but adequate, analyses to predict the thermal performance of collectors.

Longwave radiation is assumed diffuse. The radiation properties of the upper and lower surfaces are assumed equal. The temperature gradient in the covers is neglected. Referring to figure 56, the nodal equations for determining the infrared radiosity distribution are

$$J_1 = E_p + \rho_p J_2 = \frac{E_p + \rho_p [E_{c1} + \tau_{c1} E_{bs}]}{1 - \rho_p \rho_{c1}} \tag{B.3}$$

$$J_2 = E_{c1} + \rho_{c1} J_1 + \tau_{c1} E_s \tag{B.4}$$

$$J_3 = E_{c1} + \tau_{c1} J_1 + \rho_{c1} E_s \tag{B.5}$$

The above equations may be solved simultaneously using an estimated cover temperature. Improved estimates of the cover temperature follow from an energy balance on the cover which yields

$$t_{c1} = \frac{h_{pc1} t_p + h_w t_a + [E_s - J_2] + [J_1 - J_3] + G q_{ac1}}{h_w + h_{pc1}} \tag{B.6}$$

The result is used to improve the estimate of the radiosity distribution until the cover temperature converges. The possibility exists, since $t_{sky} \neq t_a$, that

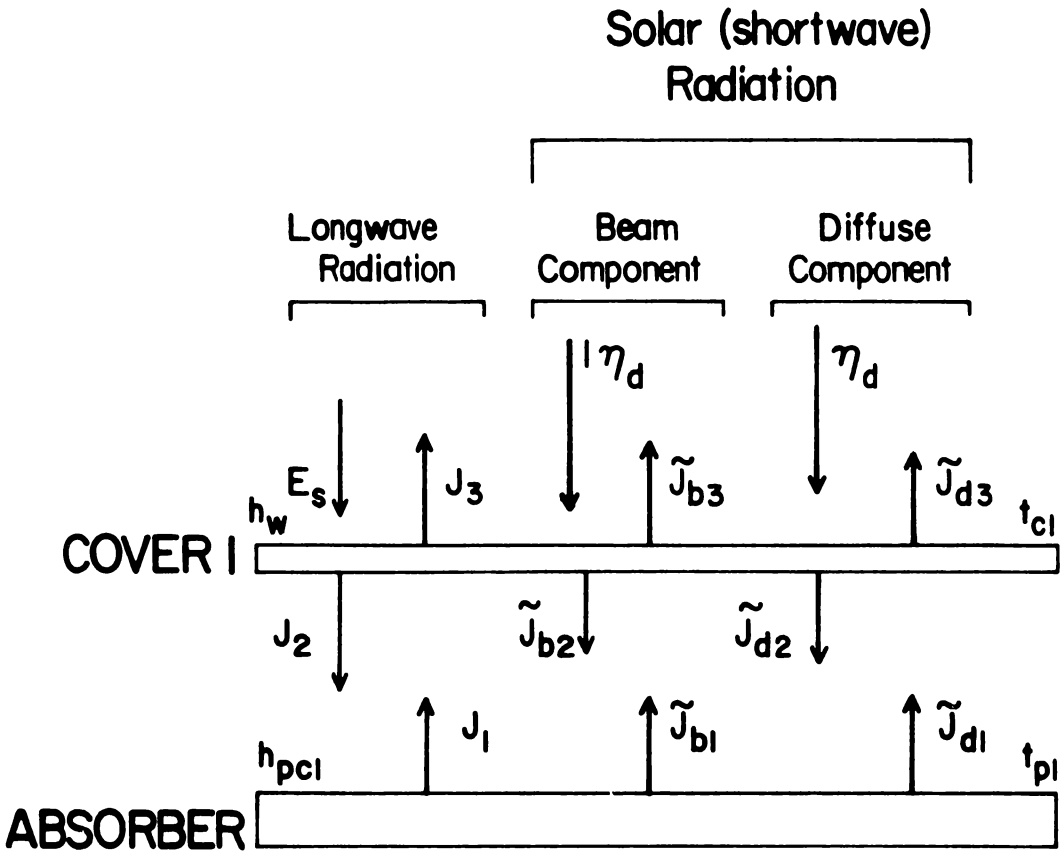

Fig. 56 Solar and infrared wavelength radiosity distributions in collectors with 1 cover

$Q_t = 0$ with $t_p = t_a$; in this case, eq (B.1) applies but eq (B.2) is meaningless. Furthermore, it is noted that if $t_{sky} > t_a$ and t_p near t_a, there can be a net heat gain, i.e. $Q_t < 0$; this condition is conceivable for indoor tests with solar simulators.

The (diffuse) longwave radiation properties of many commercially important cover materials are not as well established as corresponding properties for solar (shortwave) radiation. Nevertheless, reliable values of emittance and longwave transmittance are needed in the analysis for accurate results.

Sky temperature and h_w are estimated [12], respectively, from

$$t_{sky} = 0.0552\ (t_a/°K)^{1.5} °K \tag{B.7}$$

$$h_w = [5.7 + 3.8\ V_w]\ W/(m^2\ C) \tag{B.8}$$

The free-convection coefficients between covers and plates are calculated using the three-region correlation by Buchberg et al. [14] using temperature-dependent air properties at one atmosphere [15].

CALCULATION OF FILM CONDUCTANCE BETWEEN THE TEST FLUID AND FLOW CHANNEL WALL

The following analysis is taken directly from reference 11. Suitable expressions for calculating the film conductance between the test fluid and wall of the flow channel are required. The flow regimes of practical importance include laminar, transitional, and "fully turbulent" flow. In previous related analyses [16-18], an abrupt change from laminar to fully turbulent flow was assumed at a critical Reynolds number (of 2100). This previous procedure may cause problems in analytical approaches for estimating collector parameters. For the specified flow rate [7] of aqueous fluids, the strong dependence of viscosity on temperature frequently results in Reynolds numbers well above the practical upper limit for laminar flow.

Following a critical review of the available Nusselt number correlations [18], the practical significance of uncertainties in calculated results, and the benefit of increased computational time requirements, the following expressions were selected for laminar [19] and fully turbulent [20] flows, respectively,

$$Nu(RePrd_h/L) = 3.66 + \frac{0.0668\ Re\ Pr\ d_h/L}{1 + 0.04\ (Re\ Pr\ d_h/L)^{0.667}} \left[\frac{\mu(t_{fm})}{\mu(t_w)}\right]^{0.14} \tag{B.9}$$

where $Re\ Pr\ d_h/L < 1000$, and

$$Nu(Re, Pr) = 0.021\ Re(d_h)^{0.8}\ Pr^{1/3} \left[\frac{\mu(t_{fm})}{\mu(t_w)}\right]^{0.14} \tag{B.10}$$

where $0.7 \leq Pr \leq 120$ and $10{,}000 \leq Re \leq 120{,}000$. The latter expression is essentially the Seider-Tate correlation. The coefficient of 0.021 was

selected to better match the data [20] at lower Reynolds numbers than the value of 0.027 reported in many textbooks. Considering current designs, the L/d ratio effect is strong for laminar flow but weak for turbulent flow, i.e., less than 10 percent for L/d greater than 60 [21]. Consequently, entrance effects are neglected for turbulent flow.

In the transition region $Re_{c1} \leq Re \leq Re_{c2}$, a parabola is used for interpolation, i.e.

$$Nu = a + b\,[Re - Re_{c1}] + c\,[Re - Re_{c2}]^2 \tag{B.11}$$

where a, b, and c are selected to satisfy

$$Nu\,(Re_{c1}\,Pr\,d_h/L) = Nu_1 \text{ (from eq (B.9))} \tag{B.12}$$

$$Nu\,(Re_{c2}Pr) = Nu_2 \text{ (from eq (B.10))} \tag{B.13}$$

$$\frac{d}{d\,Re}\,Nu\Big|_{Re_{c2}} = \frac{d}{d\,Re}\left[0.021\,Pr^{1/3}\,Re^{0.8}\right]\Big|_{Re_{c2}} =$$

$$0.8\,\frac{Nu_2}{Re_{c2}} \tag{B.14}$$

As supported by reference 20, the slope of the interpolating curve and fully turbulent correlation are matched by eq (B.14) at Re_{c2} and the transition range is taken as $2100 < Re < 4000$.

APPENDIX C

DIMENSIONS AND PROPERTIES OF SOLAR COLLECTOR
INSTRUMENTATION SPECIFICATIONS
DATA CHANNEL ASSIGNMENT

DIMENSIONS AND PROPERTIES OF SOLAR COLLECTOR

Manufacturer and Model: Lennox LSC18-15

Component/Property	
Absorber	
Material	Steel
Flow configuration	Parallel
Effective length	1.730 m
Effective width	0.813 m
Flow tubes: number	10
Material	Copper
OD	6.35 mm
Hyd diameter	4.93 mm
Wetted perimeter	15.5 mm
Thickness	0.90 mm
Thermal conductivity	47.6 W/m-C
Emittance	0.10
Solar absorptance (est)	0.94
Cover	
Material	Glass
Number of covers	1
Air space under cover	65.2 mm
Emittance	0.88 mm
Transmittance	0.04
Index of refraction, solar	1.51
Extinction coeff, solar	0.010 mm^{-1}
Thickness	3.18 mm
Insulation	
Material	Glass Fiber
Thickness: back	89.0 mm
edge	25.4 mm
Conductivity: back	0.040 W/m-C
edge	0.040 W/m-C
Estimated U_b	1.4 W/m^2-C
Gross Area	1.662 m^2

SUPERIOR ELECTRIC COMPANY
AUTOTRANSFORMER SPECIFICATIONS

Voltage input	240 volts ac
Voltage output	0 - 280 volts ac
Maximum amperage output	28
Maximum output	7.8 kVa
Phase	Single

SCIENTIFIC COLUMBUS XL5C5-A2-1-7
WATT TRANSDUCER SPECIFICATIONS

Connection	Single Phase
Input voltage	0 - 240 Vac
Current input, nominal	0 - 15 a
Potential input	120 Vac
Potential burden	0.1 Va at 120 Vac
Watt input range	0 - 3.5 kW
Output signal	0 - 100 mv
Accuracy	$\pm$ 0.25 percent of indicated reading
Output ripple peak	$\leq$ 0.5 percent of output
Response time (to 99 percent)	< 400 ms
Power factor range	Unity to zero lead or lag
Temperature range	-20 C to +70 C
Temperature influence (max.)	$\pm$ 0.005 percent/C
Operating humidity	0 - 95 percent
Stability (per year)	$\pm$ 0.1 percent of output

SCIENTIFIC COLUMBUS DIGITAL WATTMETER
MODEL 6335 PF SPECIFICATIONS

Function	Three-phase, two-element wattmeter One-phase, one-element wattmeter
Full scale watts	Three phase: 0.4, 0.8, 1.2, 2, 2.4, 4, 6, 8, 12, 20, 24, 60 kW total Single Phase: 0.2, 0.4, 0.6, 1, 1.2 2, 3, 4, 6, 10, 12, 30 kW per element
Input voltage	0-100, 200, 500 Vac, push button select Max. with linearity 125 percent of range Max. without linearity 150 percent of range Burden 0.5 Va per element
Input current	2, 6, 20, 60 amps, push button select Max. with linearity 124 percent of range Max. without damage 200 percent of range
Frequency	60 $\pm$ 5 Hz
Power factor range	Unity to zero lead or lag
Operating temperature effect on accuracy	0 C to 50 C max. $\pm$ 0.015 percent/G
Accuracy at 25 C	Digital Readout $\pm \frac{0.25 \text{ percent of reading}}{\text{Power factor}}$ + 1 digit Analog Output $\pm \frac{.2 \text{ percent of reading}}{\text{Power factor}}$ $\pm$ 0.03 percent of R.O
Digital readout	Direct reading in kW

EPPLEY PRECISION SPECTRAL PYRANOMETER MODEL PSP SPECIFICATIONS

Sensitivity	9 microvolts per watt m^{-2} approx.
Impedance	650 ohms approx.
Receiver	circular, coated with Parsons' bla optical lacquer
Temperature dependence	± 1 percent over ambient temperature range -20 to +40 C
Linearity	± 0.5 percent
Response time	1 second (1/e signal)
Cosine	± 1 percent from normalization, 0-70° zenith angle ± 3 percent, 70-80° zenith angle

---

EPPLEY PRECISION INFRARED RADIOMETER (PYRGEOMETER) MODEL PIR SPECIFICATIONS

Sensitivity	3 microvolts/W m^{-2} approx.
Impedance	700 ohms approx.
Temperature dependence	± 1 percent, -20 to 40 C (nominal)
Linearity	± 1 percent
Response time	2 seconds (1/e signal)
Cosine response	better than 5 percent from normalization, insignificant for a diffuse source

NBS SOLAR DOMESTIC HOT WATER TEST FACILITY
DATA CHANNEL ASSIGNMENT

SYSTEM EMPLOYING ACTUAL SOLAR COLLECTORS EXPOSED
TO OUTSIDE METEOROLOGICAL CONDITIONS

CHANNEL NO.	MEASUREMENT	
0	Temperature	Tank 0.15 m (6 in.) Elevation
1	Temperature	Tank 0.30 m (12 in.) Elevation
2	Temperature	Tank 0.46 m (18 in.) Elevation
3	Temperature	Tank 0.61 m (24 in.) Elevation
4	Temperature	Tank 0.76 m (30 in.) Elevation
5	Temperature	Tank 0.91 m (36 in.) Elevation
6	Temperature	Tank 1.07 m (42 in.) Elevation
7	Temperature	Tank 1.22 m (48 in.) Elevation
8	Temperature	Tank 1.37 m (54 in.) Elevation
9	Temperature	Tank 1.52 m (60 in.) Elevation
10	None	
11	None	
12	Temperature	Collector Supply at Tank
13	Temperature	Collector Return at Tank
14	Temperature	Collector Supply at Solar Array
15	Temperature	Collector Return at Solar Array
16	Voltage (mV)	Temperature Difference Across Solar Storage Tank, Six-Junction Thermopile
17	Voltage (V)	Flowmeter Analog Signal Output
18	Voltage (V)	Circulator Pump Status, 1.5 Vdc On - 0.0 Vdc Off
19	Voltage (V)	Wind Speed Anemometer
20	Voltage (mV)	Storage Tank Heating Element Watt Transducer Output
21	Voltage (mV)	Temperature Difference Across Collector Array, Six-Junction Thermopile
22	Voltage (mV)	Radiation Level on Collector Surface
23	Voltage (mV)	Effective Sky Temperature
24	Temperature	Controller Tank Temperature Sensor
25	Temperature	Controller Plate Temperature Sensor
26	Temperature	Controller Collector Exit Pipe Temperature Sensor
27	Temperature	Collector Plate Temperature 1/4 Length
28	Temperature	Collector Plate Temperature 1/2 Length
29	Temperature	Collector Plate Temperature 3/4 Length
30	Temperature	Supply Circulation Loop Temperature
31	Temperature	Calibration Input Channel 1
32	None	
33	Voltage (V)	Storage Tank Heating Element Status 1.5 Vdc On - 0.0 Vdc Off

(CONTINUED)

CHANNEL NO.	MEASUREMENT	
34	None	
35	Temperature	Ambient Temperature Surrounding Tank 1.14 m Elevation
36	Temperature	Ambient Temperature Surrounding Tank 0.62 m Elevation
37	None	
38	None	
39	Temperature	Ambient Temperature Outdoors
40	Voltage (mV)	Temperature Difference Across Hot Water Load Three-Junction Thermopile
41	None	
42	None	
43	None	
44	Voltage (mV)	Integrated Temperature Difference Across Hot Water Load
45	Temperature	Cold Water Supply to Storage Tank
46	Temperature	Hot Water Outlet From Storage Tank
47	Voltage (mV)	Calibration Input Channel 2
48	None	
49	None	
50	None	

NBS SOLAR DOMESTIC HOT WATER TEST FACILITY
DATA CHANNEL ASSIGNMENT

SYSTEM EMPLOYING NONIRRADIATED SOLAR COLLECTORS

CHANNEL		MEASUREMENT
31	Temperature	Calibration Channel No. 1
32	None	
33	None	
34	Voltage (V)	Storage Tank Heating Element Status 1.5 Vdc On - 0.0 Vdc Off
35	None	
36	None	
37	Temperature	Ambient Temperature Surrounding Tank 1.14 m Elevation
38	Temperature	Ambient Temperature Surrounding Tank 0.62 m Elevation
39	None	
40	Voltage (mV)	Temperature Difference Across Hot Water Load, Three-Junction Thermopile
41	Temperature	Collector 1 Sky Cover
42	Temperature	Collector 2 Sky Cover
43	Voltage (mV)	Temperature Difference Across Collector Inlet and Heat Source Outlet, Six-Junction Thermopile
44	Voltage (mV)	Integrated Temperature Difference Across Hot Water Load, Three-Junction Thermopile
45	None	
46	None	
47	Temperature	Calibration Channel No. 2
48	None	
49	None	
50	Temperature	Tank 0.15 m (6 in.) Elevation
51	Temperature	Tank 0.30 m (12 in.) Elevation
52	Temperature	Tank 0.46 m (18 in.) Elevation
53	Temperature	Tank 0.61 m (24 in.) Elevation
54	Temperature	Tank 0.76 m (30 in.) Elevation
55	Temperature	Tank 0.91 m (36 in.) Elevation
56	Temperature	Tank 1.07 m (42 in.) Elevation
57	Temperature	Tank 1.22 m (48 in.) Elevation
58	Temperature	Tank 1.37 m (54 in.) Elevation
59	Temperature	Tank 1.52 m (60 in.) Elevation
60	Temperature	Cold Water Supply to Storage Tank
61	Temperature	Hot Water Supply from Storage Tank
62	None	
63	None	
64	Temperature	Collector Supply at Solar Array

CHANNEL		MEASUREMENT
65	Temperature	Collector Outlet at Solar Array
66	Temperature	Ambient Temperature Above Collectors
67	Voltage (mV)	Temperature Difference Between Inlet to Solar Collector Array and Ambient Above Solar Collector Array, Six-Junction Thermopile
68	None	
69	Temperature	Heat Source Outlet
70	Voltage (mV)	Temperature Difference Across Solar Collector Array, Six-Junction Thermopile
71	Temperature	Inlet to Heat Source
72	Temperature	Outlet from Heat Source
73	Voltage (mV)	Temperature Difference Across Heat Source, Six-Junction Thermopile
74	Temperature	Supply at Tank
75	Temperature	Return at Tank
76	Voltage (mV)	Temperature Difference Across Solar Storage Tank, Six-Junction Thermopile
77	Temperature	Controller Tank Temperature Sensor
78	Temperature	Controller Exit Pipe Temperature Sensor
79	Temperature	Controller Plate Temperature 1/4 Length
80	Temperature	Controller Plate Temperature 1/2 Length
81	Temperature	Controller Plate Temperature 3/4 Length
82	Voltage (mV)	Flowmeter
83	None	
84	Voltage (mV)	Heat Source Watt Transducer Output
85	Voltage (mV)	Storage Tank Watt Transducer Output
86	Voltage (mV)	Effective Sky Temperature
87	Temperature	Collector Plate Temperature 1/8 Length
88	Voltage (V)	Zone Valve Status 1.5 Vdc Collector-Heat Source-Tank Loop 0.0 Vdc Collector-Heat Source Loop
89	Temperature	Inlet Temperature to Solar Collector Array

TRENDSCAN 1000 PERFORMANCE SPECIFICATIONS

Measurement technique: Dual slope integrating auto-zeroing measuring circuit, fully-guarded for high common mode rejection.

Linearization: Variable-length segment digital linearization.

Reference junction compensation (T.C. Ranges): Electrically compensated to 0 C reference junction. A temperature sensitive component for each T.C. range is located on the range card for each range in the Trendscan 1000.

Temperature Coefficient: (5 to 20 C and 30 to 45 C)	± (0.015 percent of reading ±0.001 percent of range/C)
Normal mode rejection: (At range card input terminals)	70 dB at 50-60 Hz, 50 dB at 100/120 Hz increasing 12 dB/octave beyond 100/120 Hz
Common mode rejection:	120 db at DC, 130 dB at 50/60 Hz with 1000 Ω line unbalance
Self-test voltage accuracy:	± (0.05 percent of reading)
Max. common-mode voltage:	250 Vdc or Vac Peak
Max. source resistance:	2500 Ω
Input impedance	100 Megohms (all ranges)
Repeatability:	± (0.05 percent of reading)

Range Description	Total Range	Display Resolution	System Accuracy
			1 Year 25 ± 10 C
Copper-Constantan	-200 C to + 400 C	0.1 C	0.9 C
EMF	+ 4 V Linear	0.1 mV	± (0.02 percent ± 0.4 mV)
EMF	+ 10 V Linear	1 mV	± (0.02 percent ± 4 mV)

NBS-114A (REV. 2-8C)

U S DEPT. OF COMM. BIBLIOGRAPHIC DATA SHEET (See instructions)	1. PUBLICATION OR REPORT NO. NBS BSS 140	2. Performing Organ. Report No.	3. Publication Date February 1982

4. TITLE AND SUBTITLE

Analytical and Experimental Analysis of Procedures for Testing Solar Domestic Hot Water Systems

5. AUTHOR(S)

A.H. Fanney, W.C. Thomas, C.A. Scarbrough, C.P. Terlizzi

6. PERFORMING ORGANIZATION (If joint or other than NBS, see instructions)

NATIONAL BUREAU OF STANDARDS
DEPARTMENT OF COMMERCE
WASHINGTON, D C 20234

7. Contract/Grant No.

8. Type of Report & Period Covered

Final

9. SPONSORING ORGANIZATION NAME AND COMPLETE ADDRESS (Street, City, State, ZIP)

Office of Solar Applications for Buildings
U.S. Department of Energy
Washington, D C 20585

Library of Congress Catalog Card Number: 81-600191

10. SUPPLEMENTARY NOTES

11. ABSTRACT

A repeatable test method independent of outdoor environmental conditions and laboratory geographical location is required in order to provide a means by which solar domestic hot water systems may be rated and compared. Three experimental techniques which allow the net thermal output of an irradiated solar collector array to be reproduced indoors without the use of a solar simulator are investigated. These techniques include use of an electric heat source only, use of a nonirradiated collector array in series with an electric heat source, and the use of electric strip heaters which are attached to the back of nonirradiated absorber plates. Expressions are developed to compute the input power required for each experimental technique. Solar collectors connected in parallel and series combinations are considered.

All three test techniques were shown to reproduce the outdoor daily collector array thermal output within four percent. Two of the techniques allow the actions of the circulator controller for an outdoor irradiated system to be duplicated indoors. One technique applies to solar hot water systems which operate on the thermosyphon principle.

Experiments conducted to determine the effect of storage tank temperature stratification on system performance for a single-tank direct solar hot water system are described. Several return tube designs, which introduce the solar heated water into the storage tank, were fabricated and tested to determine the influence of thermal stratification on system performance. The best return tube design increased the performance of the single-tank direct system approximately ten percent compared to a conventional return tube design.

An analytical model for a single-tank direct hot water system is developed. The model is used to support parametric studies for the thermal performance characteristics which result from the use of each test method to duplicate the net thermal output of an irradiated array. The model is also used to assess thermal performance differences which occur due to indoor versus outdoor environmental conditions.

12. KEY WORDS (Six to twelve entries; alphabetical order; capitalize only proper names; and separate key words by semicolons)

ASHRAE Standard 95; collectors in parallel; electric strip heaters; environmental conditions; indoor testing; modeling; NBS; solar; solar domestic hot water system; stratification; test method

13. AVAILABILITY

[X] Unlimited
[ ] For Official Distribution. Do Not Release to NTIS
[X] Order From Superintendent of Documents, U.S. Government Printing Office, Washington, D C 20402.
Order From National Technical Information Service (NTIS), Springfield, VA 22161

14. NO. OF PRINTED PAGES 158

15. Price $6.00

☆ U.S. GOVERNMENT PRINTING OFFICE : 1982 0 - 366-393

USCOMM-DC 6043-P80

NBS TECHNICAL PUBLICATIONS

PERIODICALS

JOURNAL OF RESEARCH—The Journal of Research of the National Bureau of Standards reports NBS research and development in those disciplines of the physical and engineering sciences in which the Bureau is active. These include physics, chemistry, engineering, mathematics, and computer sciences. Papers cover a broad range of subjects, with major emphasis on measurement methodology and the basic technology underlying standardization. Also included from time to time are survey articles on topics closely related to the Bureau's technical and scientific programs. As a special service to subscribers each issue contains complete citations to all recent Bureau publications in both NBS and non-NBS media. Issued six times a year. Annual subscription: domestic $18; foreign $22.50. Single copy $4.25 domestic; $5.35 foreign.

NOTE: The Journal was formerly published in two sections: Section A "Physics and Chemistry" and Section B "Mathematical Sciences."

DIMENSIONS/NBS—This monthly magazine is published to inform scientists, engineers, business and industry leaders, teachers, students, and consumers of the latest advances in science and technology, with primary emphasis on work at NBS. The magazine highlights and reviews such issues as energy research, fire protection, building technology, metric conversion, pollution abatement, health and safety, and consumer product performance. In addition, it reports the results of Bureau programs in measurement standards and techniques, properties of matter and materials, engineering standards and services, instrumentation, and automatic data processing. Annual subscription: domestic $11; foreign $13.75.

NONPERIODICALS

Monographs—Major contributions to the technical literature on various subjects related to the Bureau's scientific and technical activities.

Handbooks—Recommended codes of engineering and industrial practice (including safety codes) developed in cooperation with interested industries, professional organizations, and regulatory bodies.

Special Publications—include proceedings of conferences sponsored by NBS, NBS annual reports, and other special publications appropriate to this grouping such as wall charts, pocket cards, and bibliographies.

Applied Mathematics Series—Mathematical tables, manuals, and studies of special interest to physicists, engineers, chemists, biologists, mathematicians, computer programmers, and others engaged in scientific and technical work.

National Standard Reference Data Series—Provides quantitative data on the physical and chemical properties of materials, compiled from the world's literature and critically evaluated. Developed under a worldwide program coordinated by NBS under the authority of the National Standard Data Act (Public Law 90-396).

NOTE: The principal publication outlet for the foregoing data is the Journal of Physical and Chemical Reference Data (JPCRD) published quarterly for NBS by the American Chemical Society (ACS) and the American Institute of Physics (AIP). Subscriptions, reprints, and supplements available from ACS, 1155 Sixteenth St., NW, Washington, DC 20056.

Building Science Series—Disseminates technical information developed at the Bureau on building materials, components, systems, and whole structures. The series presents research results, test methods, and performance criteria related to the structural and environmental functions and the durability and safety characteristics of building elements and systems.

Technical Notes—Studies or reports which are complete in themselves but restrictive in their treatment of a subject. Analogous to monographs but not so comprehensive in scope or definitive in treatment of the subject area. Often serve as a vehicle for final reports of work performed at NBS under the sponsorship of other government agencies.

Voluntary Product Standards—Developed under procedures published by the Department of Commerce in Part 10, Title 15, of the Code of Federal Regulations. The standards establish nationally recognized requirements for products, and provide all concerned interests with a basis for common understanding of the characteristics of the products. NBS administers this program as a supplement to the activities of the private sector standardizing organizations.

Consumer Information Series—Practical information, based on NBS research and experience, covering areas of interest to the consumer. Easily understandable language and illustrations provide useful background knowledge for shopping in today's technological marketplace.

Order the **above** *NBS publications from: Superintendent of Documents, Government Printing Office, Washington, DC 20402.*

Order the **following** *NBS publications—FIPS and NBSIR's—from the National Technical Information Services, Springfield, VA 22161.*

Federal Information Processing Standards Publications (FIPS PUB)—Publications in this series collectively constitute the Federal Information Processing Standards Register. The Register serves as the official source of information in the Federal Government regarding standards issued by NBS pursuant to the Federal Property and Administrative Services Act of 1949 as amended, Public Law 89-306 (79 Stat. 1127), and as implemented by Executive Order 11717 (38 FR 12315, dated May 11, 1973) and Part 6 of Title 15 CFR (Code of Federal Regulations).

NBS Interagency Reports (NBSIR)—A special series of interim or final reports on work performed by NBS for outside sponsors (both government and non-government). In general, initial distribution is handled by the sponsor; public distribution is by the National Technical Information Services, Springfield, VA 22161, in paper copy or microfiche form.